

ESCUELA TÉCNICA SUPERIOR DE INGENIERÍA (ICAI)

INGENIERO INDUSTRIAL

SIMULACIÓN DE UNA TURBINA DE VAPOR DE UNA CENTRAL NUCLEAR CON ATHLET

Autor: Vega Gómez de la Rosa
Director: Prof. Dr. Rafael Macián-Juan

Madrid
Mayo 2015

AUTORIZACIÓN PARA LA DIGITALIZACIÓN, DEPÓSITO Y DIVULGACIÓN EN ACCESO *ABIERTO* (*RESTRINGIDO*) DE DOCUMENTACIÓN

1º. Declaración de la autoría y acreditación de la misma.

El autor D. VEGA GÓMEZ DE LA ROSA , como ALUMNA de la UNIVERSIDAD PONTIFICIA COMILLAS (COMILLAS), **DECLARA**

que es el titular de los derechos de propiedad intelectual, objeto de la presente cesión, en relación con la obra PROYECTO FIN DE CARRERA : SIMULACIÓN DE UNA TURBINA DE VAPOR DE UNA CENTRAL NUCLEAR CON ATHUET [1], que ésta es una obra original, y que ostenta la condición de autor en el sentido que otorga la Ley de Propiedad Intelectual como titular único o cotitular de la obra.

En caso de ser cotitular, el autor (firmante) declara asimismo que cuenta con el consentimiento de los restantes titulares para hacer la presente cesión. En caso de previa cesión a terceros de derechos de explotación de la obra, el autor declara que tiene la oportuna autorización de dichos titulares de derechos a los fines de esta cesión o bien que retiene la facultad de ceder estos derechos en la forma prevista en la presente cesión y así lo acredita.

2º. Objeto y fines de la cesión.

Con el fin de dar la máxima difusión a la obra citada a través del Repositorio institucional de la Universidad y hacer posible su utilización de *forma libre y gratuita* (*con las limitaciones que más adelante se detallan*) por todos los usuarios del repositorio y del portal e-ciencia, el autor **CEDE** a la Universidad Pontificia Comillas de forma gratuita y no exclusiva, por el máximo plazo legal y con ámbito universal, los derechos de digitalización, de archivo, de reproducción, de distribución, de comunicación pública, incluido el derecho de puesta a disposición electrónica, tal y como se describen en la Ley de Propiedad Intelectual. El derecho de transformación se cede a los únicos efectos de lo dispuesto en la letra (a) del apartado siguiente.

3º. Condiciones de la cesión.

Sin perjuicio de la titularidad de la obra, que sigue correspondiendo a su autor, la cesión de derechos contemplada en esta licencia, el repositorio institucional podrá:

[1] Especificar si es una tesis doctoral, proyecto fin de carrera, proyecto fin de Máster o cualquier otro trabajo que deba ser objeto de evaluación académica

(a) Transformarla para adaptarla a cualquier tecnología susceptible de incorporarla a internet; realizar adaptaciones para hacer posible la utilización de la obra en formatos electrónicos, así como incorporar metadatos para realizar el registro de la obra e incorporar "marcas de agua" o cualquier otro sistema de seguridad o de protección.

(b) Reproducirla en un soporte digital para su incorporación a una base de datos electrónica, incluyendo el derecho de reproducir y almacenar la obra en servidores, a los efectos de garantizar su seguridad, conservación y preservar el formato. .

(c) Comunicarla y ponerla a disposición del público a través de un archivo abierto institucional, accesible de modo libre y gratuito a través de internet.[2]

(d) Distribuir copias electrónicas de la obra a los usuarios en un soporte digital. [3]

4º. Derechos del autor.

El autor, en tanto que titular de una obra que cede con carácter no exclusivo a la Universidad por medio de su registro en el Repositorio Institucional tiene derecho a:

a) A que la Universidad identifique claramente su nombre como el autor o propietario de los derechos del documento.

b) Comunicar y dar publicidad a la obra en la versión que ceda y en otras posteriores a través de cualquier medio.

c) Solicitar la retirada de la obra del repositorio por causa justificada. A tal fin deberá ponerse en contacto con el vicerrector/a de investigación (curiarte@rec.upcomillas.es).

d) Autorizar expresamente a COMILLAS para, en su caso, realizar los trámites necesarios para la obtención del ISBN.

---

[2] En el supuesto de que el autor opte por el acceso restringido, este apartado quedaría redactado en los siguientes términos:

(c) Comunicarla y ponerla a disposición del público a través de un archivo institucional, accesible de modo restringido, en los términos previstos en el Reglamento del Repositorio Institucional

[3] En el supuesto de que el autor opte por el acceso restringido, este apartado quedaría eliminado.

d) Recibir notificación fehaciente de cualquier reclamación que puedan formular terceras personas en relación con la obra y, en particular, de reclamaciones relativas a los derechos de propiedad intelectual sobre ella.

5º. Deberes del autor.

El autor se compromete a:

a) Garantizar que el compromiso que adquiere mediante el presente escrito no infringe ningún derecho de terceros, ya sean de propiedad industrial, intelectual o cualquier otro.

b) Garantizar que el contenido de las obras no atenta contra los derechos al honor, a la intimidad y a la imagen de terceros.

c) Asumir toda reclamación o responsabilidad, incluyendo las indemnizaciones por daños, que pudieran ejercitarse contra la Universidad por terceros que vieran infringidos sus derechos e intereses a causa de la cesión.

d) Asumir la responsabilidad en el caso de que las instituciones fueran condenadas por infracción de derechos derivada de las obras objeto de la cesión.

6º. Fines y funcionamiento del Repositorio Institucional.

La obra se pondrá a disposición de los usuarios para que hagan de ella un uso justo y respetuoso con los derechos del autor, según lo permitido por la legislación aplicable, y con fines de estudio, investigación, o cualquier otro fin lícito. Con dicha finalidad, la Universidad asume los siguientes deberes y se reserva las siguientes facultades:

a) Deberes del repositorio Institucional:

- La Universidad informará a los usuarios del archivo sobre los usos permitidos, y no garantiza ni asume responsabilidad alguna por otras formas en que los usuarios hagan un uso posterior de las obras no conforme con la legislación vigente. El uso posterior, más allá de la copia privada, requerirá que se cite la fuente y se reconozca la autoría, que no se obtenga beneficio comercial, y que no se realicen obras derivadas.

- La Universidad no revisará el contenido de las obras, que en todo caso permanecerá bajo la responsabilidad exclusiva del autor y no estará obligada a ejercitar acciones legales en nombre del autor en el supuesto de infracciones a derechos de propiedad intelectual derivados del depósito y archivo de las obras. El autor renuncia a cualquier reclamación frente a la Universidad por las formas no ajustadas a la legislación vigente en que los usuarios hagan uso de las obras.

- La Universidad adoptará las medidas necesarias para la preservación de la obra en un futuro.

b) Derechos que se reserva el Repositorio institucional respecto de las obras en él registradas:

- retirar la obra, previa notificación al autor, en supuestos suficientemente justificados, o en caso de reclamaciones de terceros.

Madrid, a 26 de Mayo de 2015

ACEPTA

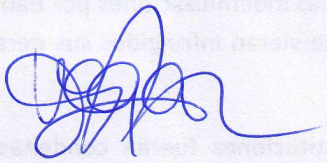

Fdo.....

Proyecto realizado por el alumno/a:

Vega Gómez de la Rosa

Fdo.: 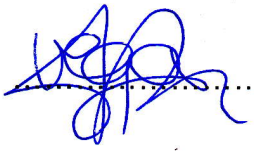 Fecha: 21 / 05 / 2015

Autorizada la entrega del proyecto cuya información no es de carácter confidencial

EL DIRECTOR DEL PROYECTO

Rafael Macián Juan

Fdo.:  Fecha: 15 / 05 / 2015

Vº Bº del Coordinador de Proyectos

Fdo.: ..... Fecha: ...../ ...../ .....



ESCUELA TÉCNICA SUPERIOR DE INGENIERÍA (ICAI)

INGENIERO INDUSTRIAL

SIMULACIÓN DE UNA TURBINA DE VAPOR DE UNA CENTRAL NUCLEAR CON ATHLET

Autor: Vega Gómez de la Rosa
Director: Prof. Dr. Rafael Macián-Juan

Madrid
Mayo 2015

SIMULACIÓN DE UNA TURBINA DE VAPOR DE UNA CENTRAL NUCLEAR CON ATHLET

Autor: Gómez de la Rosa, Vega.

Director: Prof. Dr. Macián-Juan, Rafael.

Entidad Colaboradora: TUM – Technische Universität München

RESUMEN DEL PROYECTO

Introducción

La turbina de vapor es una parte muy importante del circuito secundario de una central nuclear. Debido a que desde el punto de vista del análisis de la seguridad de una central nuclear, la turbine de vapor tiene una menor prioridad que el circuito primario, normalmente se emplean modelos muy simples para representarla. Esto implica que su influencia en el circuito primario no puede considerarse.

El código termo-hidráulico ATHLET (Analysis of Thermal-hydraulics of Leaks ant Transients) se emplea normalmente para analizar el circuito primario de centrales nucleares. Sin embargo, la simulación de la turbina de vapor, donde la energía térmica producida en el circuito primario se convierte en energía mecánica, y más tarde en electricidad en el generador, se ha considerado de interés, ya que una buena simulación del circuito secundario proporciona una visión más realista del comportamiento de la central nuclear a distintos estados de operación y durante transitorios. Por este motivo, ATHLET se ha empleado en este proyecto para simular la parte de la turbina de vapor de la central nuclear.

El propósito de este proyecto es modelar la turbina de vapor y sus componentes adyacentes con la ayuda del código alemán ATHLET. La turbina considerada existe, y se utiliza en el circuito secundario de un reactor nuclear a presión alemán (PWR).

El sistema modelado está formado por una turbina de alta presión, un separador de agua y vapor, un calentador, una turbina de baja presión y un condensador.

Metodología

El objetivo final de este proyecto era simular condiciones transitorias para este sistema de la turbina de vapor. Para poder simular transitorios, la simulación del sistema bajo condiciones normales de operación fue necesaria previamente. Por este motivo, el trabajo fue dividido en dos partes:

1. La simulación de la turbina de alta y de baja, y del sistema conectado bajo condiciones normales de operación.
2. La simulación de transitorios para el sistema completo

Se han modelado dos turbinas distintas empleando los datos de diseño disponibles, porque la información referente a medidas reales durante transitorios no estaba disponible al comenzar el proyecto. Por este motivo, el modelo de una antigua turbina fue realizado primero. Finalmente, cuando se consiguieron las medidas reales de

transitorios, el modelo fue adaptado a través de varias modificaciones a la nueva turbina.

El sistema se ha modelado utilizando datos reales y nominales de un reactor nuclear a presión alemán del tipo Convoy. La información de la planta que ha sido empleada durante el proceso de modelado y simulación incluía potencia, entalpía, presión, temperatura y flujo másico a la entrada y salida de los componentes principales del sistema. Debido a la confidencialidad de los datos reales de la planta, todos los resultados incluidos en el proyecto están normalizados, tomando como referencia los valores a la entrada de la nueva turbina de alta presión.

El sistema de la turbina de vapor está formado por dos partes principales: la turbina de alta presión y la de baja presión. Como el vapor procedente del circuito primario se encuentra a una elevada presión, se expande primero en la turbina de alta, y después en la de baja. Con el fin de aumentar la eficiencia de la turbina de baja, hay dos componentes entre ambas turbinas que también han sido modelados: un separador de vapor y agua y un calentador. Cuando el vapor sale de la turbina de baja se condensa en el condensador.

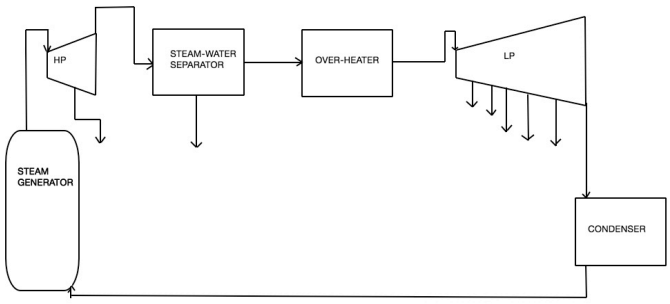

Esquema del sistema modelado

El sistema descrito se ha modelado en ATHLET conectando los objetos termodinámicos a través de sus correspondientes métodos de conexión. Se han empleado objetos especiales para simular las turbinas, el separador y el condensador.

El proceso seguido para simular transitorios ha sido el siguiente:

1. Desarrollo del modelo de la antigua turbina bajo condiciones normales:
    - Mejora de un modelo existente para la turbina de alta presión.
    - Diseño y desarrollo de un separador de vapor y agua, y su conexión a la salida de la turbina de alta presión.
    - Diseño y desarrollo de un calentador, y su conexión a la salida del separador.
    - Mejora de un modelo existente para la turbina de baja presión, y su conexión a la salida del calentador.
    - Diseño y desarrollo de un condensador, y su conexión a la salida de la turbina de baja formando un sistema conectado.

2. Introducción de cambios para el modelo de la nueva turbina bajo condiciones normales:
    - Condiciones diferentes del vapor a la entrada de la turbina de alta.
    - Aproximaciones para flujo másico en las extracciones de la turbina.

3. Introducción de cambios para la simulación de transitorios:
    - Introducción de señales de control para los flujos másicos a la entrada de la turbina de alta y en las extracciones de la turbina.
    - Flujo másico variando en el tiempo a la entrada de la turbina de alta.

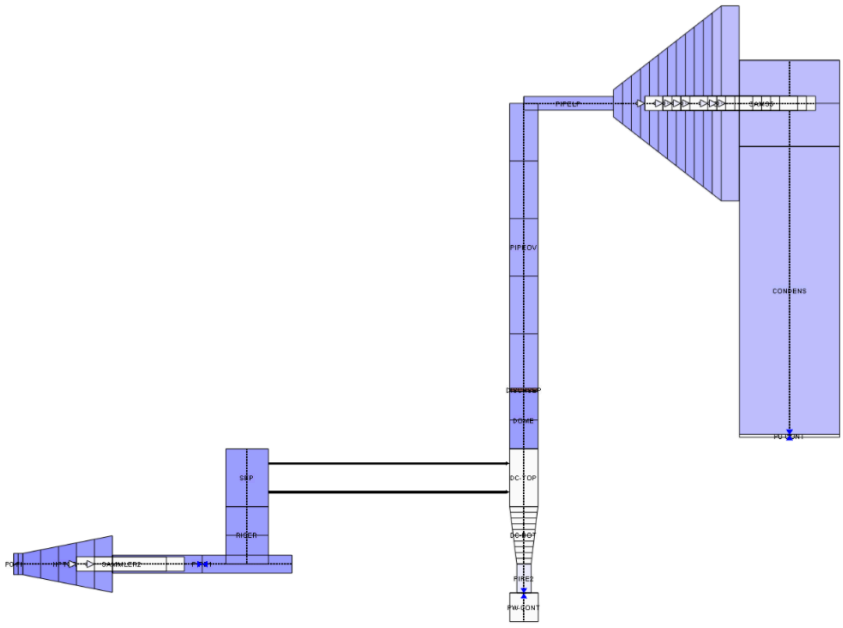

Visualización del sistema de la turbina modelado

Resultados

Los resultados obtenidos en la simulaciones se han comparado con los datos disponibles de la turbina. En total se han realizado las simulaciones de la antigua turbine bajo condiciones normales, la nueva turbina bajo condiciones normales y tres distintas simulaciones de transitorios. Los resultados más relevantes se muestran en las siguientes imágenes.

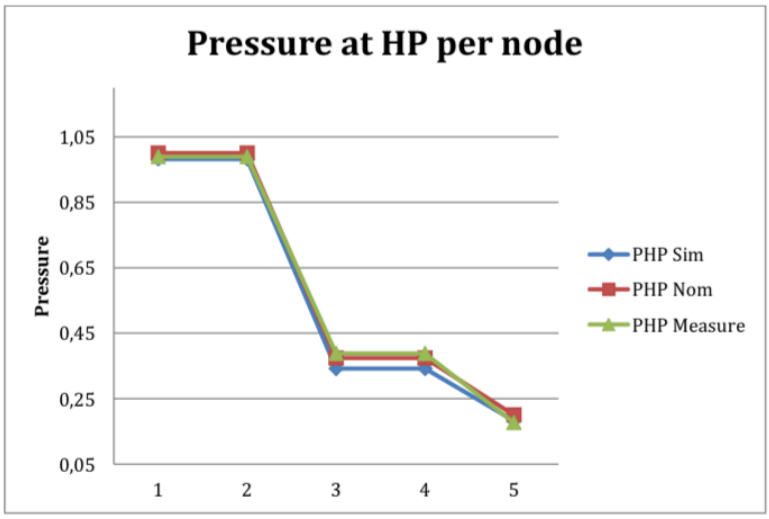

Presión en la nueva turbina de alta presión por nodo bajo condiciones normales

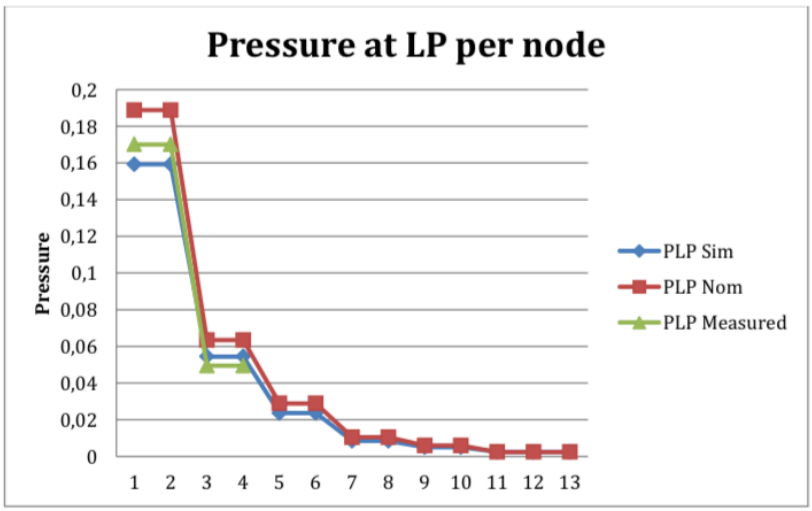

Presión en la nueva turbina de baja presión bajo condiciones normales

La distribución de presión obtenida a lo largo de la turbina (azul) se aproxima mucho a la distribución nominal de presión (roja), así como a la distribución nominal de presión (verde) tanto para la turbina de alta como para la de baja presión bajo condiciones normales de operación.

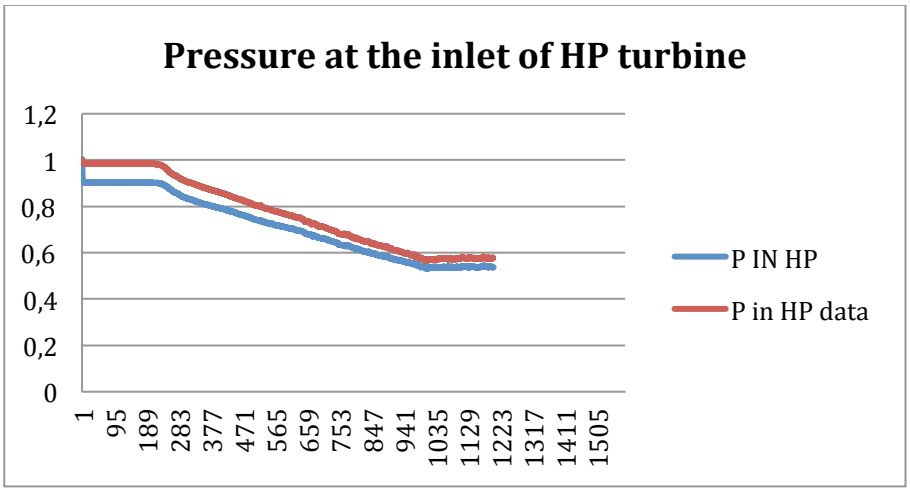

Presión a la entrada de la turbina de alta presión durante el primer transitorio

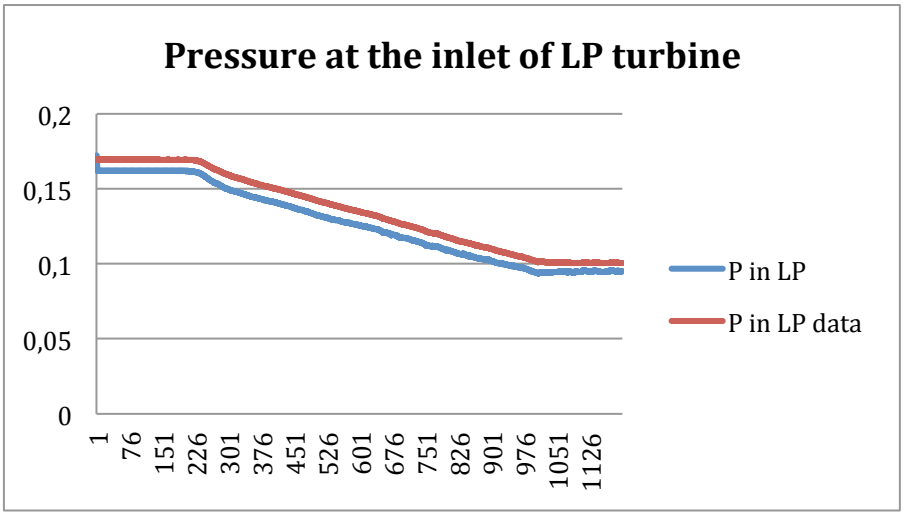

Presión a la entrada de la turbina de baja presión durante el primer transitorio

La presión obtenida a la entrada de la turbina de alta (azul) varía a lo largo del tiempo de simulación, así como la presión real medida durante el transitorio (roja), y estas dos curvas son muy próximas. Además, la presión obtenida con la simulación en la entrada de la turbina de baja (azul) sigue el mismo patrón que la presión a la entrada de la turbina de alta y que la medida real de la presión en el transitorio (roja).

Conclusiones

El modelo desarrollado con ATHLET en este proyecto describe bastante bien el comportamiento de la turbina de vapor del típico reactor nuclear alemán PWR durante condiciones de operación normales y condiciones adversas o transitorias. Este modelo ha sido desarrollado partiendo de dos modelos separados para la turbina de alta presión y para la de baja. Estos modelos para cada turbina se han mejorado y han sido conectados a través de tuberías y componentes adicionales como el separador de vapor y agua o el calentador para obtener un sistema de turbina más realista.

El principal objetivo de este proyecto era simular una turbina de vapor de una central nuclear durante condiciones normales y transitorias. Este objetivo se ha alcanzado y los resultados obtenidos se presentan en el quinto capítulo del proyecto. Tanto las simulaciones bajo condiciones normales como bajo condiciones transitorias presentan resultados muy próximos a los datos reales de la planta, por lo que se considera que el objetivo del proyecto se ha conseguido.

SIMULATION OF A NPP STEAM TURBINE WITH ATHLET SYSTEM CODE

Introduction

The steam turbine component is an important part of the secondary side of a nuclear power plant. Because it has a lower priority in the safety analysis of a plant, the turbine is usually only modeled as either a set of control signals in the system code ATHLET (Analysis of Thermal-hydraulics of Leaks ant Transients) or a turbine valve in TRACE. That means that the influence of the turbine system on the primary side cannot be taken into consideration.

The thermal-hydraulic computer code ATHLET has been mainly applied for the analysis of the primary loop of a NPP. However, the simulation of the steam turbine, where the thermal energy produced by the primary loop is converted into mechanical energy and further in the generator into electricity, has been considered interesting, since a good simulation of the secondary loop provides a more realistic view of the behavior of a NPP at different operation states and during transients. For this reason, ATHLET has been used in this work to simulate the steam turbine part of the NPP.

The purpose of this Master's Thesis is to model a steam turbine and its adjacent components with the help of the German system code ATHLET, developed by GRS (Geschellschaft für Anlagen- und Nukleartechnik mbH). The considered turbine exists,

and it is used in the secondary loop of a typical German Pressurized Water Reactor (PWR).

The system modeled consists of a high-pressure turbine, a steam-water separator, an over-heater, a low-pressure turbine and a condenser.

Methodology

The final goal of this Master's Thesis was to simulate transient conditions for this modeled steam turbine system. In order to simulate transients, the simulation of the system at nominal operational conditions was required first. Therefore, the work has been divided into two parts:

1. The steady state simulation of the HP and LP turbines and connected systems

2. The simulation of transients for the modeled system

Two different turbines have been modeled using the available design data because the transient measurements data of the new turbine was not available at the beginning of work. For this reason the model of an older turbine was developed first. Finally, when the data for transient's simulations was available, the model was adapted to the new turbine by inserting some modifications.

The system has been modeled using design and measurement data from a typical German PWR of Convoy type. The plant data used during the modeling and simulation process included system power, enthalpies, pressures, temperatures and mass flows of the inlet and outlet of main components. Since the real data of the plant is confidential, all the values included here are normalized. The values that have been taken as the reference for the normalization are those at the inlet of the high-pressure new turbine under normal operation conditions.

The steam turbine system consists of two main parts: the high-pressure turbine and the low-pressure turbine. Since the steam that comes from the steam generator is at high pressure, it is expanded first in the high-pressure turbine, and later in the low-pressure turbine. In order to raise the efficiency of the low- pressure turbine, there are two components in between the two turbines that have been modeled as well: the steam-water separator and the over-heater. The steam is expanded in the low-pressure turbine, and then it flows to the condenser, the last component of the modeled system, where it is condensed.

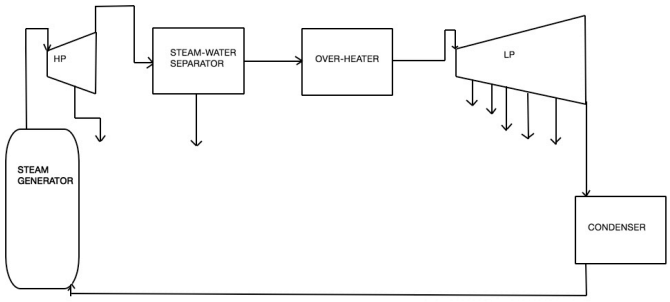

Scheme of the modeled system

The system described before has been modeled in ATHLET by connecting the thermo-

fluid dynamic objects (TFOs) through their corresponding linkage methods. Special objects have been modeled in order to simulate the turbines, the steam-water separator and the condenser.

The procedure followed in order to run transient simulations has been the following one:

1. Development of the steady state model for the old turbine:
    - Further development and improvement of an existing model for the high-pressure (HP) turbine.
    - Design and development of a steam-water separator, and its connection to the HP turbine.
    - Design and development of an over-heater, and its connection to the separator.
    - Further development and improvement of an existing model for the low-pressure (LP) turbine, and its connection at the end of the over-heater.
    - Design and development of a condenser, and its connection to the LP turbine, setting up a connected system.

2. Introduction of changes for the steady state model of the new turbine:
    - Different fluid conditions at the inlet of the HP turbine.
    - Approximations for mass flows in turbine extractions.

3. Introduction of changes for the simulation of transients:
    - Introduction of control signals for fill and turbine extractions mass flows.
    - Transient mass flow conditions at the inlet of the HP turbine.

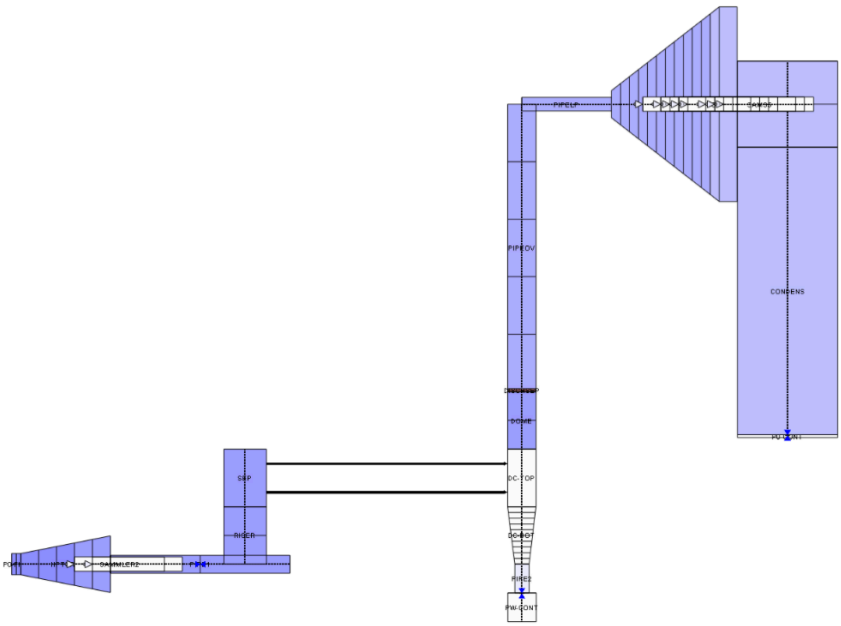

Visualization of the modeled turbine system

Results

The results obtained by the simulations have been compared to the available data of the turbine. In total, the steady state simulation of the old turbine, the steady state simulation of the new turbine, and three different transient simulations have been run. The most interesting results are shown in the following pictures.

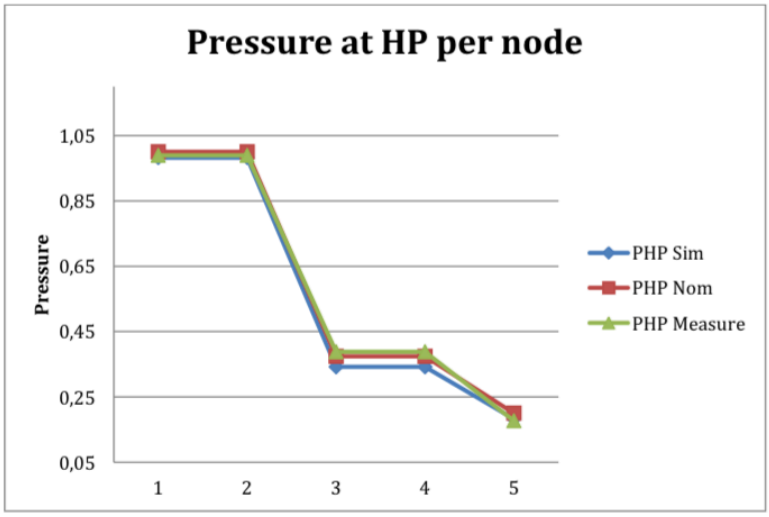

Pressure at the HP turbine per node for the new turbine steady state

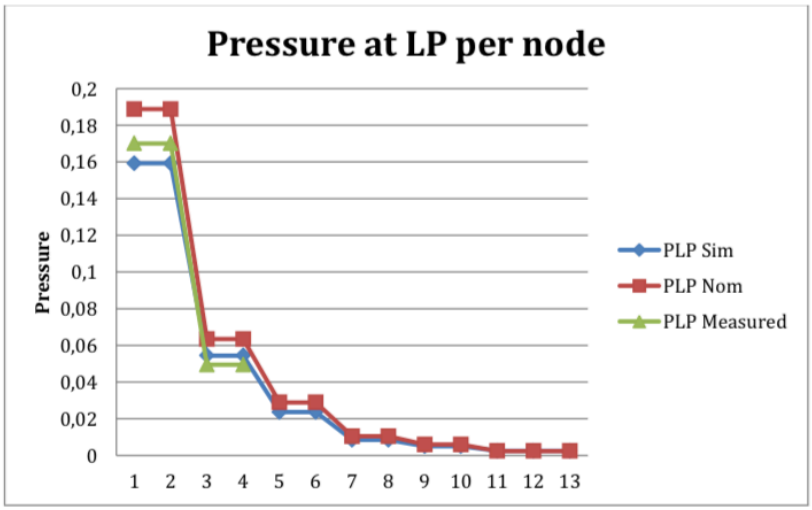

Pressure at the LP turbine per node for the new turbine steady state

The obtained pressure distribution within the turbine (blue) is very close to the nominal pressure distribution (red), as well as to the real measured distribution (green) for both the HP and the LP turbines for the steady state simulation.

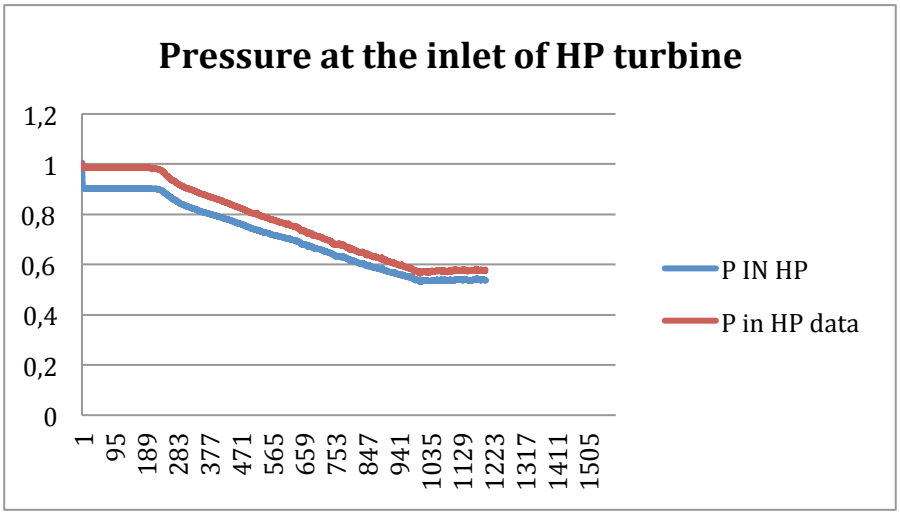

Pressure at the inlet of the HP turbine during the first transient

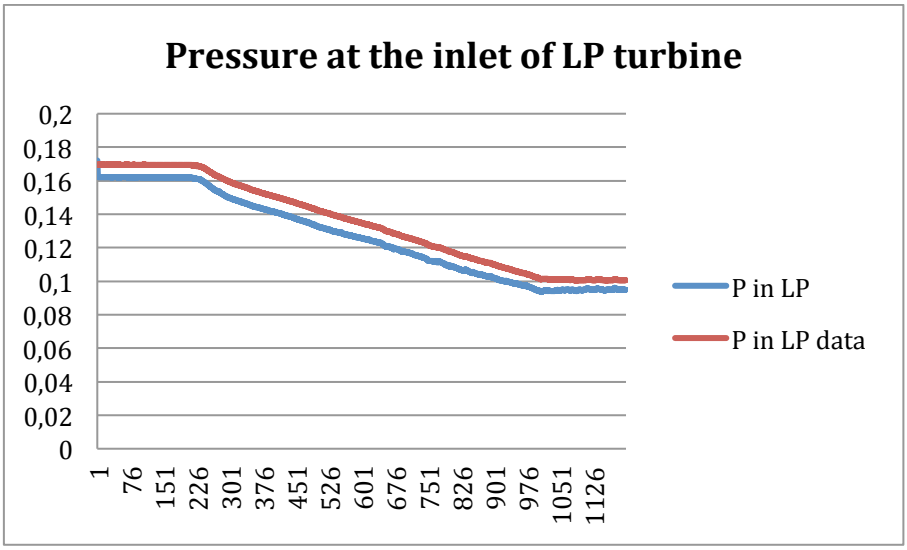

Pressure at the inlet of the LP turbine during the first transient

The obtained pressure at the inlet of the HP turbine (blue) varies over time as the real measured pressure for the transient (red) also changes, and these curves are very close to each other. In addition, the obtained pressure at the LP turbine inlet follows the same pattern as the HP turbine pressure and the real measured pressure in the LP turbine.

Conclusions

The ATHLET model developed in this work is able to describe relatively well the behavior of the steam turbine of a typical German PWR during normal operation as well as load change transients. The model has been designed starting from two separated models for the HP and LP turbines. These turbine models were improved and then connected through several pipes and additional components such as water separator and over-heater in order to obtain a more realistic turbine system.

The main objective of the Master´s Thesis was to simulate the steam turbine of a NPP during normal as well as transient operation. This has been achieved and the results obtained are presented and analyzed in the fifth chapter of the thesis. Both steady state and transient simulations results were close to the real plant measurements; therefore, it is considered that the objective of the Master's Thesis has been successfully reached.



NTech
Lehrstuhl für
Nukleartechnik

Technische Universität München

Master's Thesis

Vega Gómez de la Rosa

Simulation of a NPP steam turbine with ATHLET system code

Betreuer TUM: Prof. Dr. Rafael Macián-Juan
Betreuer: Dipl.-Ing. Dan-Ovidiu Melinte
Ausgegeben: 01.11.14
Abgegeben: 30.04.15

Acknowledgements

This work is part of the Research Project No. 1501441 - “Plant specific dynamic modeling of LWR turbo generator sets by adjustment of general models with measurement data” which has been financed by the German Federal Ministry for Economic Affairs and Energy (BMWi).

I would like to express my deepest gratitude to my supervisors, Dipl.-Ing. Dan-Ovidiu Melinte and Prof. Dr. Rafael Macián-Juán for the guidance provided throughout the course of my work, their constructive criticism, many valuable suggestions and continuous support. Without their help this work would have not been possible. Special thanks have to be given to Mr. Dan-Ovidiu Melinte for his patience, support, understanding and all the possible facilities to help me through the development of this work and the difficult times. To all the members of the Department of Nuclear Engineering, for making my time here very pleasant.

I would also like to thank my family, for all their support and for always encouraging me, as well as for the trust and confidence they placed in me year after year.

To all my friends with whom I have shared my wonderful experience in Munich because they have been by far my best German family, especially the people from Ludwigskolleg. To finish with, I would like to particularly mention my PC-Raum mates, without whom working hard would have never been so funny.

Declaration

I hereby declare that I have made this thesis independently and without the help of others. Ideas and quotes that I have taken over directly or indirectly from other sources are marked as such. This thesis has not been submitted to any inspection authority in the same or similar form and has not been published.

I hereby agree that this thesis can be made available to the public by Lehrstuhl für Nukleartechnik.

Munich, April the 30th, 2015

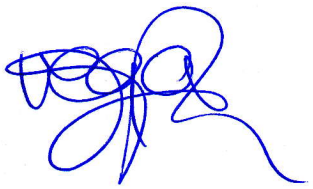

Vega Gómez de la Rosa

TABLE OF CONTENTS

TABLE OF CONTENTS 9
ABSTRACT 13
LIST OF FIGURES 15
LIST OF TABLES 21
LIST OF ACRONYMS 23
1. INTRODUCTION 25
2. THEORETICAL BACKGROUND 27
2.1. Nuclear Power Plant (NPP) 27
2.2. Pressurized Water Reactor (PWR) 28
2.3. Secondary Loop of a PWR 29
2.3.1. Rankine Cycle 30
2.3.2. Steam Turbine 32
2.4. ATHLET 32
2.4.1. Code Structure 33
2.4.2. Fluid Dynamics 34
2.4.3. Heat Conduction and Heat Transfer 35
2.4.4. Simulation of Components 35
2.4.5. Simulation of Control and Balance of Plant 36
2.4.6. The Steady State Calculation 36
3. SYSTEM DESCRIPTION 37
3.1. High-Pressure Turbine 38
3.2. Steam-Water Separator 39
3.3. Over-heater 39
3.4. Low-Pressure Turbine 40
3.5. Condenser 41
4. ATHLET MODEL 43
4.1. Steady State Model 43
4.1.1. Parameters 43
4.1.2. Topology 43
4.1.3. Simulation of Components 44
- FILL 45
- HIGH-PRESSURE TURBINE 46

- STEAM-WATER SEPARATOR 50
- OVER-HEATER 52
- LOW-PRESSURE TURBINE 54
- CONDENSER 55
- DISCHARGE AFTER SEPARATOR 57
- TIME DEPENDENT VOLUMES 57
- CHECK VALVES 58

4.2. Changes introduced for the new turbine steady state model 58

4.2.1. Parameters 58

4.2.2. Extractions 59

4.3. Changes introduced for simulation of transients 59

4.3.1. Tables for the FILL mass flow and enthalpy GCSM signals 59

4.3.2. GCSM signal controlling the mass flows of the turbine extractions 59

4.3.3. GCSM signals controlling the enthalpy of TDV 60

4.3.4. Pressure at the inlet of the high-pressure turbine 60

4.4. Detailed Procedure to model the system 61

4.4.1. Old Turbine Steady State Model 61

4.4.2. New Turbine Steady State Model 61

4.4.3. Transient Model 61

5. RESULTS 65

5.1. Steady State Simulation for the Old Turbine 65

5.2. Steady State Simulation for the New Turbine 75

5.3. First Transient Simulation for the New Turbine 86

5.4. Second Transient Simulation for the New Turbine 94

5.5. Third Transient Simulation for the New Turbine 100

6. CONCLUSIONS 107

7. POSSIBLE FUTURE IMPROVEMENTS OF THE MODEL 109

7.1. High-pressure turbine and low-pressure turbine at the same elevation 109

7.2. Model over-heater as a heat exchanger 109

7.3. Heat source controlled by a signal instead of a constant source for the over-heater 109

8. BIBLIOGRAPHY 111

ANNEXES 113

ABSTRACT

The steam turbine component is an important part of the secondary side of a nuclear power plant. Because it has a lower priority in the safety analysis of a plant, the turbine is usually only modeled as either a set of control signals in the system code ATHLET or a turbine valve in TRACE. That means that the influence of the turbine system on the primary side cannot be taken into consideration.
The purpose of this Master's Thesis is to model a steam turbine and its adjacent components with the help of the German system code ATHLET, developed by GRS. This is a first step towards considering the feedback of the turbine when simulating an entire nuclear power plant; thus, improving the behavior of the model. The considered turbine exists, and it is used in the secondary loop of a typical German Pressurized Water Reactor (PWR).
The model consists of a high-pressure (HP) turbine connected through a piping system with a water separator and an over heater to a low-pressure (LP) turbine which is followed by a condenser.
Steady state and transient simulations using real plant measurements have been run for the HP and LP models separately as well as for the connected model. The results have been compared to the available measurements and have shown good agreement.

LIST OF FIGURES

Figure 1: Chain fission reaction 28
Figure 2: Basic scheme of a pressurized water reactor (PWR) 29
Figure 3: Rankine Cycle 30
Figure 4.1: T-s diagram of an ideal Rankine Cycle 30
Figure 4.2: T-s diagram of a real Rankine Cycle 31
Figure 4.3: Detailed comparison between the isentropic and the real work produced by the fluid within a turbine stage 32
Figure 5: A Standard Pipe TFO 33
Figure 6: TFO Network of a branching 34
Figure 7: Scheme of the modeled system 38
Figure 8: Scheme of the first PC 44
Figure 9: Fill simulation at the left end of a dead end pipe 45
Figure 10: ATHLET discretization of a turbine with two stages 47
Figure 11: ATLAS visualization of the modeled high-pressure turbine 49
Figure 12: TFO arrangement for the simulation of a water-steam separator 50
Figure 13: ATLAS visualization of the temperature gradient in the modeled over-heater 54
Figure 14: ATLAS visualization of the modeled low-pressure turbine 55
Figure 15: ATLAS visualization of the modeled condenser at the exit of the low-pressure turbine 57
Figure 16: ATLAS visualization of the whole modeled system 58
Figure 17: Process followed to model the old turbine's steady state *64*
Figure 18: Process followed to model the new turbine's steady state *65*
Figure 19: Process followed to model the new turbine's transients *65*
Figure 20.1: Mass flow in the high-pressure turbine per node 65
Figure 20.2: Pressure at each node of the high-pressure turbine 66
Figure 20.3: Pressure drop in high-pressure turbine 66
Figure 20.4: Fluid temperature at each high-pressure turbine node 67
Figure 20.5: Pressure at each node of the low-pressure turbine 67
Figure 20.6: Fluid temperature at each node of the low-pressure turbine 68
Figure 20.7: Mass flow at each node of the low-pressure turbine 69

Figure 20.8: Pressure drop in the low-pressure turbine 69
Figure 20.9: Void fraction at the inlet of the separator 70
Figure 20.10: Mass flow at the inlet of the separator 70
Figure 20.11: Mass flow of the separated steam in the separator 71
Figure 20.12: Mass flow of the separated water in the separator 71
Figure 20.13: Pressure at each node of the over-heater 72
Figure 20.14: Fluid temperature at each node of the over-heater 72
Figure 20.15: Enthalpy at each node of the over-heater 73
Figure 20.16: Pressure of the steam at the inlet of the condenser 73
Figure 20.17: Pressures in the condenser 74
Figure 20.18: Steam mass flow at the inlet of the condenser 74
Figure 20.19: Mass flows balance in the condenser 75
Figure 21.1: Mass flow at each node of the high-pressure turbine 76
Figure 21.2: Pressure at each node of the high-pressure turbine 76
Figure 21.3: Pressure drop in high-pressure turbine 77
Figure 21.4: Fluid temperature at each high-pressure turbine node 78
Figure 21.5: Pressure at each node of the low-pressure turbine 78
Figure 21.6: Fluid temperature at each node of the low-pressure turbine 79
Figure 21.7: Mass flow at each node of the low-pressure turbine 79
Figure 21.8: Pressure drop in the low-pressure turbine 80
Figure 21.9: Void fraction at the inlet of the separator 80
Figure 21.10: Mass flow at the inlet of the separator 81
Figure 21.11: Mass flow of the separated steam in the separator 81
Figure 21.12: Mass flow of the separated water in the separator 82
Figure 21.13: Pressure at each node of the over-heater 82
Figure 21.14: Fluid temperature at each node of the over-heater 83
Figure 21.15: Enthalpy at each node of the over-heater 83
Figure 21.16: Pressure of the steam at the inlet of the condenser 84
Figure 21.17: Pressures in the condenser 84
Figure 21.18: Steam mass flow at the inlet of the condenser 85
Figure 21.19: Mass flows balance in the condenser 85
Figure 22.1: Mass flow introduced by the fill (normalized values) during transient .. 86

Figure 22.2: Pressure at the inlet of the high-pressure turbine during transient simulation 87
Figure 22.3: Pressure at the high-pressure turbine extraction during transient simulation 88
Figure 22.4: Steam mass flow extracted in the high-pressure turbine 88
Figure 22.5: Pressure at the outlet of the high-pressure turbine during transient simulation 89
Figure 22.6: Pressure drop in high-pressure turbine comparison for simulation and measurements 89
Figure 22.7: Pressure at the exit of the steam-water separator during transient simulation 90
Figure 22.8: ΔT and ΔH in the over-heater during the first transient simulation 90
Figure 22.9: Pressure in the first extraction of the low-pressure turbine 91
Figure 22.10: Pressure in the second extraction of the low-pressure turbine 91
Figure 22.11: Steam mass flow extracted in the first steam extraction of the low-pressure turbine 92
Figure 22.12: Steam mass flow extracted in the second steam extraction of the low-pressure turbine 92
Figure 22.13: Pressure at the inlet of the condenser during transient simulation 93
Figure 22.14: Pressure in the condenser 93
Figure 23.1: Mass flow introduced by the fill (normalized values) during transient 94
Figure 23.2: Pressure data at the inlet of the High-Pressure Turbine during transient simulation 95
Figure 23.3: Pressure at the extraction of the high-pressure turbine during transient simulation 95
Figure 23.4: Pressure at the outlet of the high-pressure turbine during transient simulation 96
Figure 23.5: Pressure drop within the high-pressure turbine for the measured and the simulated data 96
Figure 23.6: Pressure at the exit of the steam-water separator during transient simulation 97
Figure 23.7: ΔT and ΔH in the over-heater during the second transient simulation 97
Figure 23.8: Pressure in the first extraction of the low-pressure turbine 98

Figure 23.9: Pressure in the second extraction of the low-pressure turbine 98
Figure 23.10: Pressure at the inlet of the condenser during transient simulation 99
Figure 23.11: Pressure in the condenser 99
Figure 24.1: Mass flow introduced by the fill (normalized values) during transient 100
Figure 24.2: Pressure at the inlet of the high-pressure turbine during transient simulation 101
Figure 24.3: *Pressure at the extraction of the high-pressure turbine during transient simulation* 101
Figure 24.4: Pressure at the outlet of the high-pressure turbine during transient simulation 102
Figure 24.5: Pressure drop within the high-pressure turbine for the measured and the simulated data 102
Figure 24.6: pressure at the exit of the steam-water separator during transient simulation 103
Figure 24.7: Pressure in the first extraction of the low-pressure turbine 103
Figure 24.8: pressure in the second extraction of the low-pressure turbine 104
Figure 24.9: Pressure at the inlet of the condenser during transient simulation 104
Figure 24.10: Pressure in the condenser 105
Figure A.2: ΔT in the Over-heater during the old turbine´s steady state model 113
Figure A.3: ΔH in the Over-heater during the old turbine´s steady state 113
Figure A.4: ΔT in the Over-heater during the new turbine´s steady state model 114
Figure A.5: ΔH in the Over-heater during the new turbine´s steady state model 114
Figure A.6: Pressure drop in LP turbine during the first transient simulation 114
Figure A.7: Pressure drop in LP turbine during the second transient simulation 115
Figure A.8: Mass flow at HP steam extraction during the second transient simulation 115
Figure A.9: Mass flow at LP first steam extraction during the second transient simulation 115
Figure A.10: Mass flow at LP second extraction during the second transient simulation 116
Figure A.11: Mass flow at the inlet of the condenser during the second transient simulation 116

Figure A.12: Pressure drop in LP turbine during the third transient simulation 116
Figure A.13: Mass flow at HP steam extraction during the third transient simulation 117
Figure A.14: Mass flow at LP first steam extraction during the third transient simulation 117
Figure A.15: Mass flow at LP second steam extraction during the third transient simulation 117
Figure A.16: Mass flow at the inlet of the condenser during the third transient simulation 118
Figure A.17: ΔT in the over-heater during the third transient simulation 118
Figure A.18: ΔH in the over-heater during the third transient simulation 118

LIST OF TABLES

Table 1: Old High-Pressure Turbine Fluid conditions.....38
Table 2: New High-Pressure Turbine Fluid conditions 38
Table 3: Geometrical data of the High-Pressure Turbine 39
Table 4: Old separator fluid conditions.....39
Table 6: Old Over-heater fluid conditions 40
Table 7: New Over-heater fluid conditions 40
Table 9: New Low-Pressure Turbine fluid conditions.....41
Table 10: Geometrical data for the Low-Pressure Turbine 41
Table 11: Old Condenser fluid conditions.....41
Table 12: New Condenser fluid conditions.....42

LIST OF ACRONYMS

ATHLET	Analysis of Thermal-Hydraulics of Leaks and Transients
CV	Control Volume
EXT	Extraction
GCSM	General Control Simulation Module
GRS	Gesellschaft für Anlagen- und Nukleartechnik mbH.
HCO	Heat Conduction Object
HECU	Heat Transfer and Heat Conduction
HP	High-pressure
In	Inlet
LP	Low-pressure
ML	Mixture Level
Nom	Nominal
NPP	Nuclear Power Plant
Out	Outlet
PC	Priority Chain
PWR	Pressurized Water Reactor
Sim	Simulated
TDV	Time Dependent Volume
TFD	Thermo-fluiddynamics
TFO	Thermo-fluiddynamic Object

1. INTRODUCTION

The thermal-hydraulic computer code ATHLET has been mainly applied for the analysis of the primary loop of a NPP. However, the simulation of the steam turbine, where the thermal energy produced by the primary loop is converted into mechanical energy and further in the generator into electricity, has been considered interesting, since a good simulation of the secondary loop provides a more realistic view of the behavior of a NPP at different operation states and during transients. For this reason, ATHLET has been used in this work to simulate the steam turbine part of the NPP.
The system modeled consists of a high-pressure turbine, a steam-water separator, an over-heater, a low-pressure turbine and a condenser.
The final goal of this Master's Thesis was to simulate transient conditions for this modeled steam turbine system. In order to simulate transients, the simulation of the system at nominal operational conditions was required first. Therefore, the work has been divided into two parts:

1. The steady state simulation of the HP and LP turbines and connected systems
2. The simulation of transients for the modeled system

Two different turbines have been modeled using the available design data because the transient measurements data of the new turbine was not available at the beginning of work. In addition, the older turbine data included design data at different power levels. For this reason the model of the old turbine was developed first. This offered the possibility to compare turbine simulation results for different generator powers. Finally, when the data for transient's simulations was available, the model was adapted to the new turbine by inserting some modifications.

The structure of this Master's Thesis consists of the following parts:

- An introduction to NPP and steam turbine theory, which is necessary to understand the concepts used next.
- A description of ATHLET, its main structure and modules used during the work.
- A description of the real system that has been modeled, including the available data.
- A detailed description of the modelling process for each component, as well as for each type of simulation.
- A comparison and analysis of the obtained results.

- Conclusions.
- Possible improvements of the model for the future.

Every step of the modelling process has been performed within the ATHLET allowed limits, and some assumptions have been taken when the available data was not enough for the model.
Since the simulated turbine exists and its data is confidential, all the data and results included in this Master's Thesis are normalized. The analysis consists of comparisons between the obtained values and the nominal or real measurement data.
Auxiliary tools of ATHLET have been used to represent and post process data, and ATLAS has been used for the visualization of the simulation results.

2. THEORETICAL BACKGROUND

The goal of this Master's Thesis is to model the steam turbine of a nuclear power plant, as well as its main secondary side components, and simulate the system during transient conditions. A brief introduction to NPPs and steam turbines is given next.

2.1. Nuclear Power Plant (NPP)

A nuclear power plant is a thermal power plant, in which the heat source is a nuclear reactor. The heat produced by fission reactions in the nuclear reactor is used to generate steam that drives a steam turbine connected to an electric generator in order to produce electrical power.

"*Nuclear Reactors are machines in which controlled nuclear fission chain reactions can be sustained.*" [1]

The fission reaction takes place when a fissile atom (e.g. ^{235}U) absorbs a neutron, and as a consequence, this atom splits into two new atoms (fission fragments) releasing several additional neutrons and energy (200 MeV per fission). These neutrons can either interact with another atom or not collide with anything (Leakage). In the first case, a neutron can interact with two different kinds of atoms. In this way, if the neutron is absorbed by an atom of ^{238}U or by another absorber, the reaction does not continue (Absorption). On the contrary, if the neutron collides with a fissile atom (e.g. ^{235}U) which then fissions and releases additional neutrons, the reaction continues (Chain Reaction). [2]

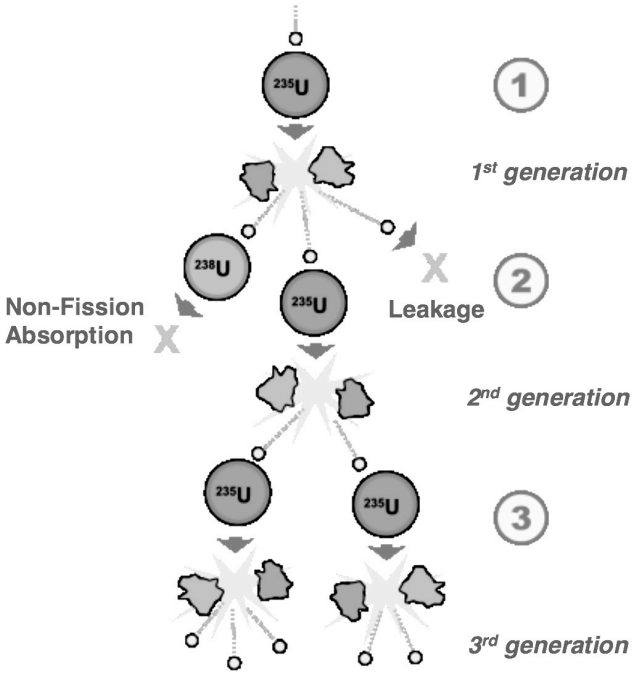

Figure 1: Chain fission reaction

"In general, a nuclear reactor is simply a sufficiently large mass of fissile material for a given shape (e.g., ^{235}U or ^{239}Pu) in which such a controlled fission chain reaction can be sustained." [3].

2.2. Pressurized Water Reactor (PWR)

A pressurized water reactor (PWR) consists of three main cooling loops: The primary loop, which is in contact to the reactor core; the secondary loop, where the steam generators produce the steam; and a Third loop for the condenser. Since the primary and secondary loops are separated, the coolant that contains radioactivity is contained only in the primary loop, and its transfer to the secondary side of the nuclear reactor is avoided.

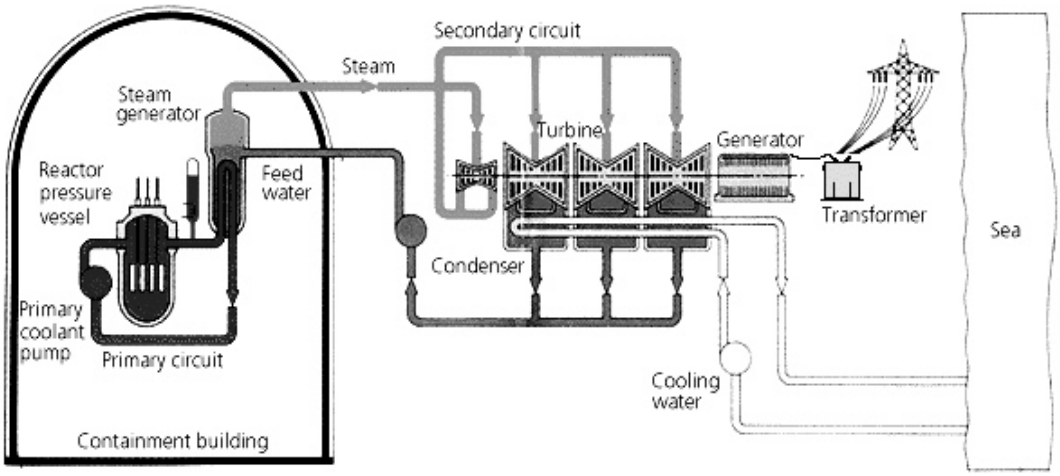

Figure 2: Basic scheme of a pressurized water reactor (PWR)

The primary loop of a PWR consists of a reactor pressure vessel containing the nuclear fuel where the energy from fission is transformed into heat in the coolant-moderator (water). Furthermore, a pressurizer maintains the pressure above the saturation pressure (at around 15 MPa) so that bulk boiling does not occur. In this way, when the pressure in the primary loop decreases, the pressurizer boils water; hence, the pressure increases. On the contrary, when the primary loop pressure increases, it sprays water to compensate the pressure rise. The heated coolant flows through several U-type tubes in the steam generators, where the secondary coolant, or feedwater, flows around the outside of the tubes picking up the heat from the primary coolant. When the feedwater absorbs enough heat, it starts to boil and form steam. After transferring the heat, the cold primary coolant is pumped back to the reactor core so that the process continues. [4]

2.3. Secondary Loop of a PWR

The secondary loop of a PWR is maintained at a lower pressure (7 MPa); hence, the coolant in the steam generators evaporates, and the steam/water mixture passes through multiple stages of moisture separation. The content of water of the steam must be maintained as low as possible in order to prevent damage for the turbine. This dry steam flows to the steam turbine in order to convert thermal energy into mechanical energy; therefore, into electrical energy. At the exit of the steam turbine the steam condensates and is redirected to the steam generator. [5]
The saturated steam produced in the steam generators is expanded in the high-pressure turbine, where both the pressure and the quality are reduced, and after that it is sent to a steam-water separator that increases the steam quality, followed by an over-heater that raises its temperature, in order to improve the efficiency of

the low-pressure turbine. After the low-pressure turbine, the steam is condensed and sent again to the steam generator.

2.3.1. Rankine Cycle

The performance of a steam turbine is described by the Rankine cycle, which is a heat engine with a vapor power cycle. The common fluid working is water, and it follows a closed circuit because the water is evaporated at high pressure and condensed at low pressure; hence, it is reused.

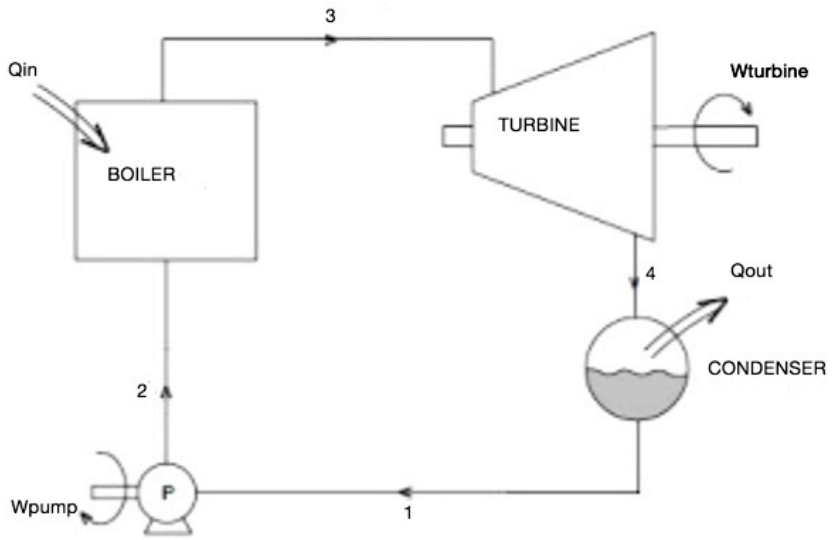

Figure 3: Rankine Cycle

This ideal cycle consists of four reversible processes as shown in the next T-s diagram: [6]

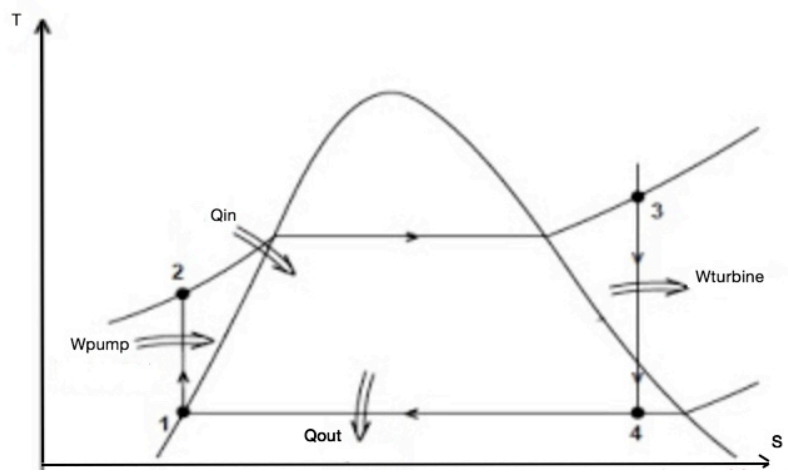

Figure 4.1: T-s diagram of an ideal Rankine Cycle

- 1-2: Isentropic compression (Pump): The saturated liquid from the condenser is compressed until the operating pressure of the boiler (steam generator). External work is done on the working fluid by means of pumping operation (W_{pump}).
- 2-3: Isobaric heat supplying (Boiler or Steam generator): The saturated liquid enters the steam generator and absorbs heat at constant pressure, leaving it as superheated steam (Q_{in}).
- 3-4: Isentropic expansion (Steam Turbine): The superheated steam is expanded in the turbine generating work ($W_{turbine}$). The fluid leaves the turbine at a lower pressure and enthalpy, but with the same entropy.
- 4-1: Isobaric heat rejection (Condenser): The steam is condensed at constant pressure (Q_{out}).

The efficiency of the cycle is defined as the ratio of the net power generated by the cycle and the thermal power used for heating the flow:

$$\eta = \frac{W_{turbine} - W_{pump}}{Q_{in}} \qquad \textit{(Equation 1)}$$

Due to mechanical friction and other pressure losses, this cycle is not reversible in practice. The processes 1-2 and 3-4 are not isentropic, and the real T-s Diagram takes this shape:

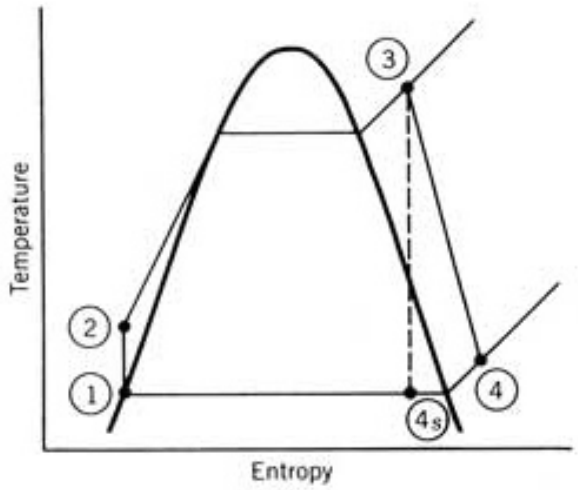

Figure 4.2: T-s diagram of a real Rankine Cycle

The point 4s corresponds to the isentropic expansion, and the point 4 corresponds to the irreversible one. [6]

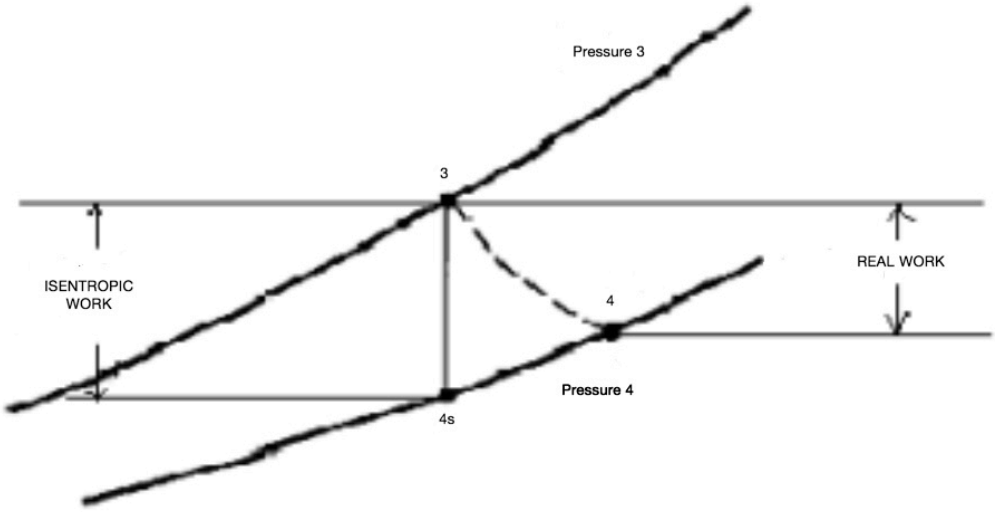

Figure 4.3: Detailed comparison between the isentropic and the real work produced by the fluid within a turbine stage

As shown in these figures 4.2 and 4.3, the power generated by the steam turbine is lower than the ideal one; hence, the efficiency of the irreversible Rankine cycle is also lower.

2.3.2. Steam Turbine

A steam turbine consists of a set of blades attached to a rotor that capture the energy of the steam and convert it into rotational energy by spinning the rotor round when the steam hits them. The expansion of the steam takes place through the blades, which can be fixed or moving. In practice, steam turbines have not a single set of blades on the rotor, but a number of different sets, each one extracting a little bit more energy from the steam. Each set of blades is called a stage. This multi-stage approach invented by Charles-Parsons means that instead of having a just one high pressure drop through the turbine, each stage is reducing the pressure of the steam by only a relatively small amount, which reduces the forces on the blades and improves the turbine overall's power output. [8]
The T-s diagram of a turbine is shown in Figure 4.3.

2.4. ATHLET

The thermal-hydraulic computer code ATHLET (Analysis of THermal-hydraulics of LEaks and Transients) is being developed by the Gesellschaft fur Anlagen- und Reaktorsicherheit (GRS) for the analysis of anticipated and abnormal plant transients and all kinds of leaks and breaks first and foremost in light water reactors. [8]

The aim of the code development is to cover the whole spectrum of design basis and beyond design basis accidents (without core degradation) for PWRs and BWRs with only one code. The main code features are:

- Advanced thermal-hydraulics
- Modular code architecture
- Separation between physical models and numerical methods
- Pre- and post-processing tools
- Portability

2.4.1. Code Structure

The ATHLET structure is highly modular so it allows an easy implementation of different physical models. The code is composed of several basic modules for the calculation of the different phenomena involved in the operation of a light water reactor: [8]

- Thermo-fluiddynamics (TFD)
- Heat Transfer and Heat Conduction (HECU)
- Neutron Kinetics (NEUKIN)
- General Control Simulation Module (GCSM)

ATHLET provides a modular network approach for the representation of a thermal-hydraulic system. A given system configuration can be simulated just by connecting basic fluid dynamic elements, called thermo-fluid dynamic objects (TFOs). There are several TFO types, each of them applying for a certain fluid dynamic model. All object types are classified into three basic categories:

- **The Pipe Object:** A pipe is a one-dimensional component for the simulation of one-dimensional fluid flow; hence, with full conservation of the momentum flux. The nodalization (number of nodes or volumes) is defined by input data. After nodalization, a pipe-object can be taken as a number of consecutive volumes (control volumes) connected by flow paths (junctions). A special application of a pipe object, called single junction pipe, consists of only one junction, without any control volumes.

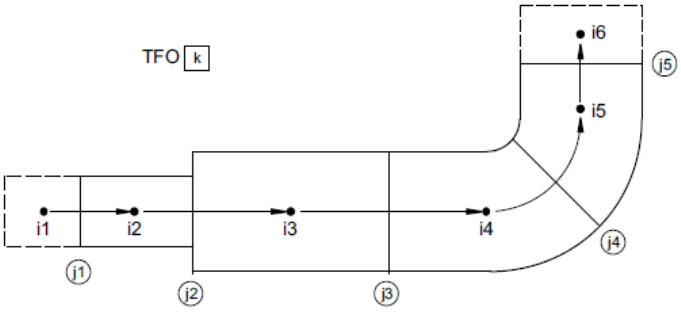

Figure 5: A Standard Pipe TFO

The different junctions of the pipe simulate junction-related components, such as pumps, valves, breaks, discharges and fills.

- **Branch Object:** A branch simply decomposes into a CV with the same features like a standard CV of a pipe object.

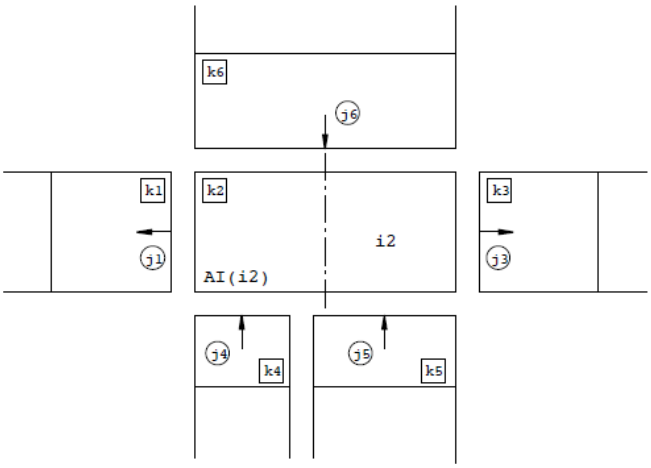

Figure 6: TFO Network of a branching

Within the branch neither a dominant flow direction nor friction losses are considered.

- **Special Objects:** used for components with complex geometry (e.g. the cross connection of pipes within a multi-channel representation).

This object structure has been developed in order to allow the coupling of models of different physical formulation and spatial discretization techniques.

2.4.2. Fluid Dynamics

ATHLET offers the possibility of choosing between different models for the simulation of fluid dynamics: [8]

- 5-equation model, with separate conservation equations for liquid and vapor mass and energy, and a mixture momentum equation. It accounts for thermal and mechanical non-equilibrium and includes a mixture level tracking capability,
- Two-fluid model, with separate conservation equations for liquid and vapor mass, energy, and momentum (without mixture level tracking capability).

The spatial discretization is performed on the basis of a finite-volume approach. The mass and energy equations are solved within control volumes, and the momentum equations are solved over flow paths (junctions) connecting the centers of the control volumes. The solution variables are the pressure, vapor temperature, liquid temperature and mass quality within a control volume, as well as the mass flow rate (5-eq. model) or the phase mass velocities (6-eq. model) in a junction, respectively.

Two types of control volumes are available. Within the so-called "ordinary" control volume, a homogeneous mass and energy distribution is assumed. Within the "non-homogeneous" control volume, a mixture level is modelled. Above the mixture level, steam with water droplets, below the mixture level, liquid with vapor bubbles may exist. The combination of ordinary and nonhomogeneous control volumes provides the option to simulate the motion of a mixture level through vertical components.
A full-range drift-flux model is available for the calculation of the relative velocity between the fluid phases. The model comprises all flow patterns from homogeneous to separated flow occurring in vertical and horizontal two-phase flow. It also takes into account countercurrent flow limitations in different geometries.

2.4.3. Heat Conduction and Heat Transfer

The simulation of the heat conduction in structures, fuel rods, and electrical heaters is performed within the basic module HECU. It permits the user to assign heat conduction objects (HCOs) to all thermal-fluid dynamic objects of a given network. [8]
The one-dimensional heat conductor module HECU provides the simulation of the temperature profile and the energy transport in solid materials. The model has the following characteristics:

- The geometry of a HCO is constant in time.
- The model can simulate the one-dimensional temperature profile and heat conduction in plates normal to the surface, as well as in hollow or full cylinders and spheres in the radial direction.
- In each HCO, up to three material zones can be modelled.
- The HCOs can be coupled on left and/or right side to TFOs by consideration of the energy transport between heat conductor surface and the surrounding fluid. It is also possible to simulate a fluid temperature as boundary condition for the HCO by means of GCSM signals.
- Heat generation can be considered in material zones. The specific heat generation rate per volume unit is assumed to be distributed uniformly either within a material zone or a material layer.

2.4.4. Simulation of Components

In general, major plant components (e.g. pressurizer, steam generators) can be modelled by connecting thermo-fluid dynamic objects (TFOs) and heat conduction

objects (HCOs) via input data. Simplified compact models for those components are also available as special objects. [8]
Additional models are provided for the simulation of valves, pumps, accumulators, steam separators, steam and gas turbines, steam condensers, single and double ended breaks, fills, leaks, and boundary conditions for pressure and enthalpy. Except for the separator model, they are comparable to the corresponding models in other advanced codes. The steam separator model is an empirical approach for the calculation of carry-over and carry-under flows by means of input functions of the inlet mass flow rates, of the void fraction in the separator region, and of the mixture level outside the separator.

2.4.5. Simulation of Control and Balance of Plant

The module GCSM (General Control Simulation Module) allows the user to model control circuits just by connecting basic functional blocks (e.g. switch, adder and integrator). Most of the system variables calculated within the fluid dynamics module (process variables) can be selected as input to these functional blocks. The output of such control blocks can be fed back to the thermo-fluid dynamics in form of boundary conditions (e.g. temperature, heat and mass sources). [8]

2.4.6. The Steady State Calculation

In general, the simulation system shall be initialized with steady state conditions.
That is, energy, mass, and momentum in all parts of the system are well-balanced, and the time derivatives of the solution variables are close to zero. In any case, residual imbalances have to be small enough not to dominate the transient that follows. In addition, the particular state at the beginning of the transient has to be represented by the simulation system, e.g. nominal operational condition of a reactor plant.
The SSC calculates the steady state of the system by means of direct algebraic solutions combined with nested iterative procedures. All independent modules (TFD, HECU, GCSM, etc.) are involved whereas the TFD module plays the leading part. [8]

3. SYSTEM DESCRIPTION

The system has been modeled using design and measurement data from a typical German PWR of Convoy type. The plant data used during the modeling and simulation process included system power, enthalpies, pressures, temperatures and mass flows of the inlet and outlet of main components. However, not enough geometrical data was available and some simplifications, approaches and assumptions were necessary.

Since the real data of the plant is confidential, all the values included here are normalized. The values that have been taken as the reference for the normalization are those at the inlet of the high-pressure new turbine under normal operation conditions. Therefore, the values at every point have been divided by their reference value for each fluid property.

Two different sets of data were used for modeling the system. One, corresponding to an older turbine from the plant, includes design data at different power levels. In contrast to that, the available data set for the newer turbine only includes design data at 100% power, but measurements during several transients have been received from the power plant later during the work.

The steam turbine system consists of two main parts: the high-pressure turbine and the low-pressure turbine. Since the steam that comes from the steam generator is at high pressure, it is expanded first in the high-pressure turbine, and later in the low-pressure turbine. In order to raise the efficiency of the low-pressure turbine, there are two components in between the two turbines that have been modeled as well: the steam-water separator and the over-heater. The steam is expanded in the low-pressure turbine, and then it flows to the condenser, the last component of the modeled system, where it is condensed. The system has been modeled in order to simulate the steady state for the older and the newer turbine, and later it has been adapted to simulate some transients during the operation of the newer turbine.

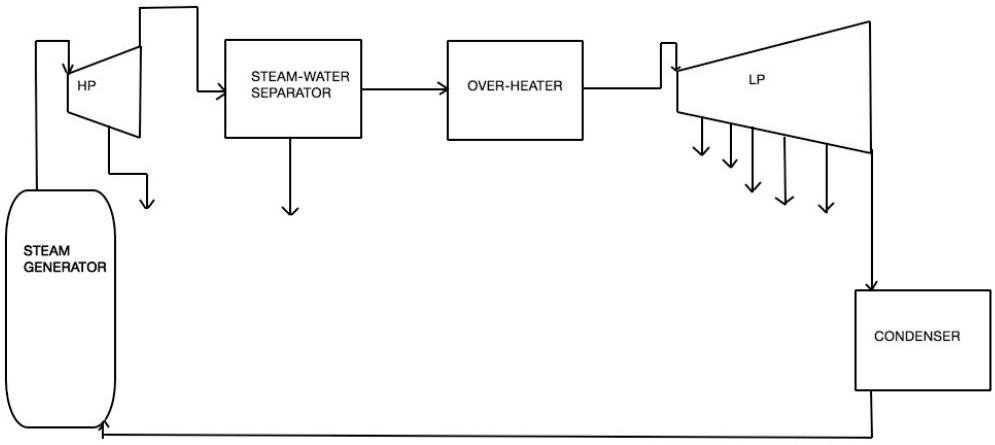

Figure 7: Scheme of the modeled system

3.1. High-Pressure Turbine

The double flux high-pressure turbine is simulated as a single turbine component in order to simplify the model.
The high-pressure turbine consists of two stages and both a steam and a water extraction.
The steam conditions for the high-pressure turbine are known at the inlet, the extractions and the outlet.

Old HP-T	P	T	G	H	Quality
Inlet	0,99516129	0,98844128	0,9635767	1,00064888	0,9953
Steam Extraction	0,37580645	0,78495229	0,08165952	0,94718818	0,907
Water Extraction	0,37580645	0,78495229	0,00096781	0,3407354	0,000239
Outlet	0,18064516	0,65881833	0,8819097	0,91144557	0,873

Table 1: Old High-Pressure Turbine Fluid conditions

New HP-T	P	T	G	H	Quality
Inlet	1	0,99876868	1	1	0,9953
Steam Extraction	0,37419355	0,78295374	0,08254261	0,94718818	0,907
Water Extraction	0,37419355	0,78295374	0,00097827	0,3407354	0,000239
Outlet	0,2	0,67419929	0,91493073	0,91452776	0,873

Table 2: New High-Pressure Turbine Fluid conditions

The available geometrical data corresponding to the high-pressure turbine is the mean diameters and blade heights at its inlet and outlet, which have also been normalized taking as the reference the value of the dimensions at the inlet.

HP-Turbine	Mean Diameter	Blade Height
Inlet	1	1
Outlet	1,11650485	2,619047619

Table 3: Geometrical data of the High-Pressure Turbine

3.2. Steam-Water Separator

The steam-water separator is modeled taking into account the steam properties at the exit of the high-pressure turbine, the target steam properties before being heated up in the over-heater, and the properties of the water after being separated. In fact, the goal of the steam-water separator is to increase the quality of the steam by removing as much condensed water as possible because the turbine's efficiency would be reduced by the liquid and the droplets could erode the turbine blades.

Old Separator	P	T	G	H	Quality
Inlet	0,18064516	0,65881833	0,87993621	0,91144557	0,873
Steam Outlet	0,18064516	0,65881833	0,7723323	0,99866619	0,873
Water Outlet	0,18064516	0,65881833	0,1076074	0,28287671	0

Table 4: Old separator fluid conditions

New Separator	P	T	G	H	Quality
Inlet	0,2	0,67419929	0,91493073	0,91452776	0,88
Steam Outlet	0,2	0,78295374	0,80449517	1,04006784	1
Water Outlet	0,19516129	0,67081851	0,11043556	0,28864456	0,000267

Table 5: New separator fluid condition

3.3. Over-heater

The over-heater is a heat exchanger whose purpose is to increase the temperature and enthalpy of the steam at a constant pressure, in order to reach super-heated steam conditions; hence, to increase the efficiency in the low-pressure turbine. The heat necessary to obtain such conditions comes from a part of the steam provided by the steam generators that does not enter the high-pressure turbine, but is directed to the over-heater.

The steam conditions for both the inlet and the outlet of the over-heater are known; thus, it is modeled as a pipe with heat conduction, where a large heat transfer surface is required.

Over-heater	P	T	G	H	Quality
Inlet	0,18064516	0,65881833	0,71484152	0,99866619	0,873
Outlet	0,17580645	0,83483578	0,71464667	1,04682769	1

Table 6: Old Over-heater fluid conditions

Over-heater	P	T	G	H	Quality
Inlet	0,2	0,78295374	0,73352935	1,04006489	1
Outlet	0,188709677	0,93487544	0,73352935	1,06896179	1

Table 7: New Over-heater fluid conditions

3.4. Low-Pressure Turbine

The low-pressure turbine consists actually of three double flux low-pressure turbines. However, as already mentioned, the whole model considers the half of the mass flow; thus, these three turbines have been brought together to one single flux low-pressure turbine. In addition, the turbine consists of six stages, each one with its water and/or steam extractions, but due to the fact that the last stage pressure is below the ATHLET pressure limits, just five stages have been modeled, including four steam extractions and four water extractions.

Moreover, the available data of the turbine differs a little bit for the new turbine in contrast to the old one; therefore, some approximations and simplifications have been taken into account in the simulation. For instance, the data for the extractions in the new turbine is given for the mixture of steam and water extracted without specifying the mass flows for each phase. These mass flows have been determined with the same percentage as given in the available data for the old turbine.

The data known for both the old turbine and the new one is shown in tables 8 and 9.

Old LP-T	P	T	G	H	Quality
Inlet	0,175806452	0,83483578	0,71484152	1,04682769	1
Steam Extraction 1	0,070483871	0,5369601	0,03083375	0,99152848	1
Steam Extraction 2	0,031451613	0,5369601	0,04122247	0,94697188	1
Water Extraction 2	0,031451613	0,42543488	0,00011512	0,18071377	0
Steam Extraction 3	0,010612903	0,42543488	0,03644772	0,89452055	1
Water Extraction 3	0,010612903	0,31462228	0,0086674	0,13334535	0
Water Extraction 4	0,005935484	0,26331355	0,00866341	0,11146359	0
Steam Extraction 5	0,002548387	0,19632715	0,02160969	0,85555155	1
Water Extraction 5	0,002548387	0,19632715	0,01178361	0,08312906	0
Outlet	0,000709677	0,10903105	0,40246611	0,83168709	0,897

Table 8: Old Low-Pressure Turbine fluid conditions

New LP-T	P	T	G	H	Quality
Inlet	0,188709677	0,934875445	0,73352935	1,06896179	1
Steam Extraction 1	0,063387097	0,59252669	0,02905412	1,0057318	1
Steam Extraction 2	0,028870968	0,41544484	0,04298714	0,97375631	1
Water Extraction 2	0,028870968	0,41544484	0,00011961	0,17660418	0
Steam Extraction 3	0,010483871	0,326512456	0,03744244	0,95753425	1
Water Extraction 3	0,010483871	0,326512456	0,00890362	0,13284066	0
Water Extraction 4	0,005935484	0,262846975	0,00866341	0,11146359	0
Steam Extraction 5	0,002419355	0,192064057	0,02583176	0,93666186	1
Water Extraction 5	0,002419355	0,192064057	0,01408352	0,08143475	0
Outlet	0,000967742	0,128683274	0,57530151	0,82591925	0,89

Table 9: New Low-Pressure Turbine fluid conditions

In addition, the available geometrical data of the Low-Pressure turbine has been normalized with reference to the inlet dimensions of the high-pressure turbine, as Table 10 shows.

LP-Turbine	Mean Diameter	Blade Height
Inlet	1,70645346	0,6031746
Outlet	2,42752713	10,623809

Table 10: Geometrical data for the Low-Pressure Turbine

3.5. Condenser

The condenser is the component where the heat of the steam that comes from the low-pressure turbine is extracted and the steam is condensed. It requires a large heat transfer surface and it is connected to the last stage of the low-pressure turbine.

The model of the condenser consists of two pipes, one responsible of containing the steam from the turbine before it condensates, in order to prevent the steam from going to the feed water circuit, and another one where the heat is extracted and the steam condensates.

The steam properties at the inlet of the condenser are known, and the same as at the outlet of the last stage of the low-pressure turbine. The water properties at the exit of the condenser are also available; therefore, the heat extracted can be calculated.

Condenser	P	T	G	H	Quality
Inlet	0,00070968	0,12898444	0,55638443	0,83168709	0,897
Outlet	0,00070968	0,12898444	0,55638443	0,04697188	0

Table 11: Old Condenser fluid conditions

Condenser	P	T	G	H	Quality
Inlet	0,00096774	0,12882562	0,5753	0,82591925	0,89
Outlet	0,00096774	0,12882562	0,5753	0,054578226	0

Table 12: New Condenser fluid conditions

4. ATHLET MODEL

The system described before has been modeled in ATHLET by connecting the thermo-fluid dynamic objects (TFOs) through their corresponding linkage methods. Special objects have been modeled in order to simulate the turbines, the steam-water separator and the condenser. The system has been modeled first for the older turbine steady state. Next some changes have been implemented to model the newer turbine steady state. The last set of modifications were the adaptations for the simulation of transients.

4.1. Steady State Model

The steady state model of the older and the newer turbine is almost the same, with several differences at the initial fluid conditions. The model has been set first for normal operational conditions of the older turbine at 100% power.

4.1.1. Parameters

First of all, the constant values or properties that are used for each component of the system are defined as Parameters, so that they can be called at any point by the code and be easily modified by the user just by changing the value assigned to the corresponding parameter. For instance, some parameters are the pressure, temperature, enthalpy and mass flow at the inlet of the new high-pressure turbine (normalized values):

PRESS1 = 1.0
TEMP1 = 1.0
H1 = 1.0
G1 = 1.0

In this way, wherever a parameter is called by %PRESS1%, the value associated to it is being used.
Furthermore, the definition of the parameter IARTO = 1, implies that the 5-equation model (with separate conservation equations for liquid and vapor mass and energy, and a mixture momentum equation) is applied when this parameter is called as %IARTO%. Actually, it has been used for every modeled component.

4.1.2. Topology

This block of data allows the user to define all the thermo-fluid dynamic objects (TFOs) and their interconnections, as well as the priority chains that define the

processing sequence during the steady state calculation. The first PC comprises generally the dominant path through the first fluid dynamic system and should represent a closed loop. All further PCs of that fluid dynamic system will start in a TFO which is part of a former PC.

Therefore, the first PC of the model is the formed by a fill that introduces the desired mass flow at the corresponding inlet pressure followed by the high-pressure turbine, the steam path of the steam-water separator, the over-heater, the low-pressure turbine and the condenser, ending in a time dependent volume (TDV) where a pressure and enthalpy boundary is set.

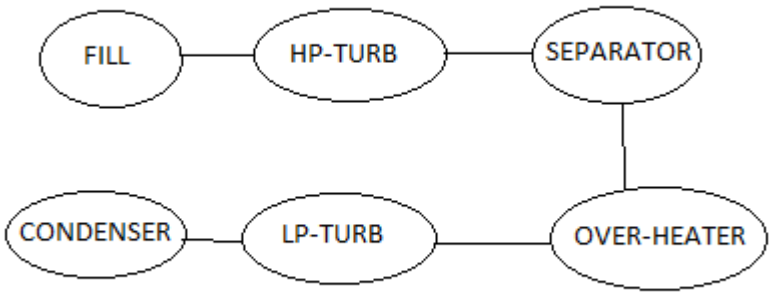

Figure 8: Scheme of the first PC

The second PC modeled is the water path of the steam-water separator, which consists of several pipes that drive the water to a TDV component.
An additional PC models a steam discharge after the steam-water separator.
All further PCs correspond to the steam and water extractions of both the high and the low-pressure turbines. These PC consist of a pipe with a TDV.

4.1.3. Simulation of Components

The OBJECT input section describes all TFOs appearing within the TOPOLOGY data concerning geometry, model options, or thermal-hydraulic initial and boundary conditions. Whereas the most important objects used in the simulation are explained here in detail, some pipes used as the connection between them are not considered. Furthermore, special component models are necessary for the simulation of some components such as the turbines or the separator.
The description of each TFO within the OBJECT input data requires at least the following input data sections:

- Name and type of TFO distinguishing between pipes with and without internal connections, branches, single junction pipes or cross connection objects and type of reactor component.

- Geometry of the TFO including for each length coordinate, the elevation and hydraulic diameter.
- Friction model, considering both friction loss models and form losses at certain lengths coordinates.
- Drift flux and interfacial shear model data, pointing out for each length coordinate the type of junction concerning flow model according to the geometry data (horizontal, vertical or inclined flow, with or without relative velocity).
- Initial Thermal-Hydraulic states of the TFO including initial pressure, temperature, mass flow, heat addition per unit length and an initial condition describing the phase of the flow.

Other input data is necessary to be input for special objects, such as the mixture level for the steam-water separator and the condenser or the junction type data for the simulation of fills, discharges or valves.

- **FILL**

The fill component is a junction related model. It consists of a pipe that simulates mass and related energy sources and sinks for liquid, vapor or mixture. Since it always has to be directed towards the thermo-fluid dynamic system, it is only allowed in the left-most junction of the pipe.

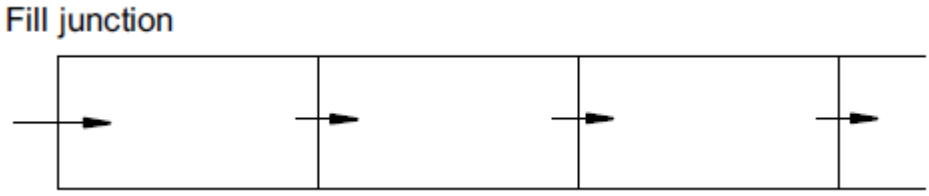

Figure 9: Fill simulation at the left end of a dead end pipe

The fill has been defined as an initialization pipe TFO without internal connection to other pipes, and as a standard pipe component regarding the type of component. Regarding the junction type data, the fill has been modeled by defining JTYPO=6 at the left-most length coordinate of the TFO.
The geometry input data of this pipe requires the hydraulic diameter of the pipe, which is the same as the inlet of the high-pressure turbine and its calculation is explained within the turbine geometry data. Its elevation is the same as for the high-pressure turbine.
The friction loss in this pipe is modeled according to the Martinelli-Nelson two phase friction loss model with constant Darcy-Weissbach friction factor, which value is defined as a parameter and used for the model of the whole system. [9] However, form losses have been neglected in order to decrease as much as possible the pressure drop due to them.

The chosen drift model for the simulation of the fill is the one recommended for horizontal flow paths without relative velocity, since the mass flow at the inlet of the high-pressure turbine is saturated steam.
As initial conditions, the pressure, temperature and mass flow at the inlet of the high-pressure turbine have been input, as well as the condition of single phase vapor or two phase flow with vapor dominant equation system (liquid saturated, high quality). This initial condition of mass flow is kept constant during the steady state simulation. However, during the simulation of transients it is controlled by a GCSM signal, which should initially match the steady state value.
Since this fill simulates a mass and enthalpy source, the mass flow must have a positive sign, and the total specific enthalpy is specified via a GCSM signal (FUNGEN) that takes the values from a table containing the enthalpy values as a function of the simulation time.

- **HIGH-PRESSURE TURBINE**

For the simulation of a steam turbine, a special pipe object type is used. Inside this turbine pipe two turbine stages are defined, and in between these two stages both a steam extraction of the working fluid and a water extraction are simulated.
The turbine stage simulation model is a junction related model, and a turbine junction can be located at every place within the turbine pipe taking into account that there must be at least two control volumes, where the extractions are located, in between two turbine junctions.

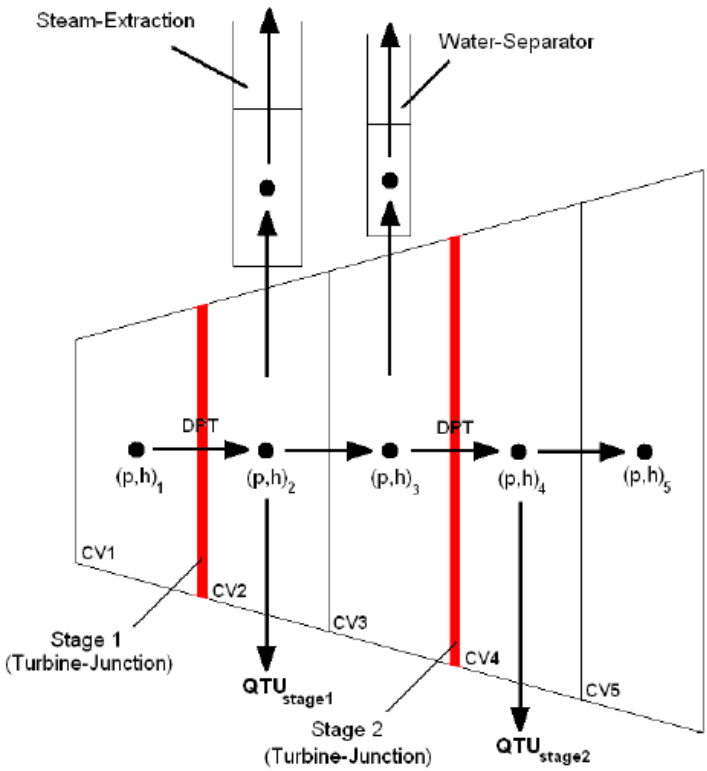

Figure 10: ATHLET discretization of a turbine with two stages

In this way, the complete model of a steam turbine consists of the definition of a special pipe object type within the OBJECT input data (HPTURB), the definition of the desired stages and extractions, and an additional input block that describes the conditions for nominal operation of every stage of the turbine.

- HPTURB OBJECT

The special pipe object type TURBINE is defined by inputting ICMPO=9, and it is divided into five control volumes so that at least two control volumes are defined in between the two stages as required. The turbine itself is implemented in the turbine stage junctions, which are defined in the third and fifth control volumes with the junction type JTYPO=7.

The available geometrical data was the mean diameter of the turbine, and it has been used in order to determine the hydraulic diameter required by the geometry data section of ATHLET, by using the following equations:

$$D_{rotor} = D_{mean} - H_{blade} \qquad \textit{(Equation 2)}$$

$$A_{flow} = A_{total} - A_{rotor} \qquad \textit{(Equation 3)}$$

$$A_{total} = \pi \cdot \left(\frac{D_{rotor} + 2 \cdot H_{blade}}{2}\right)^2 \qquad \textit{(Equation 4)}$$

$$A_{rotor} = \pi \cdot \left(\frac{D_{rotor}}{2}\right)^2 \qquad \textit{(Equation 5)}$$

$$D_{hydraulic} = 2 \cdot \sqrt{\frac{A_{flow}}{\pi}} \qquad \textit{(Equation 6)}$$

Another important restriction to consider when designing the turbine geometry is the limit of the fluid velocity by the speed of sound.
The speed of sound is given by the Newton-Laplace equation

$$v_{fluid} < c = \sqrt{\frac{K}{\rho}} \qquad \textit{(Equation 7)}$$

,where K is the modulus of bulk elasticity for gases and ρ the density of the fluid.
The friction loss model used for the turbine is the same as the one explained above for the fill, as well as the drift flux model, because the conditions of the fluid are the same. Moreover, the initial conditions of the fluid in the turbine are set to the conditions at the inlet.

- STEADY STATE TURBINE BLOCK

One turbo generating set consisting of one generator and several turbines connected to the generator shaft is simulated; therefore, all the turbines have the same shaft speed. The turbine speed at design point is the standard 1500 rpm for NPP steam turbines.
In addition, every turbine stage requires input data such as the pressures at the stage entrance and exit, the mass flow, the enthalpy at the entrance, the efficiency of the stage and the stage power under design point operation,
Whereas the pressures, mass flow and enthalpy are available data, the stage efficiency and power are determined. As work is extracted from the turbine, the pressure drops according to the Stodola's cone law, where the subscripts *a, b* and *0* mean *entrance*, *exit* and *design point value* respectively. [9]

$$\Delta p_{stage} = p_a - \sqrt{{p_a}^2 - p_a \frac{p_{a0}\left(1-\left(\frac{p_{b0}}{p_{a0}}\right)^2\right)}{\left(\frac{\dot{m}_0}{\dot{m}_0}\right)^2 \frac{\rho_{a0}}{\rho_a}}} \qquad \textit{(Equation 8)}$$

The power of a turbine stage is calculated from its pressure drop Δp_{stage}

$$Q_{stage} = \eta \cdot \dot{m} \cdot \frac{\Delta p_{stage}}{\tilde{\rho}_{stage}} \qquad \textit{(Equation 9)}$$

The stage density $\tilde{\rho}_{stage}$ is calculated as a weighted mean of the densities in front and behind the turbine stage, and the stage efficiency η depends on the operation point, but the initial value of 0.87 has been considered.
Regarding the extractions, in this block defining whether it is a steam or a water extraction is necessary. For the water extraction the efficiency of the extractor (ratio of extracted water to the overall condensed water) is required, whereas for the steam extraction the quality of the extracted steam under normal operation is to be input. Furthermore, the steam extraction requires a GCSM signal (FUNGEN) controlling the amount of steam being extracted. This signal takes the value from a table that gives the mass flow as a function of the simulation time.

- EXTRACTIONS

The extractions are modeled as standard pipes connected to the turbine pipe at the exact location where they are defined within the turbine, ending in a special object called time dependent volume that simulates a pressure-enthalpy boundary at the edge of the pipe.
Whereas the initial conditions for the extraction pipes are the same as for the turbine but with initial mass flow zero, the initial conditions for the time dependent volumes are those at the corresponding extraction with initial mass flow zero as well. Therefore, the whole mass flow at the inlet of the turbine is used as initial mass flow for the Separator.
The mass flow removed in each extraction is controlled by a GCSM signal (FUNGEN) that takes the value from an input table. This table is defined as a step taking the value of zero at the beginning of the simulation and increasing to the steady state value at a given time.

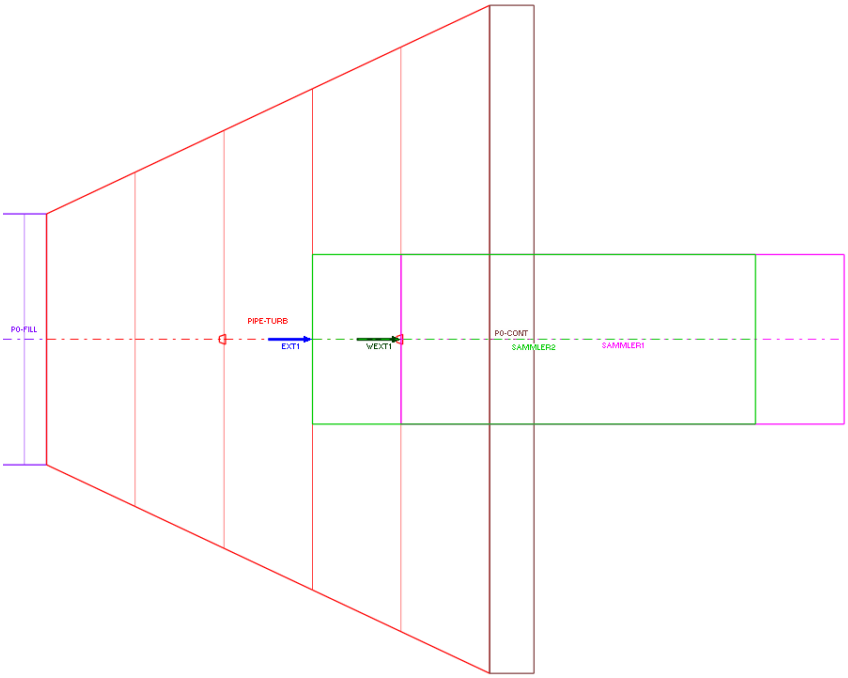

Figure 11: ATLAS visualization of the modeled high-pressure turbine

- **STEAM-WATER SEPARATOR**

The separator component model available in ATHLET is designed to simulate the separation of steam and water in the steam generator of a PWR. Although in that case the main fluid entering the separator component is water with steam droplets, and in the case of the outlet of the high-pressure turbine the main flow is steam with some condensed water, this model has been adapted and applied for the simulation.
The mentioned model requires a special arrangement of general TFOs and one separator TFO as shown in the picture below.

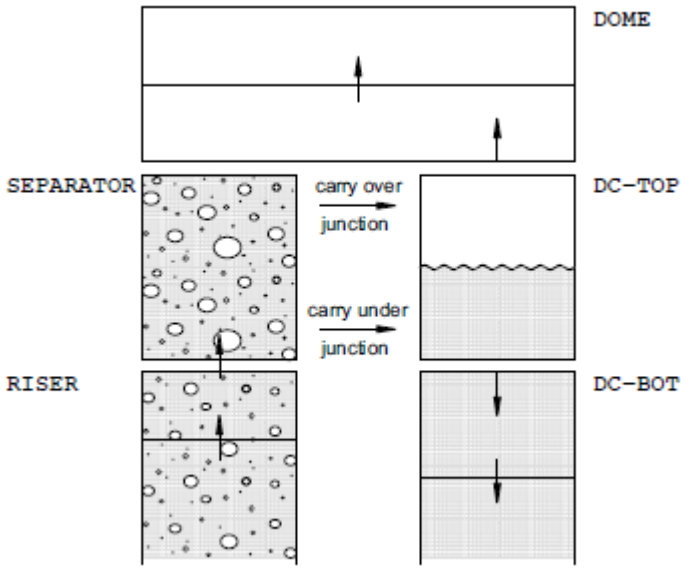

Figure 12: TFO arrangement for the simulation of a water-steam separator

- RISER

The riser is a standard vertical pipe linked to the exit of the high-pressure turbine. The friction and drift models are the same as for the high-pressure turbine and the fill, as well as the initial conditions.

- SEPARATOR

The separator object is a special vertical pipe with just one control volume, defined as a separator component by inputting ICMPO=3. Unlike a standard pipe with one CV and two junctions, three junctions are generated: one entrance and two exit junctions. Both exit junctions are automatically defined as horizontal by the code.
In contrast than for the rest of components, form losses must be input at the left and right side of a separator object. The friction and drift models applied are the same as already mentioned for the previous components.
The initial conditions have to be specified for the three junctions. Whereas the pressure and temperature are the same for the three of them, and actually those at

the inlet of the high-pressure turbine, the mass flows and kind of fluid are different. The first junction is the entrance, which works like a standard junction and its initial mass flow is the fill's one with a quality XSEP. The second junction is called carry-under junction and at operational conditions it transports water; thus, its initial mass flow is the water expected to be removed by the separator, with the condition of single phase liquid. The third one is called carry-over junction and transports steam at operational conditions, which initial mass flow input corresponds to the steam at the exit of the separator with the condition of single phase vapor.

- CARRY-OVER JUNCTION

The upper separator exit junction transports steam with quality XSEPO.

- CARRY-UNDER JUNCTION

The lower separator exit junction transports water with quality XSEPU.

- DC-TOP

At the exit of the separator pipe, a branch containing a Mixture Level (ML) is defined. This branch has the same height and elevation as the separator pipe, as well as the same initial conditions as at the entrance of the separator.
It consists of two homogenous Sub-CVs separated by a horizontal ML; the lower one contains pure liquid or liquid with vapor bubbles and the upper one pure vapor or vapor with liquid droplets.
The drift model required for this branch is that for a vertical flow path with relative velocity.
Moreover, an initial ML is defined according to the recommended value that the ATHLET manual suggests.

- DOME

At the top of the DC-TOP a standard vertical pipe is defined again with an active ML model. This pipe is filled with the separated steam; hence, the initial ML is defined at the bottom.
The drift models are the same as for the DC-TOP because of the two phases, whereas the initial thermal-hydraulic conditions correspond to those specified for the steam in the separator object.

- DC-BOT

Below the DC-TOP another standard vertical pipe with an initial ML at its top is defined. This pipe is filled with the water removed in the separator.
The drift and friction models are also the same as for the DC-TOP, and the initial conditions are those specified for the water in the separator object.

Moreover, these last three TFOs (DC-TOP, DOME and DC-BOT) make up a staggered ML track, which means that there is only one mixture level for the three of them; thus, the top elevation of the lower TFO must be equal to the bottom elevation of the upper TFO.

The mass flow quality of the separator exit junctions is defined by input separation tables that determine the mass flow void fraction as a function of the separator CV void fraction and the separator entrance mass flow, separately for the carry-under junction and for the carry-over one. Under normal operational conditions the values of these qualities are XSEPO=1 and XSEPU=0.
Separation is not possible in the whole region of separator entrance mass flows and separator qualities, but there is a limitation of the separation qualities. The most important restrictions for this case are the following ones: [8]

$$XSEPO \geq XSEP$$
$$XSEPU \leq XSEP$$
$$0 \leq XSEPU, XSEPO \leq 1$$
$$0{,}8 \leq XSEP \leq 0{,}99 \quad \text{Separation will be reduced}$$
$$0{,}99 < XSEP \quad \text{No separation}$$

The available operational data fulfills all of them; therefore, the separator model is supposed to work successfully.

- **OVER-HEATER**

The over-heater is modeled as a standard vertical pipe, connected to the end of the DOME, coupled to a heat transfer object (HCO).
Since the steam flow is expected to be saturated, the one single phase drift model is applied. As initial conditions, as well as for the rest of components, those at the inlet of the high-pressure turbine have been input, but as initial mass flow the input is the difference between the separated steam and the discharge simulated after the steam-water separator, and also the initial power per unit length QOV is taken into account.
In addition, the heat conduction object is defined as a cylinder with the same dimensions as the pipe, with just one layer of conductor material with a thickness of around 2% the cylinder diameter. It is defined as a standard HCO component ICOMPO=0, so that the simulation of heat generation within its material zone is allowed. This heat generation is simulated as a heat source constant in time through the whole length of the HCO, with a rated power per unit length QOV calculated under normal operation conditions.

(Equation 10)

$$Q = \dot{m}_{steam}(h_{out} - h_{in}) \quad [W]$$

$$QOV = \frac{Q}{L} \quad [\frac{W}{m}] \qquad \textit{(Equation 11)}$$

Since the over-heater increases the enthalpy of the steam, QOV takes a positive value.
The material properties are defined by tables, and in this model Stainless steel is used.
Furthermore, the heat transfer coefficients for the defined material zone must be determined. They have been calculated at the beginning and at the end of the pipe, defined per input data and kept constant for the whole simulation.

$$v = \frac{\dot{m}_{steam}\rho_{steam}}{A} \quad [\frac{m}{s}] \qquad \textit{(Equation 12)}$$

$$Re = \frac{\rho \cdot v \cdot D}{\mu} \qquad \textit{(Equation 13)}$$

$$Nu = 0{,}023 \cdot Re^{0,8} \cdot Pr^{0,4} \qquad \textit{(Equation 14)}$$

$$h = \frac{Nu \cdot k}{D} \quad [\frac{W}{m^2K}] \qquad \textit{(Equation 15)}$$

The HCO is coupled at its left side to the TFD pipe, whereas its right side is modeled as adiabatic. Hence, the equations above have been used for the heat transfer coefficients HTC for the left side, while for the right side the formula below has been applied.

$$h = \frac{k}{\lambda} \quad [\frac{W}{m^2K}] \qquad \textit{(Equation 16)}$$



Figure 13: ATLAS visualization of the temperature gradient in the modeled over-heater

- **LOW-PRESSURE TURBINE**

The simulation of the low-pressure turbine is the same as the model of the high-pressure one, but with five turbine stages instead of two. It has also four steam extractions and four water extractions instead of one of each type.
For these reasons, the low-pressure turbine pipe is divided into 12 CVs in order to fulfill the requirements for the extractions.

The steady state model has been input in the same way as the high-pressure turbine one, but with its corresponding pressures, enthalpies, mass flows, efficiencies and powers, as well as the simulation of extractions.
Furthermore, both the high and the low-pressure turbines are connected to the same generator shaft.

In addition, since the low-pressure turbine is the last one, a condenser component is associated to the last stage of the turbine. The data to be input is the enthalpy of the water at the exit of the condenser, which has been taken from the available data by assuming subcooled water.

In fact, the real low-pressure turbine consists of six stages. However, due to the fact that the resulting exit pressure is lower than the ATHLET pressure limit, this stage could not be modeled.

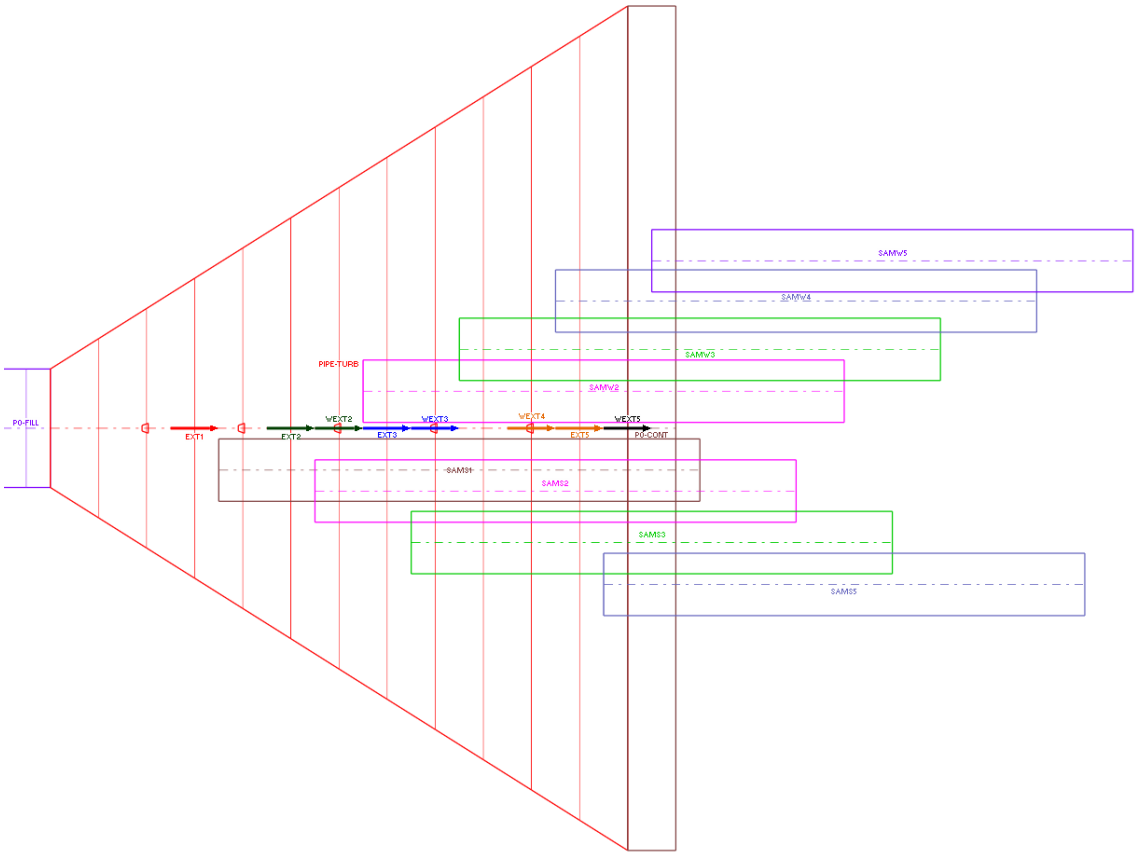

Figure 14: ATLAS visualization of the modeled low-pressure turbine

- **CONDENSER**

The condenser component follows the low-pressure turbine. Since the pressure and hence the steam density are very low, a large flow area is required behind the last turbine stage. Two condenser pipes follow the last stage of the turbine providing an adequate large flow area. These condenser pipes are vertical in order to separate the steam, which is possibly not completely condensed, and to prevent it from entering the feed water line.
The first pipe following the condenser (CONDPI) is a standard vertical pipe with two CVs and represents the steam collection, whereas the second pipe (CONDENS) is defined as a condenser component with ICOMPO=4 and consists of just one CV that represents the liquid part where the energy is removed.

- CONDPI

The dimensions of this pipe have been assumed large enough to provide a large flow area as recommended in ATHLET manuals. The drift flux model is the specified for two phase flow paths and the initial thermal-hydraulic conditions those at the inlet of the high-pressure turbine, with the mass flow expected to

enter the over-heater with the condition of single phase vapor or two phase with vapor dominant.

- CONDENS

This special pipe has been modeled with the same diameter as CONDPI and with a larger length. The friction and drift models are the same mentioned before, as well as the initial conditions but for single phase liquid, taking into account the initial power per unit length QCON.
A mixture level is also defined in this CV, since the steam condensates here, locating the initial ML at the top of the pipe.
This TFO is coupled to a HCO responsible of simulating the removal of heat. The extraction of energy has been simulated in the same way as the over-heater, with a heat source constant in time, whose rated power per unit length QCON takes a negative value since the water enthalpy is lower than the steam one.

$$Q = \dot{m}_{steam}(h_{out} - h_{in}) \quad [W] \qquad \textit{(Equation 17)}$$

$$Q_{cond} = \frac{Q}{L} \quad [\frac{W}{m}] \qquad \textit{(Equation 18)}$$

However, in order to increase the heat transfer surface without increasing the geometry, a FPARH = 1000 have been used. This command is a multiplier for parallel geometries; hence, the heat transfer is increased and the power length per unit length for each HCO is divided by 1000.

$$QCON = \frac{Q_{cond}}{1000} \quad [W/m] \qquad \textit{(Equation 19)}$$

In contrast to the over-heater simulation, the heat transfer coefficients for the condenser are calculated by means of ATHLET correlations.
As the condenser pipe is just one CV, the pressure given by ATHLET in this pipe is the pressure calculated at the center of the CV; therefore, hydrostatic pressure due to the liquid has to be taken into account.

$$P_h = \rho \cdot g \cdot \Delta H \qquad \textit{(Equation 20)}$$

$$P_{Athlet} = P_{fluid} + P_h \qquad \textit{(Equation 21)}$$

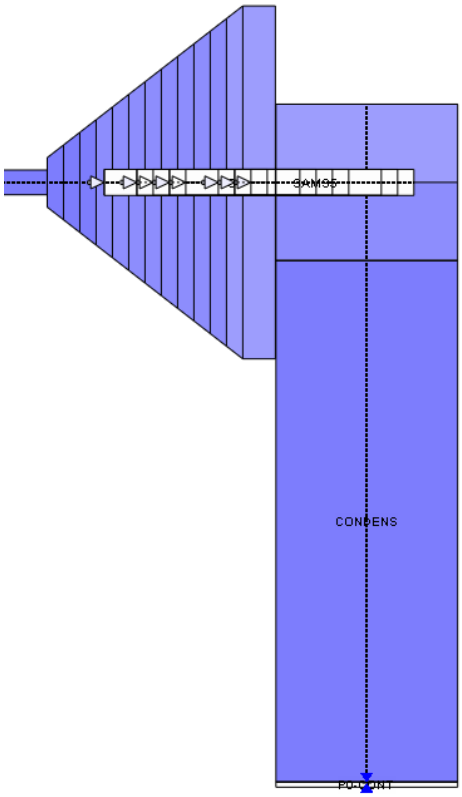

Figure 15: ATLAS visualization of the modeled condenser at the exit of the low-pressure turbine

- **DISCHARGE AFTER SEPARATOR**

A steam discharge is simulated after the steam-water separator. A standard pipe is defined at the end of the DOME, and a negative fill is inserted. The mass flow that the fill removes is controlled by a GCSM signal that takes the negative mass flow value from a table, as well as its enthalpy.

- **TIME DEPENDENT VOLUMES**

At the end of every turbine extraction, DC-BOT, and condenser, a time dependent volume (TDV) is defined in order to simulate a pressure-enthalpy boundary. These boundary conditions are controlled by GCSM signals.

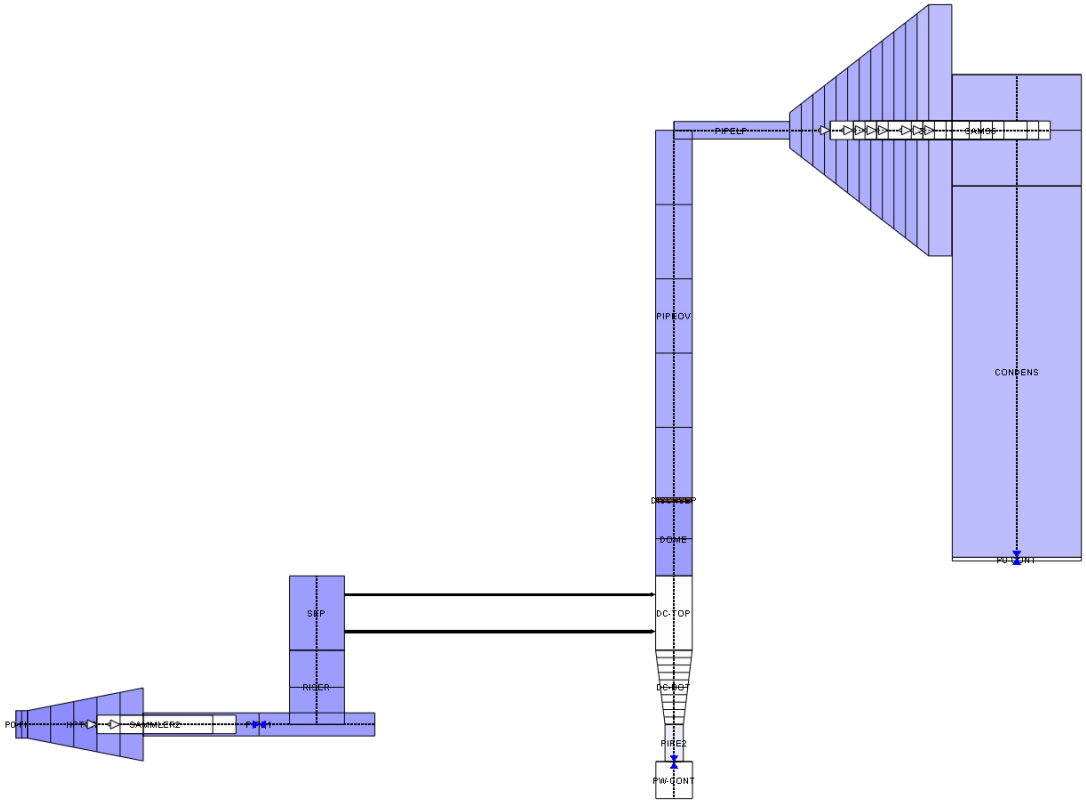

Figure 16: ATLAS visualization of the whole modeled system

- **CHECK VALVES**

The valve simulation is a junction related model and different kinds of valves can be simulated. For this model, the check valve type (JTYPO = 3) has been used in order to prevent reverse flow at some locations of the model, such as the end of the high-pressure turbine, the end of the DC-BOT of the separator, and the end of the condenser pipe CONDENS. These valves are static pressure controlled valves that close when reverse flow occurs (ITYPV = 3).

4.2. Changes introduced for the new turbine steady state model

Some changes have been introduced for the old turbine steady state model in order to adapt it to the new turbine.

4.2.1. Parameters

The conditions at the inlet of the high pressure turbine vary a little; hence, all the initial thermal-hydraulic conditions of all the components are changed just by changing the values of the parameters PRESS1, G1, H1 and TEMP1.

4.2.2. Extractions

The available data of the new turbine's extractions is given for the mixture of steam and water extracted. In order to simulate them separately, the mass flows of each phase have been estimated by applying the same percentage that they have in the old turbine.

$$\dot{m}_{mix,old} = \dot{m}_{st,old} + \dot{m}_{w,old} \qquad \textit{(Equation 22)}$$

$$x_{st} = \frac{\dot{m}_{st,old}}{\dot{m}_{mix,old}} \qquad \textit{(Equation 23)}$$

$$x_{w} = \frac{\dot{m}_{w,old}}{\dot{m}_{mix,old}} \qquad \textit{(Equation 24)}$$

$$\dot{m}_{st,new} = x_{st} \cdot \dot{m}_{mix,new} \qquad \textit{(Equation 25)}$$

$$\dot{m}_{w,new} = x_{w} \cdot \dot{m}_{mix,new} \qquad \textit{(Equation 26)}$$

4.3. Changes introduced for simulation of transients

The transients are simulated by introducing the available measurements of the operation of the system. Since the fill requires the values of the mass flow and enthalpy, which are controlled by GCSM signals, some modifications have been made in order to achieve the correct simulation of transients.

4.3.1. Tables for the FILL mass flow and enthalpy GCSM signals

The input conditions of the fill are responsible for introducing the transient. The GCSM signal (FUNGEN) for the mass flow takes the values from a table containing the available measurements as a function of time. These measurements during transient calculation do not contain the enthalpy values, but pressure values; therefore, the enthalpy of the fill is controlled by a special GCSM signal (PROP), which, instead of taking the values directly from a table, calculates these values as a function of pressure. The pressure signal (FUNGEN) is defined as usually and takes the values from a table where the available transient measurements are introduced.

4.3.2. GCSM signal controlling the mass flows of the turbine extractions

During the transient simulation, the mass flow of the system changes in time; hence the mass flow of the turbines varies as well. However, for the steady state the mass flows removed in the turbine extractions are controlled by signals that take values from an input table data. These values of extraction mass flows are not

available in the transient measurements; therefore, they cannot be inserted to make the signal value change.
An approximation has been made in order to simulate this variation of mass flows. The mass flow fraction of each extraction has been calculated under normal operational conditions as the ratio of the extracted mass flow to the mass flow at the turbine location where the extraction is placed.

$$x_{ext} = \frac{\dot{m}_{extracted}}{\dot{m}_{turbine\ CV}} \qquad \textit{(Equation 27)}$$

In this way, a GCSM signal (ADDER) is defined in order to control the mass flows as desired. This signal can multiply the value of a signal X1 by a constant value A1; therefore, for each extraction, X1 is a signal that measures the turbine mass flow in the extraction CV, and A1 is its calculated x_{ext}.

4.3.3. GCSM signals controlling the enthalpy of TDV

During the transient calculation, the p-h boundary CV works like a standard CV and the mass and energy equations in the CV are not solved. The CV related solution variables are not described by differential equations but defined by GCSM signals. For this reason, the enthalpy signals of the time dependent volumes have also been modified to the PROP type one. However, in this case the transient measurement pressure is not known at every extraction; thus, the pressure of the extraction under normal operational conditions is kept constant.

4.3.4. Pressure at the inlet of the high-pressure turbine

The available pressure data at the inlet of the high-pressure turbine, both for the old and for the new turbine, was not really the pressure at the inlet, but before a valve. Since all the values are normalized it was not a problem for the simulation of the steady state, because it was taken as the reference value so that the pressure at the inlet of the high-pressure turbine was 1. However, it is a problem for the simulation of transients, since the available data for the pressure at the inlet of the high-pressure turbine are not before the valve, but the real ones. For this reason, the pressure at the inlet of the high-pressure turbine taken as a reference both for the simulation of the steady state and transients has been calculated, assuming a pressure loss due to the valves of around 4-5%.

4.4. Detailed Procedure to model the system

The procedure followed to model the turbine system is explained here in detail because it has been the most laborious part of the Master's Thesis. As already mentioned, firstly the model of the older turbine has been designed, and later it has been adapted to the newer one.

4.4.1. Old Turbine Steady State Model

The following points describe the main process followed to achieve the design of each element as well as their connections setting up a system. Moreover, Figure 17 shows a blocks diagram describing the procedure.

- An initial model of the HP turbine has been further developed. As a result, the turbine extractions have been fixed. The model consisted of a fill, a turbine pipe and a time dependent volume.
- A steam-water separator has been added next, as well as connected at the exit of the HP turbine, leaving the TDV at the end of the separator.
- An over-heater has been developed and connected at the end of the separator's steam path, with the TDV at the end of the over-heater.
- An initial model of the LP turbine has been further developed in the same way as the HP one, and it has been joined at the exit of the over-heater.
- A condenser has been defined and connected at the end of the LP turbine, leaving the TDV at the end.

At the end of each described point, the steady state simulation has been performed, and its results have been analyzed in order to modify the model before going ahead with the next point. When introducing new components to the system, the fluid properties varied, especially the pressure because of the introduction of pressure losses.

4.4.2. New Turbine Steady State Model

The developed system for the old turbine steady state has been modified and adapted to the new one's properties and characteristics.
Figure 18 shows a blocks diagram of the followed process to model this new turbine.

4.4.3. Transient Model

The transient's fluid properties and some modifications have been input to the adapted system for the new turbine.

The following block diagrams show these three main processes followed to achieve the complete system model for the old turbine steady state, the new turbine steady state, and the transients.

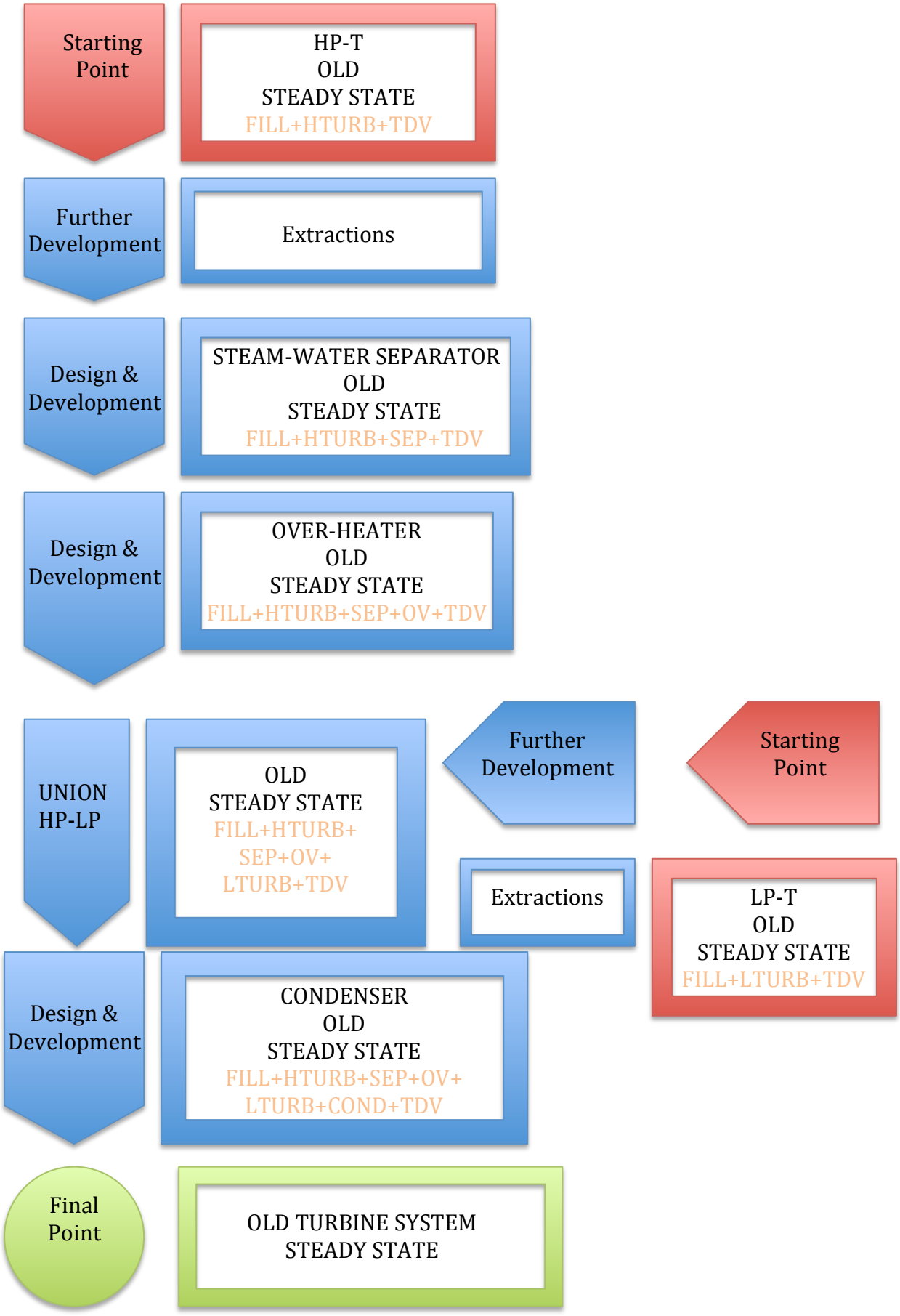

Figure 17: Process followed to model the old turbine´s steady state

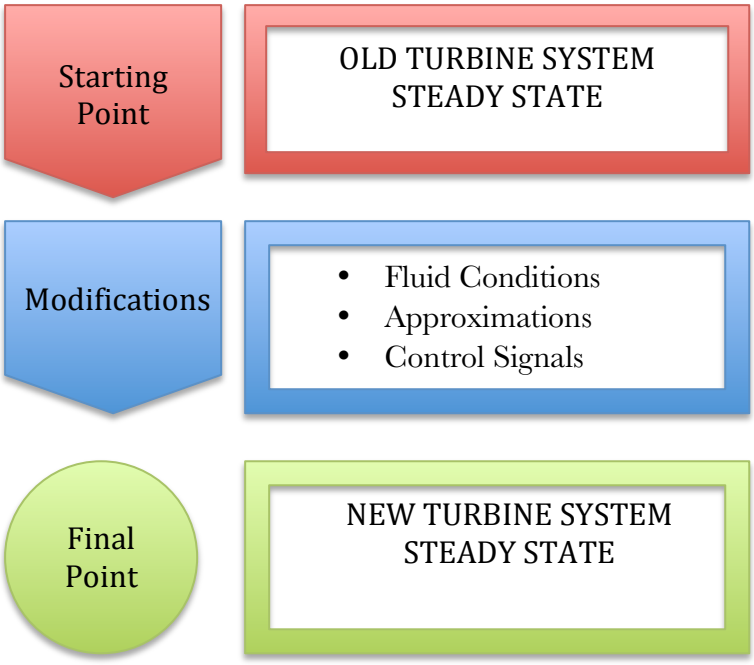

ure 18: Process followed to model the new turbine´s steady state

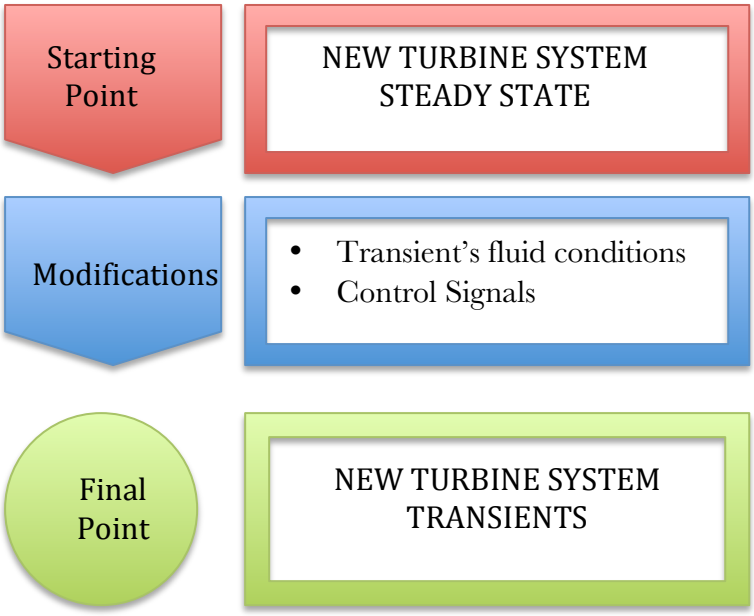

Figure 19: Process followed to model the new turbine´s transients

5. RESULTS

This section contains an analysis of the most relevant achieved results that have been compared to the real or nominal data for the five simulations that have been carried out.

5.1. Steady State Simulation for the Old Turbine

The steady state for the old turbine is simulated during 300 seconds, which is considered enough time to reach the desired steady state. The initial mass flow and pressure are input with the fill GCSM signals, and correspond to the new turbine nominal values G1 and H1.
Since there are no real measurements during the steady state operation of the plant, the obtained values have been compared to the nominal ones.

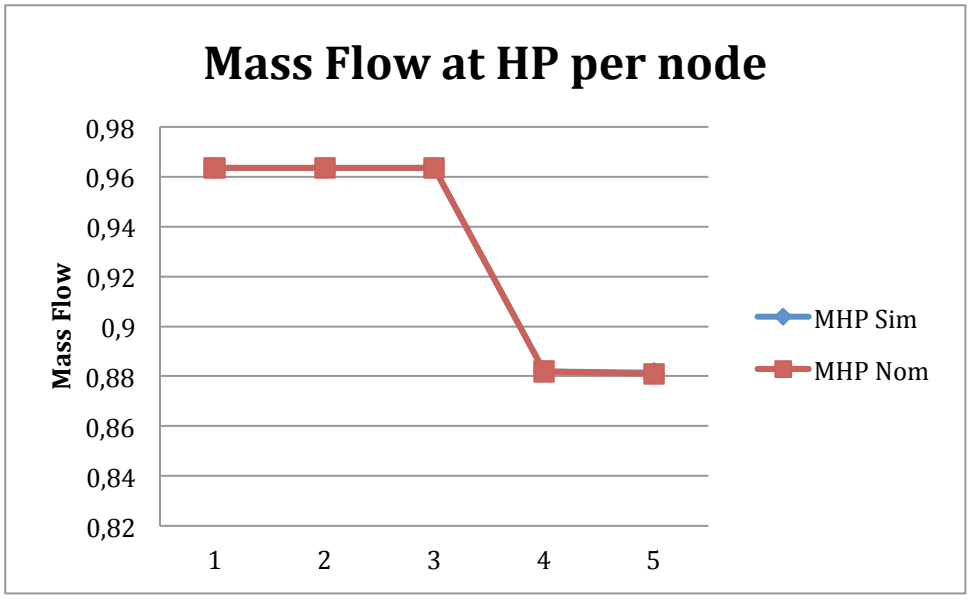

Figure 20.1: Mass flow in the high-pressure turbine per node

As Figure 20.1 shows, the simulated mass flow through the high-pressure turbine coincides with the nominal one. The mass flow decreases between node 3 and 4 because the steam extraction is placed there. Furthermore, a lower mass flow decrease takes place between nodes 4 and 5 due to the water extraction.

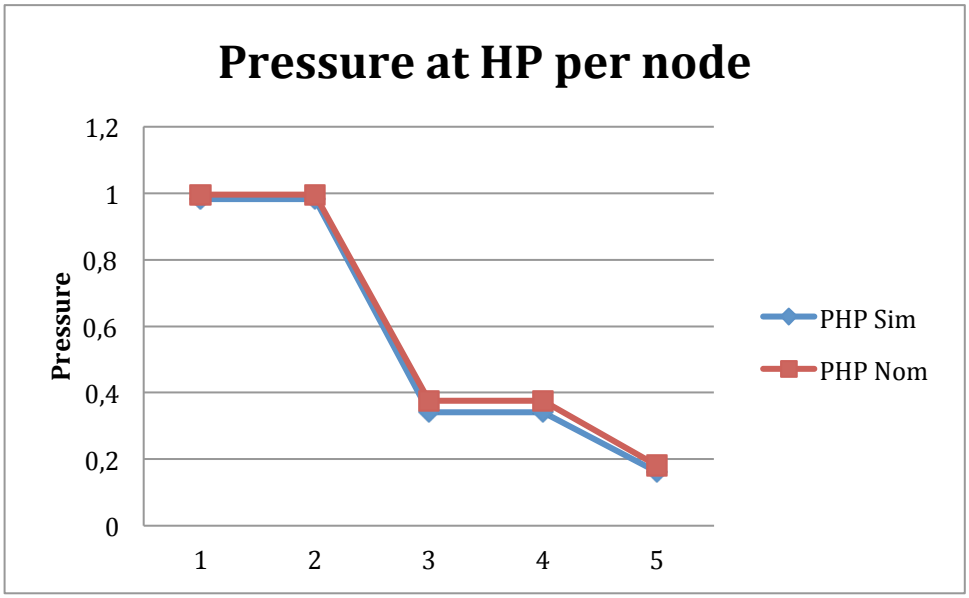

Figure 20.2: Pressure at each node of the high-pressure turbine

The simulated results curve and the nominal one are pretty close. The two turbines that simulate the high-pressure turbine are placed in CVs two and five respectively, which means in between 2 and 3 node for the first one, and in between 4 and 5 nodes for the second one. As expected, the pressure decreases in both cases due to the expansion of fluid.

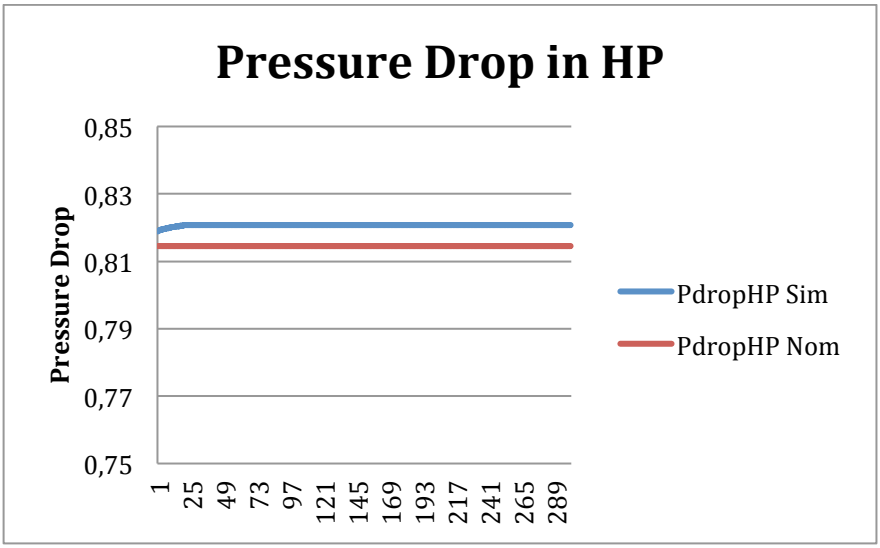

Figure 20.3: Pressure drop in high-pressure turbine during steady state

The precision of the simulation of the high-pressure turbine can be measured with the following percentage error formula.

$$\%Error = \left|\frac{Value_{simulated} - Value_{nominal}}{Value_{nominal}}\right| \cdot 100 \qquad \textit{(Equation 28)}$$

The maximum percentage error for the pressure drop in the high-pressure turbine is 0,7585%; hence, the precision of the simulation is good.

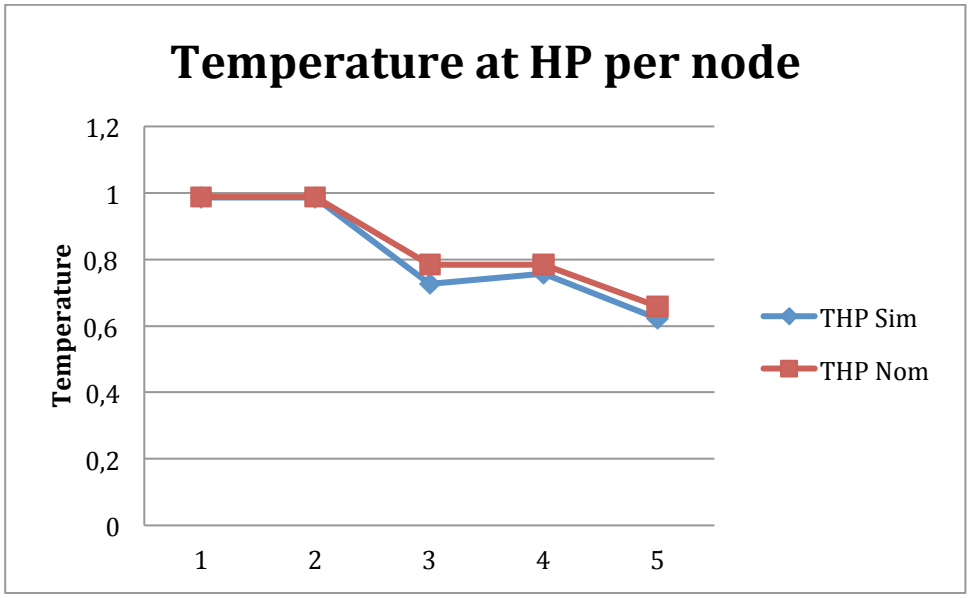

Figure 20.4: Fluid temperature at each high-pressure turbine node

The temperature decrease follows the same shape as the pressure; therefore, it decreases where the turbines are placed.

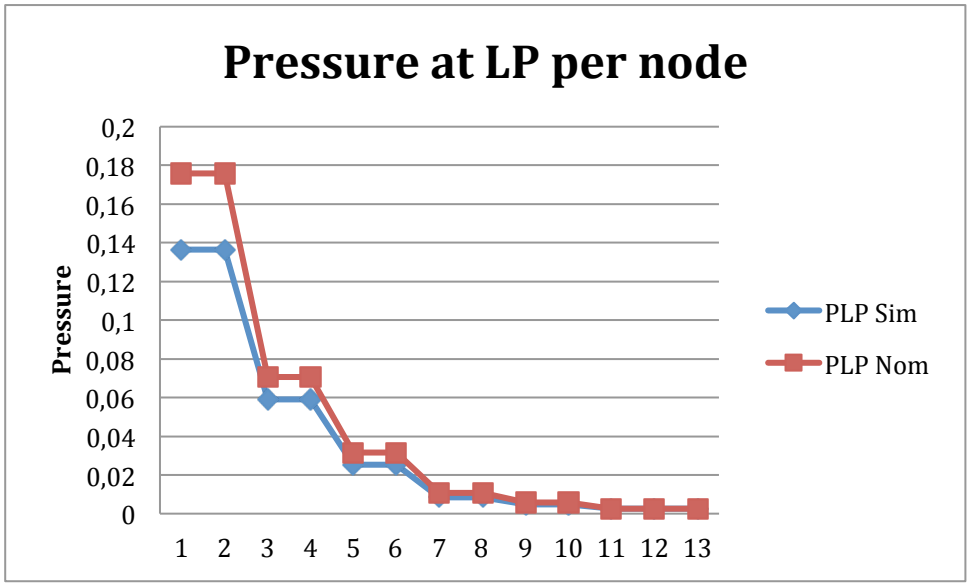

Figure 20.5: Pressure at each node of the low-pressure turbine

As Figure 20.5 shows, five stages of the low-pressure turbine are simulated. The pressure decreases in the CVs where the turbines simulating the whole low-pressure turbine are located. It is important to notice that the pressure at the inlet of the low-pressure simulated turbine is lower than the nominal one, which may be consequence of friction or form losses through the components in between the high-pressure and the low-pressure turbine, since the pressure at the exit of the simulated high-pressure turbine does coincide with the nominal one.

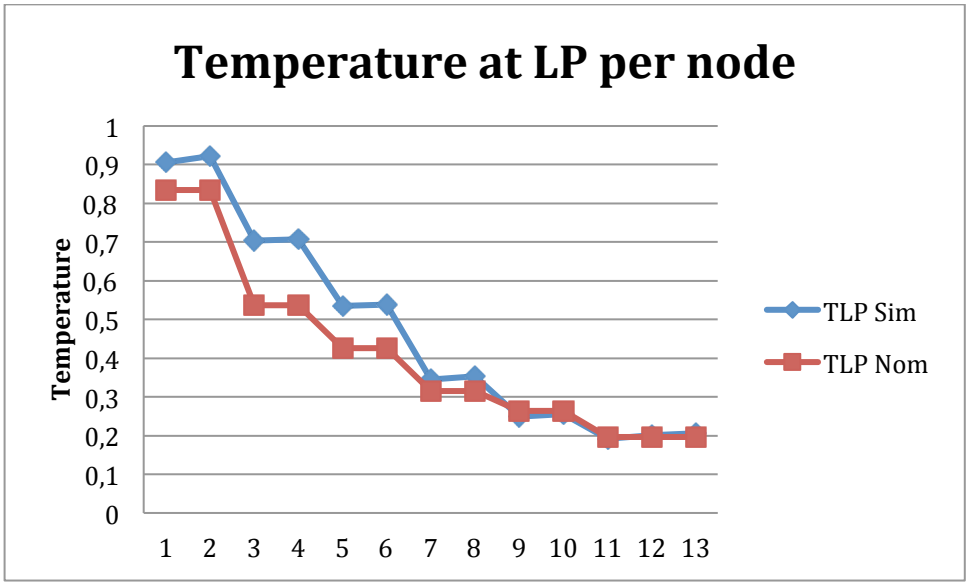

Figure 20.6: Fluid temperature at each node of the low-pressure turbine

In contrast to the pressure case, the temperature at the inlet of the simulated low-pressure turbine is higher than the nominal one, which may be caused by a higher heat addition in the over-heater, as Figure 20.14 shows. However, the temperature at the exit of the simulated turbine is the same as the nominal one.

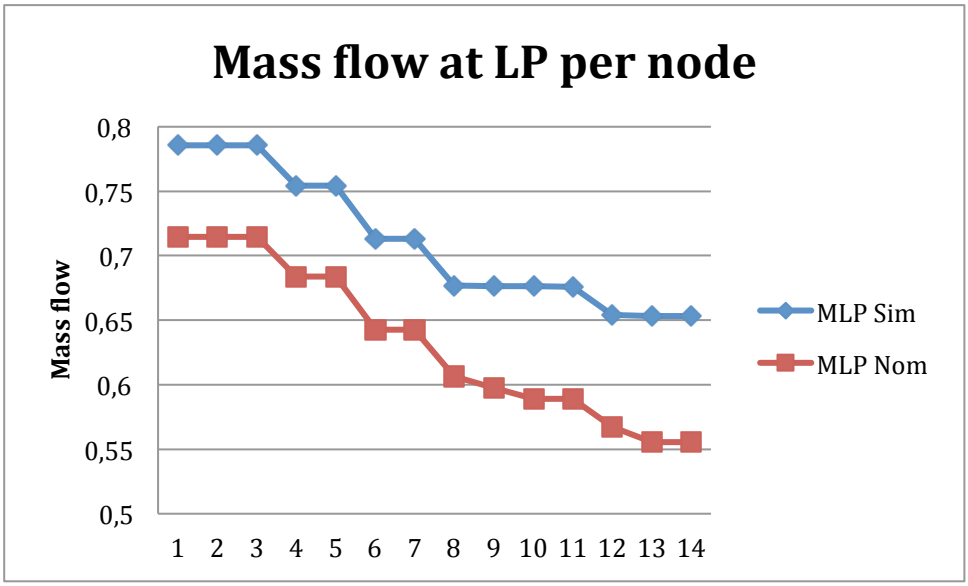

Figure 20.7: Mass flow at each node of the low-pressure turbine

As already explained for the high-pressure turbine, the mass flow through the low-pressure turbine decreases in the CVs where the steam and water extractions are located. The reason why the simulated mass flow is higher than the nominal one may be a lower separation of mass flow in the separator, explained in Figure 20.11.

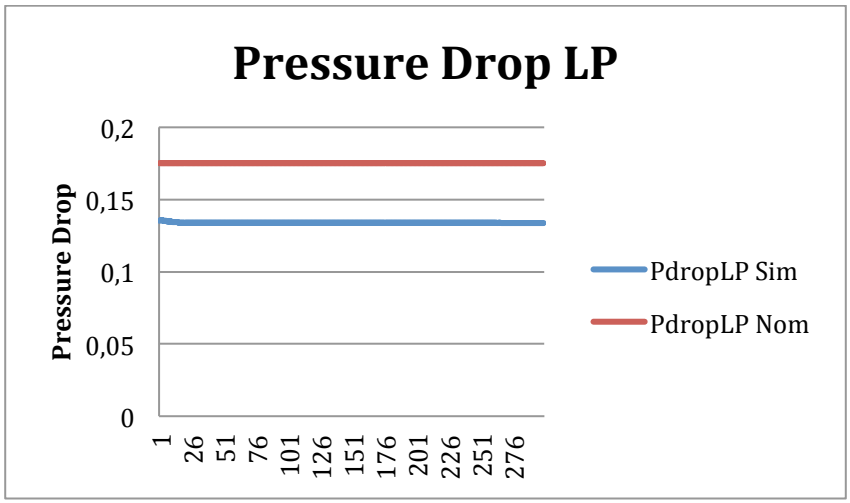

Figure 20.8: Pressure drop in the low-pressure turbine

The maximum percentage error for the pressure drop between the inlet and outlet of the old low-pressure turbine is 23,6%, which is considerable high and may be due to the fact that the last stage of the low-pressure turbine cannot be modeled.

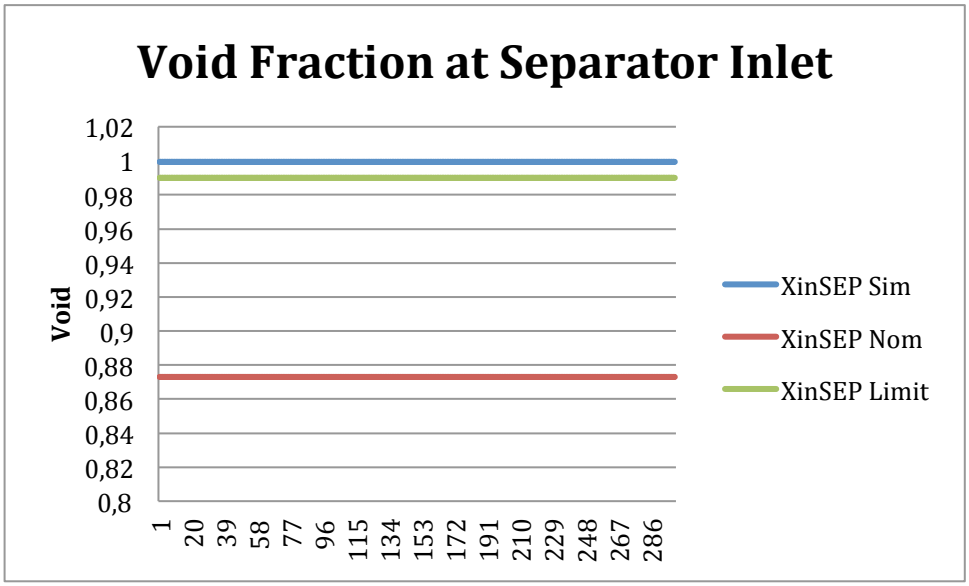

Figure 20.9: Void fraction at the inlet of the separator

As it is shown in Figure 20.9, the limit separation void fraction for which the separator works successfully is overtaken by the simulated void fraction at the inlet of the separator (0,99936>0,99). Therefore, no separation of water or a very little one is expected to happen. If the quality of the fluid were the nominal one (0,88) the separator would work within its separation limits and it would separate the desired water.

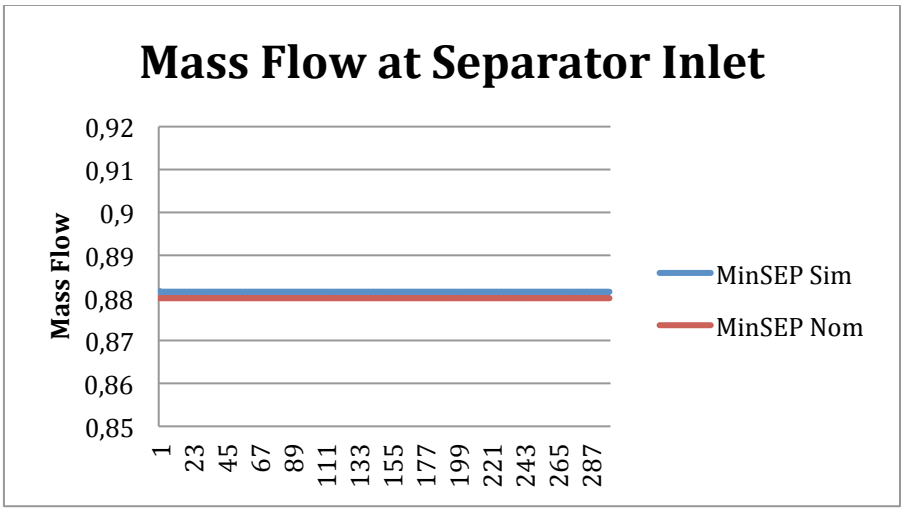

Figure 20.10: Mass flow at the inlet of the separator

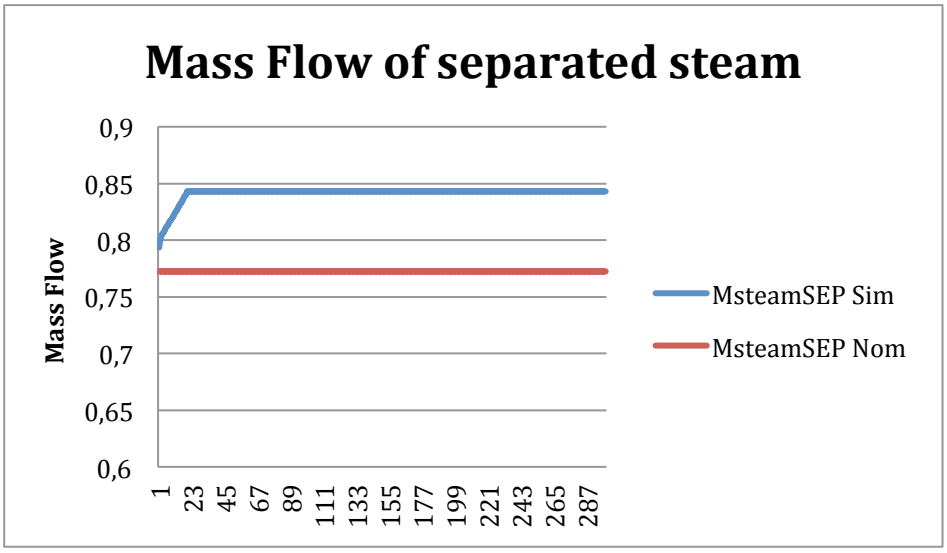

Figure 20.11: Mass flow of the separated steam in the separator

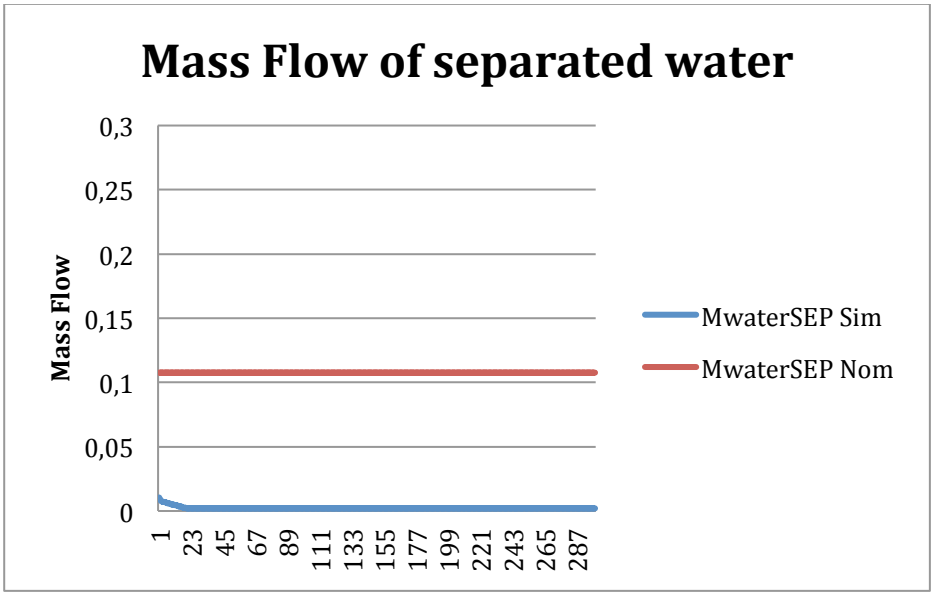

Figure 20.12: Mass flow of the separated water in the separator

As figure 20.12 shows, the water separated during the simulation is very close to zero, while it was expected to be close to the 10% of the total mass flow at the inlet of the high-pressure turbine.
These graphics explain the higher simulated mass flow at the inlet of the low-pressure turbine with respect to the nominal value.

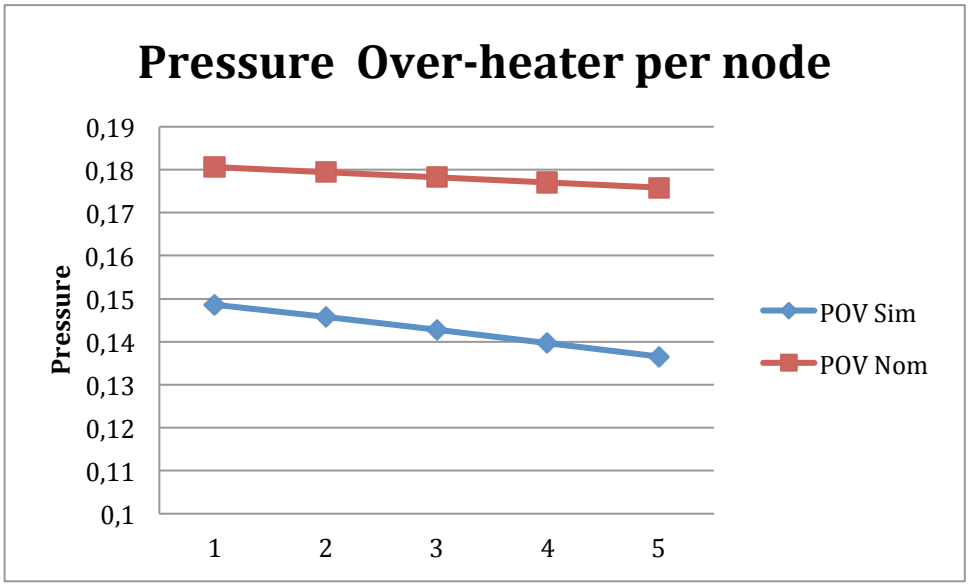

Figure 20.13: Pressure at each node of the over-heater

Although the inlet pressure for the simulated over-heater is lower than the nominal value, the pressure loss in the over-heater is higher for the simulated over-heater, which contributes to an even lower pressure at the inlet of the low-pressure turbine.

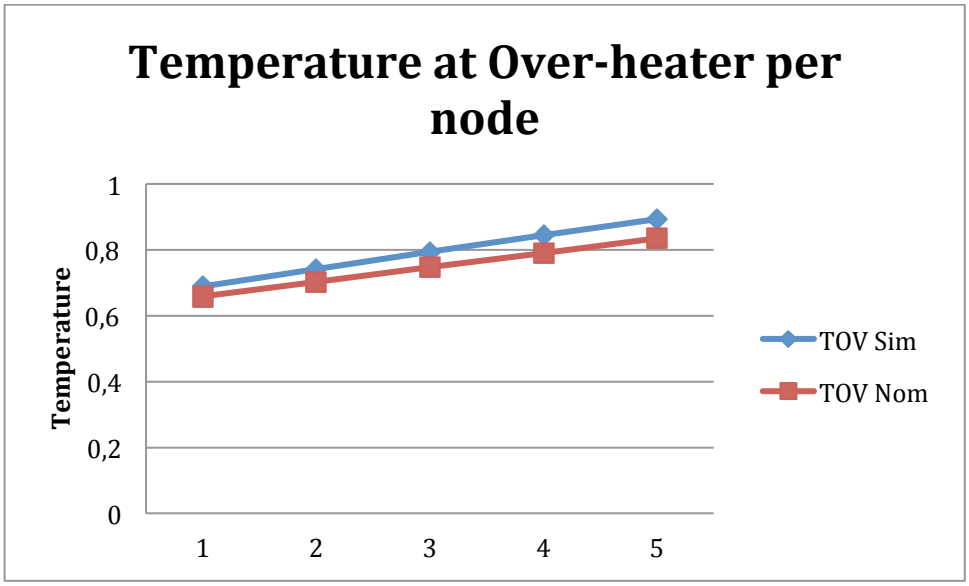

Figure 20.14: Fluid temperature at each node of the over-heater

Figure 20.14 shows that the temperature rise in the simulated over-heater follows the nominal temperature increase. However, since the pressure is lower than the nominal one, the enthalpy increase is also a little lower than the nominal one.

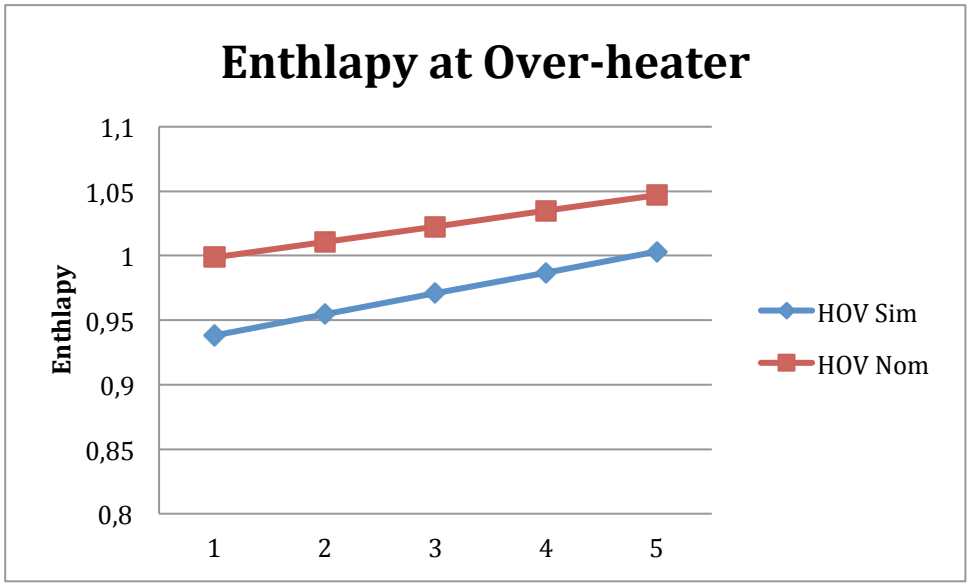

Figure 20.15: Enthalpy at each node of the over-heater

In addition, since the last stage of the low-pressure turbine is not simulated due to ATHLET pressure restrictions, the simulated pressure at the inlet of the condenser is a little higher than the nominal value.

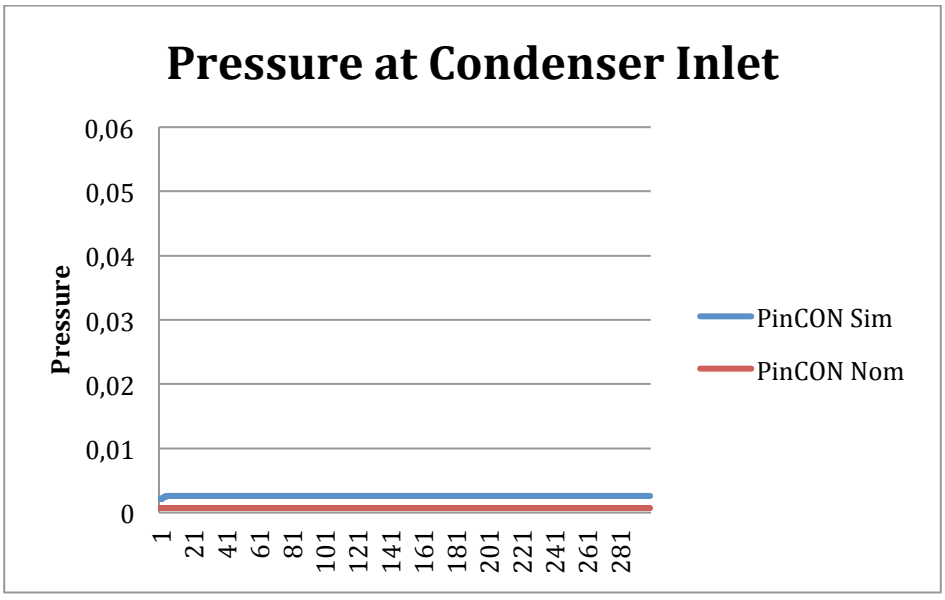

Figure 20.16: Pressure of the steam at the inlet of the condenser

The pressure at the inlet of the condenser is the same as the one at the exit of the low-pressure turbine; therefore, since its last stage could not be modeled, this pressure is not as low as the nominal value.

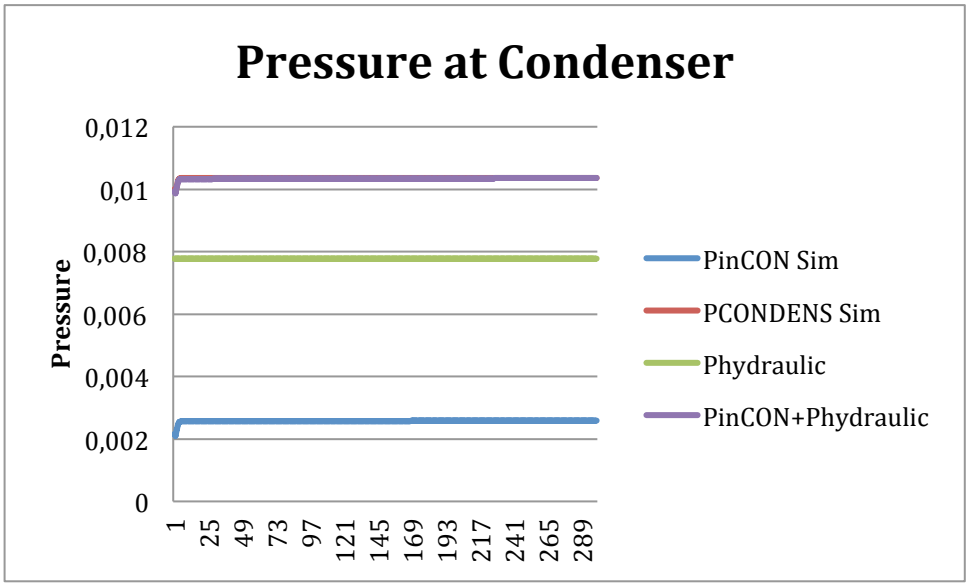

Figure 20.17: Pressures in the condenser

Figure 20.17 shows the presence of hydraulic pressure in the condenser, due to the fact that it is a pipe with a high length that is full of condensed water. Since the condenser pipe is modeled as one CV, the pressure of the fluid given by ATHLET (PCONDENS Sim) is the pressure at the center of this CV. Therefore, this pressure is the sum of the pressure of the fluid at the inlet of the condenser (PinCON Sim) and the hydraulic pressure at the center of the CV (Phydraulic).

$$PCONDENS\ Sim = PinCON\ Sim + Phydraulic \qquad \textit{(Equation 29)}$$

$$Phydraulic = \rho \cdot g \cdot \frac{L_{condenser}}{2} \qquad \textit{(Equation 30)}$$

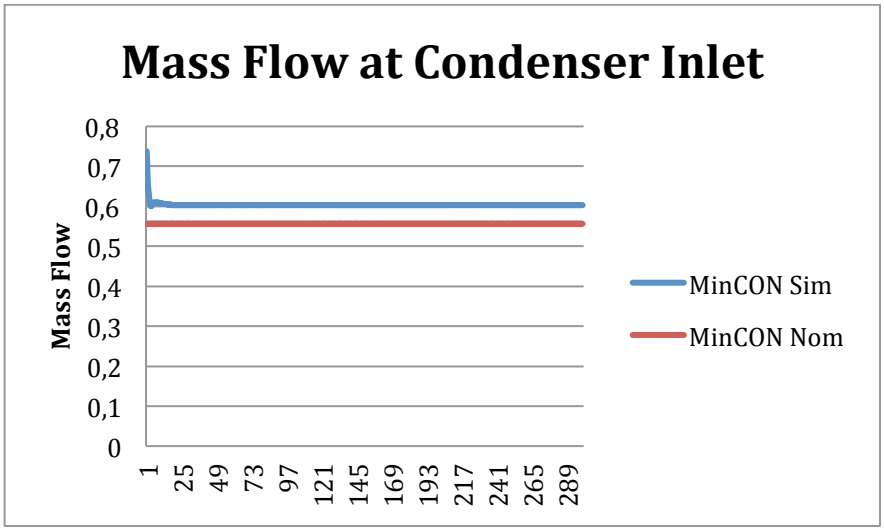

Figure 20.18: Steam mass flow at the inlet of the condenser

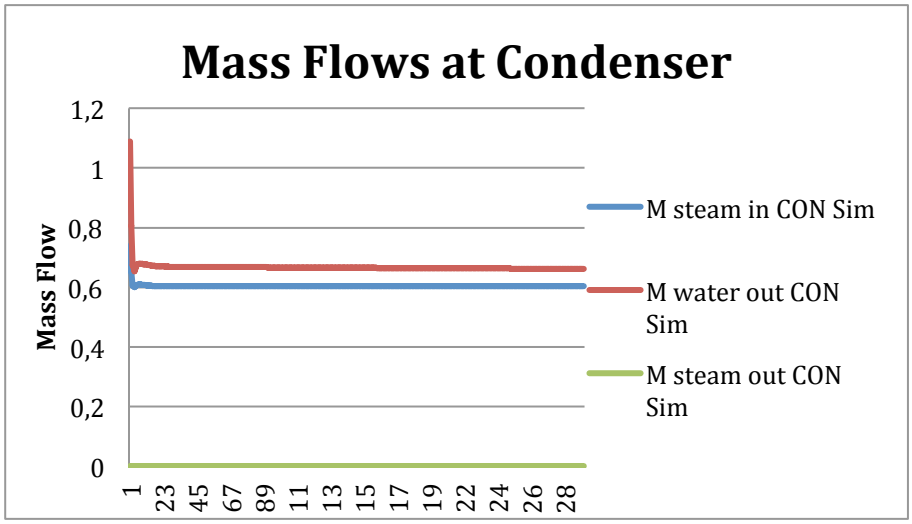

Figure 20.19: Mass flows balance in the condenser

Figure 20.19 shows that the condenser transforms all the steam that exits the low-pressure turbine into water by extracting heat. The vapor mass flow that enters the condenser (blue) is absolutely condensed into water; hence, the final mass flow of water in the condenser (red) is the sum of all the condensed steam and the little amount of water present in the fluid at the exit of the low-pressure turbine, which explains that the red line is higher than the blue one. Finally, the mass flow of steam at the exit of the condenser is zero (green).

5.2. Steady State Simulation for the New Turbine

As well as for the old turbine, the new one's steady state has also been simulated during 300 seconds.

Whereas for the simulation of the old turbine steady state no measurement data was available and the comparison was only possible with the nominal values, a further comparison can be performed in some cases for the new turbine simulation by using the available real measurement data for the transients, since also long times of steady state operation are included.

The initial mass flow and pressure are input with the fill GCSM signals, and correspond to the nominal values G1 and H1.

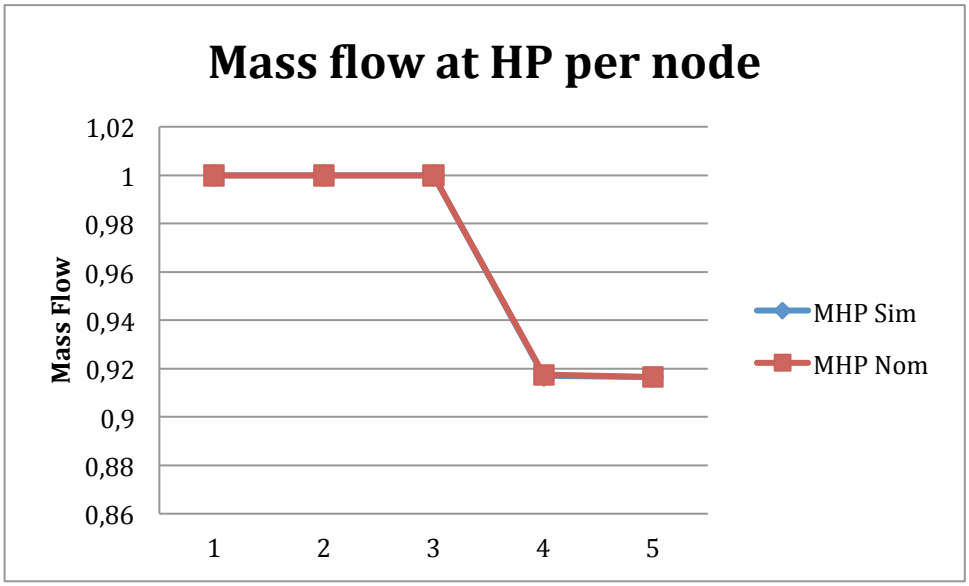

Figure 21.1: Mass flow at each node of the high-pressure turbine

As Figure 21.1 shows, the simulated mass flow through the high-pressure turbine coincides with the nominal one. The mass flow decreases between node 3 and 4 because the steam extraction is placed there. Furthermore, a lower mass flow decrease takes place between nodes 4 and 5 due to the water extraction.

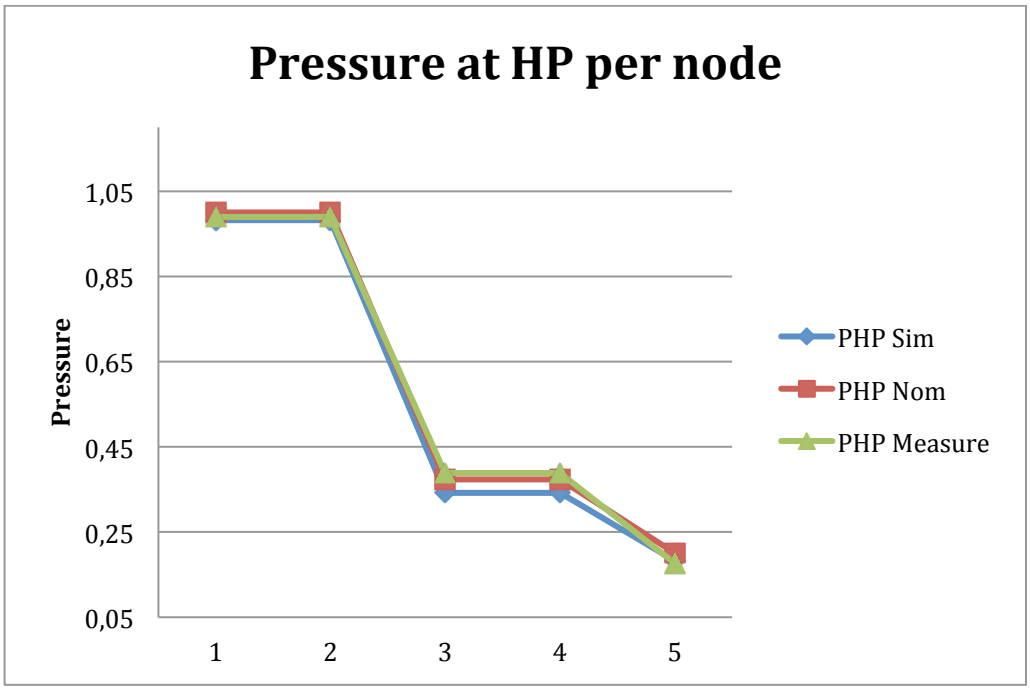

Figure 21.2: Pressure at each node of the high-pressure turbine

The measurement data includes the pressure at the inlet, steam extraction and outlet of the high-pressure turbine; thus, the pressure per node in the simulated model can be compared with both the nominal data and the measured ones. The

simulated results are pretty close to the nominal and the measured ones. The two turbines that simulate the high-pressure turbine are placed in CVs two and five respectively, which means in between 2 and 3 node for the first one and in between 4 and 5 nodes in the second one. As expected, the pressure decreases in both cases due to the expansion of fluid.

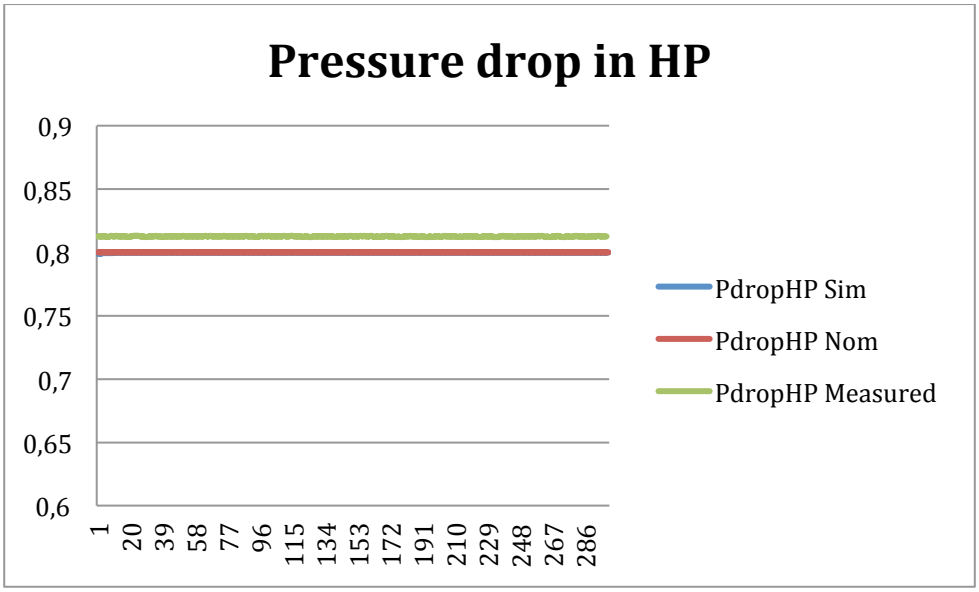

Figure 21.3: Pressure drop in high-pressure turbine

The pressure drop in the simulated high-pressure turbine is very close to the nominal pressure drop, while the pressure drop in the real measurements is higher. The maximum percentage error for the simulated pressure taking as the reference the nominal value is 0,0067%; while taking as the reference the real measured value it is 1,55%. In both cases this error is low enough to consider a good precision.

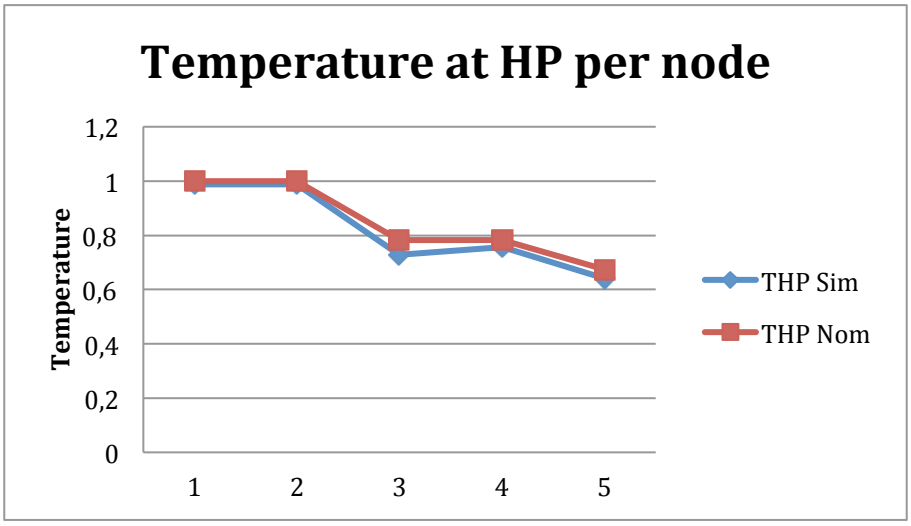

Figure 21.4: Fluid temperature at each high-pressure turbine node

The temperature decrease follows the same shape as the pressure; therefore, it decreases where the turbines are placed.

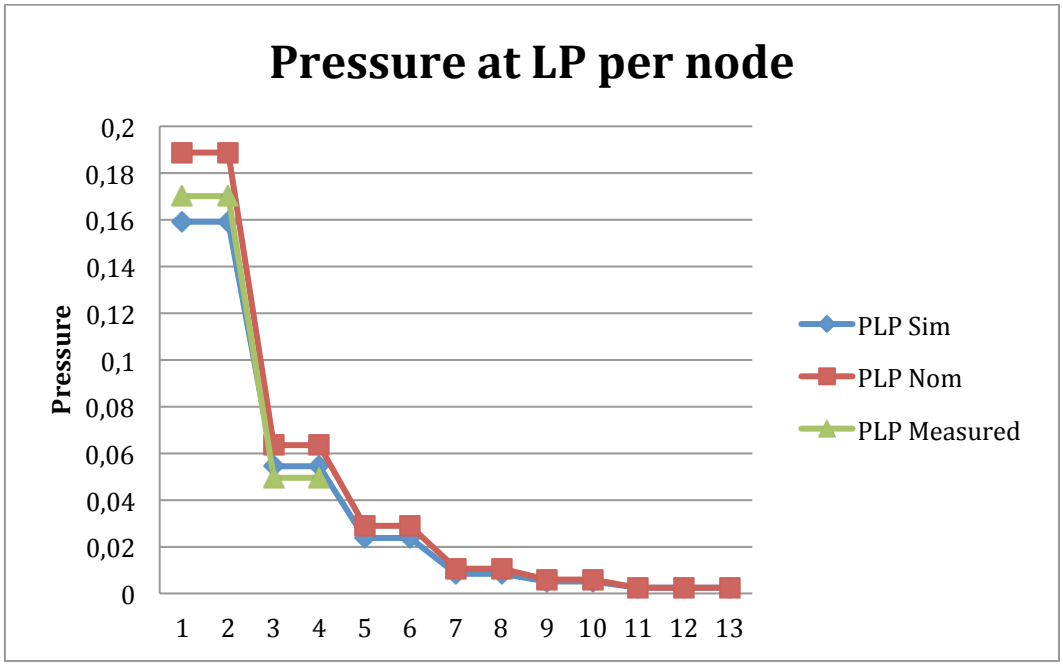

Figure 21.5: Pressure at each node of the low-pressure turbine

In the same way as for the older turbine, five stages of the new low-pressure turbine are simulated. The pressure decreases in the CVs where the turbines simulating the whole low-pressure turbine are located. The difference between the simulated and the nominal pressures at the inlet of the low-pressure turbine is lower than for the older turbine, although it is also a considerable pressure difference. However, for the new low-pressure turbine the pressures at the inlet, first steam extraction and second steam extraction are available as real

measurements; hence, a further comparison is possible. Figure 21.5 shows that the real (green) and simulated (blue) inlet pressures are lower than the nominal (red) one. This difference may be caused by pressure losses in the components that precede the low-pressure turbine.

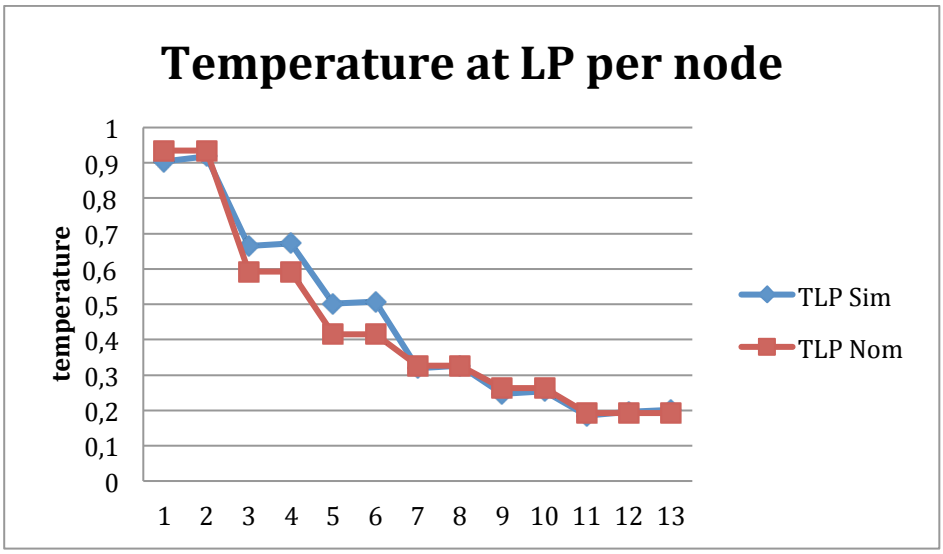

Figure 21.6: Fluid temperature at each node of the low-pressure turbine

The temperature at the inlet of the low-pressure turbine matches the nominal value, as well as the exit temperature.

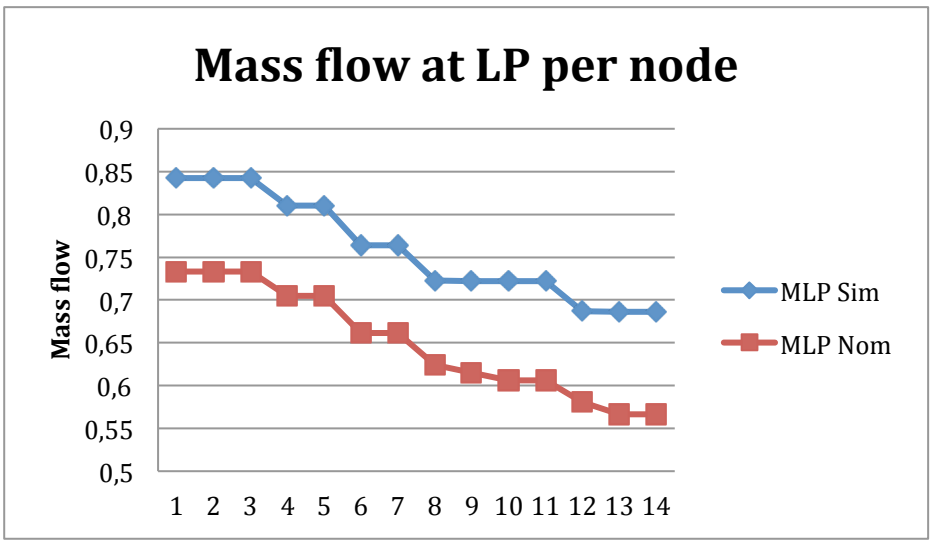

Figure 21.7: Mass flow at each node of the low-pressure turbine

As already explained for the high-pressure turbine, as well as for the older turbine, the mass flow through the low-pressure turbine decreases in the CVs where the steam and water extractions are located. The reason why the simulated mass flow

is higher than the nominal one may be a lower separation of mass flow in the separator, explained in Figure 21.11.

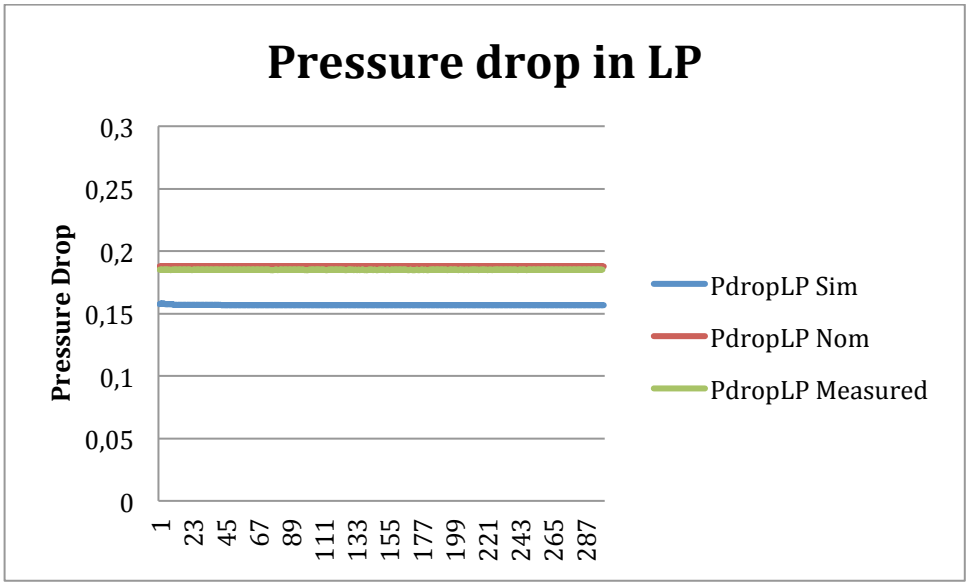

Figure 21.8: Pressure drop in the low-pressure turbine

The maximum percentage error of the simulated pressure drop in the low-pressure turbine taking the nominal value as the reference is 16,53%, and 15,3% taking as the reference the real measurement. However, this high percentage error is probably a consequence of not simulating the last stage of this turbine; thus, it does not determine the precision of the simulation.

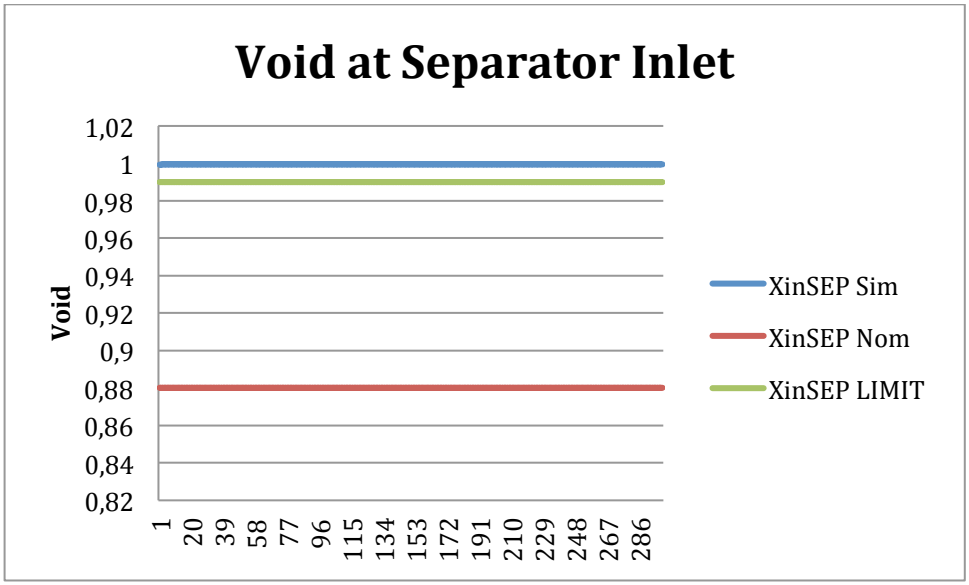

Figure 21.9: Void fraction at the inlet of the separator

As well as for the old turbine, Figure 21.9 shows that the limit separation void fraction for which the separator works successfully is overtaken by the simulated

void fraction at the inlet of the separator (0,99936>0,99). Therefore, no separation of water or a very little one is expected to happen. If the quality of the fluid were the nominal one (0,88) the separator would work within its separation limits and it would separate the desired water.

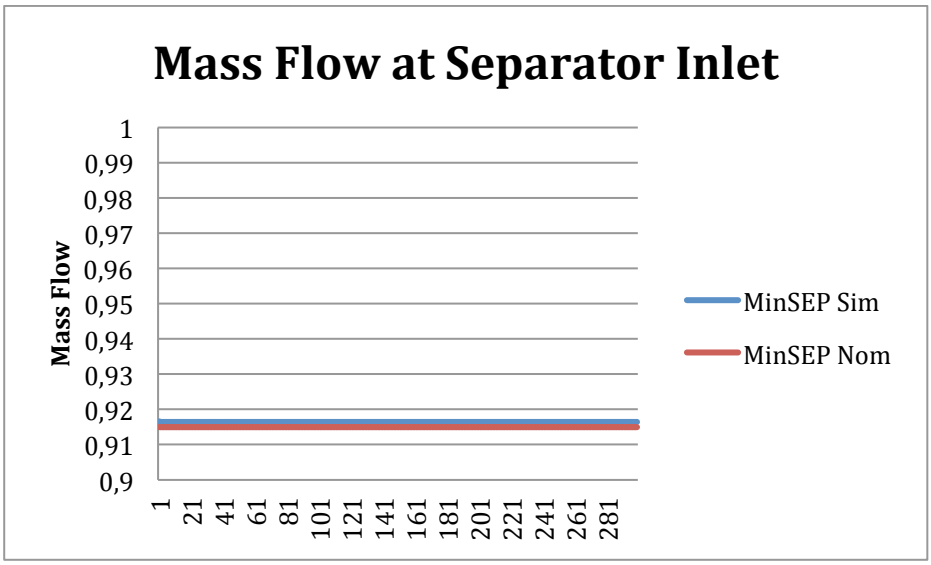

Figure 21.10: Mass flow at the inlet of the separator

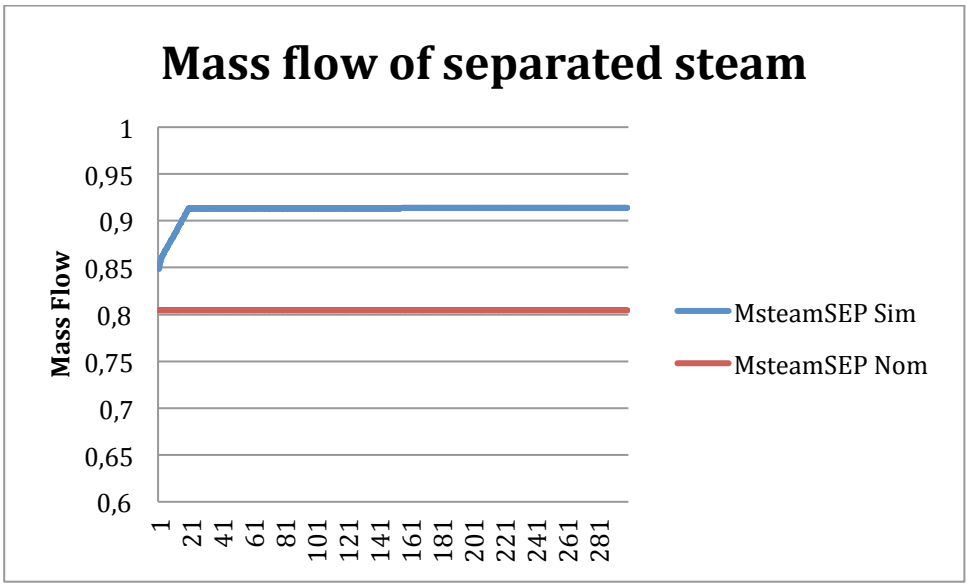

Figure 21.11: Mass flow of the separated steam in the separator

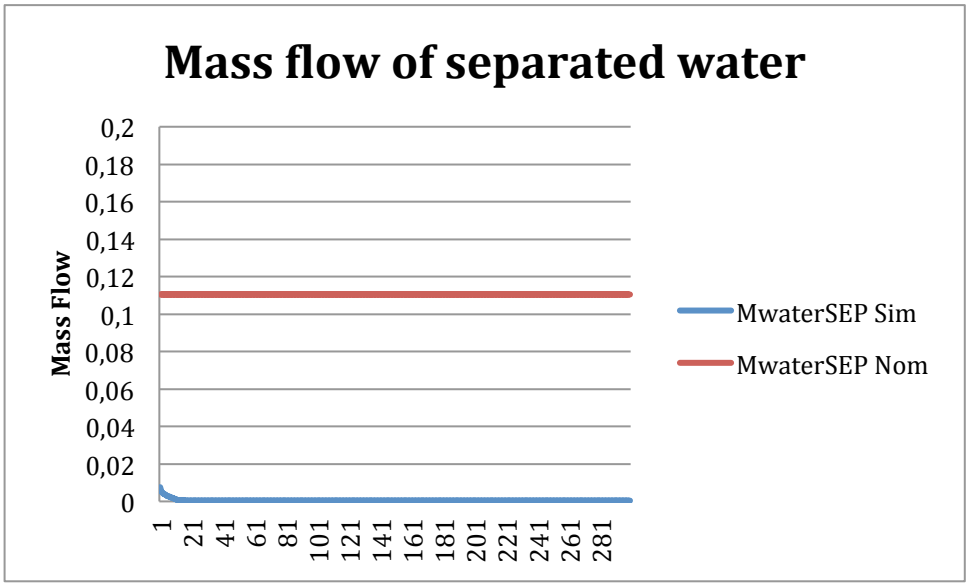

Figure 21.12: Mass flow of the separated water in the separator

As figure 21.12 shows, the water separated with the simulation is very close to zero, while it was expected to be close to the 10% of the total mass flow at the inlet of the high-pressure turbine.
These graphics explain the higher simulated mass flow at the inlet of the low-pressure turbine with respect to the nominal value.

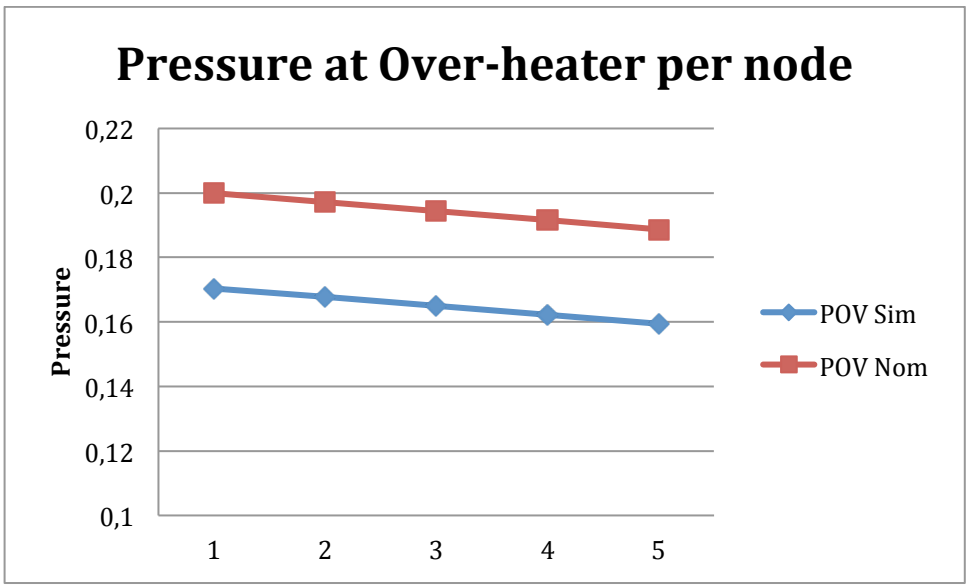

Figure 21.13: Pressure at each node of the over-heater

Although the inlet pressure for the simulated over-heater is lower than the nominal value, the pressure loss in the over-heater is higher for the simulated over-heater, which contributes to an even lower pressure at the inlet of the low-pressure turbine.

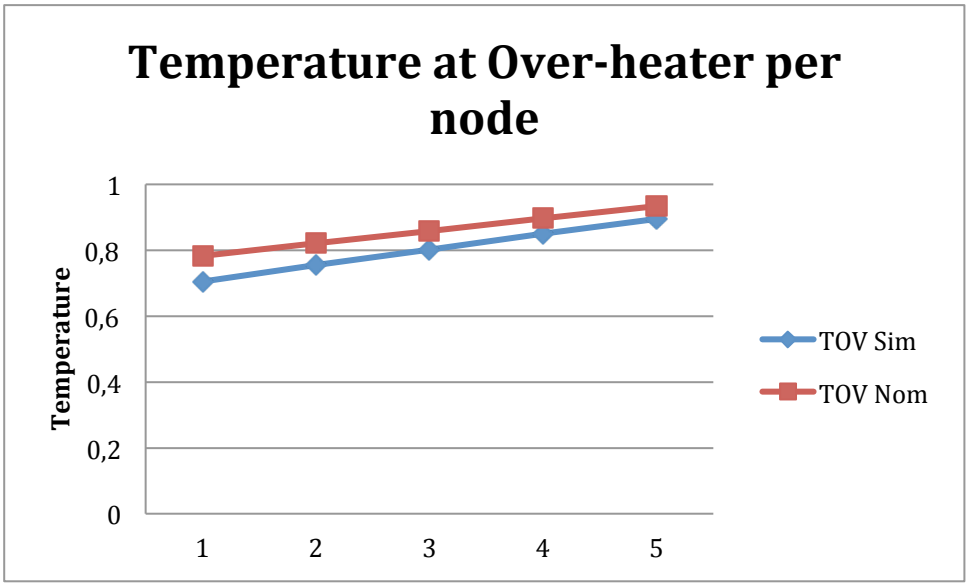

Figure 21.14: Fluid temperature at each node of the over-heater

Figure 21.14 shows that the temperature rise in the simulated over-heater follows the nominal temperature increase. However, since the pressure is lower than the nominal one, the enthalpy increase is also a little lower than the nominal one.

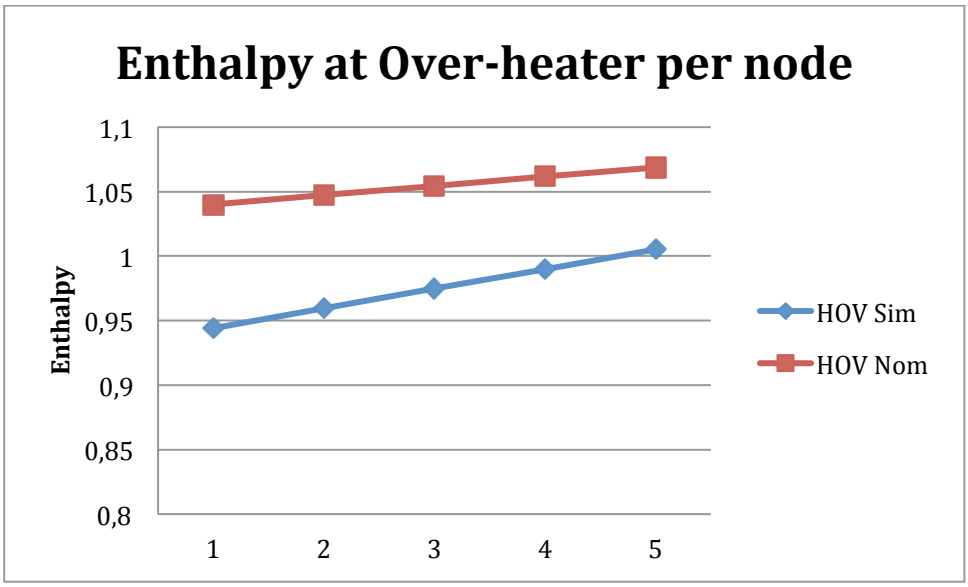

Figure 21.15: Enthalpy at each node of the over-heater

In addition, since the last stage of the low-pressure turbine is not simulated due to ATHLET pressure restrictions, the simulated pressure at the inlet of the condenser is a little higher than the nominal value.

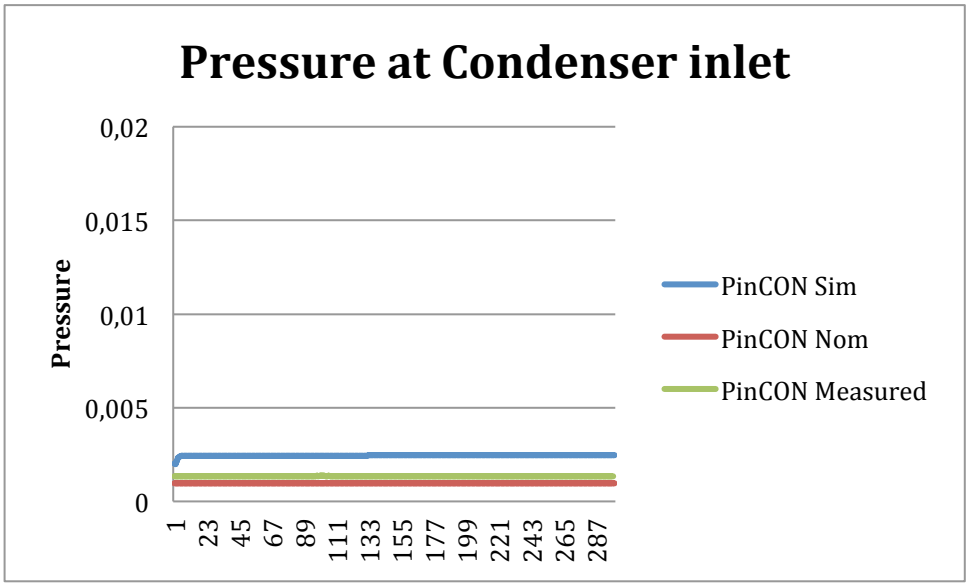

Figure 21.16: Pressure of the steam at the inlet of the condenser

Figure 18.21 shows the difference between the nominal, simulated and real pressure at the inlet of the condenser. As the last stage of the low-pressure turbine has been not modeled, it is reasonable that the simulation pressure at the inlet of the condenser is higher than the nominal and real value.

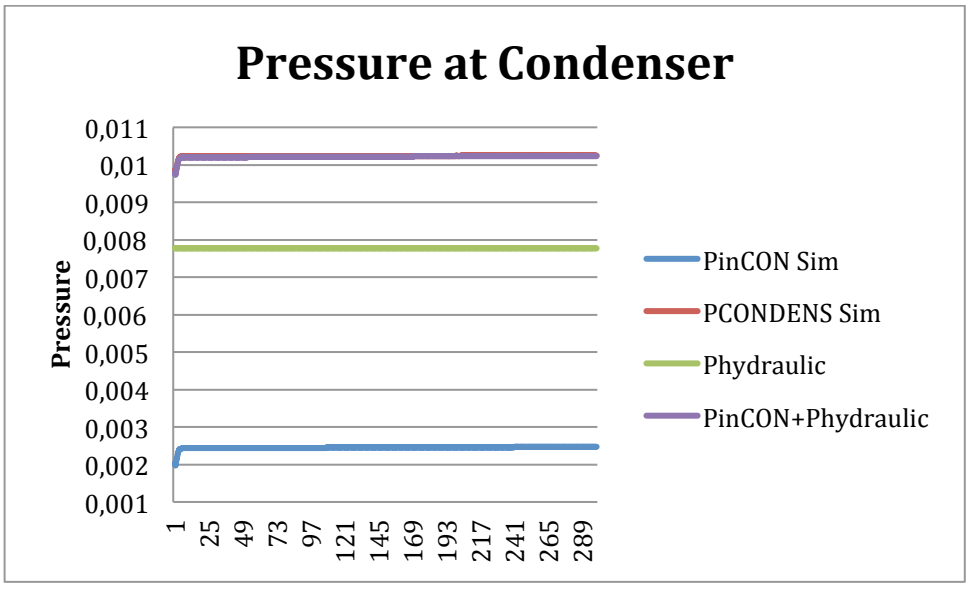

Figure 21.17: Pressures in the condenser

Figure 21.17 shows the presence of hydraulic pressure in the condenser, due to the fact that it is a pipe with a high length that is full of condensed water. Since the condenser pipe is modeled as one CV, the pressure of the fluid given by ATHLET (PCONDENS Sim) is the pressure at the center of this CV. Therefore, this pressure is the sum of the pressure of the fluid at the inlet of the condenser (PinCON Sim) and the hydraulic pressure at the center of the CV (Phydraulic).

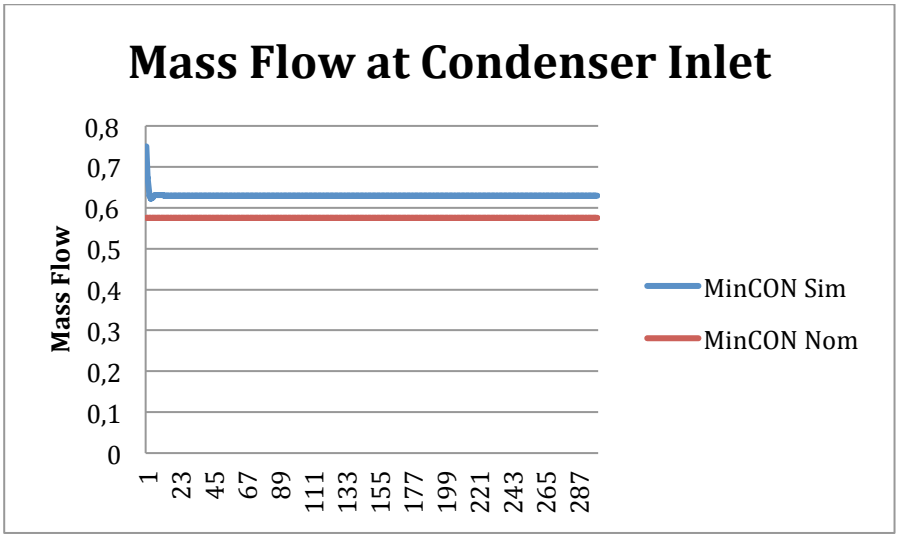

Figure 21.18: Steam mass flow at the inlet of the condenser

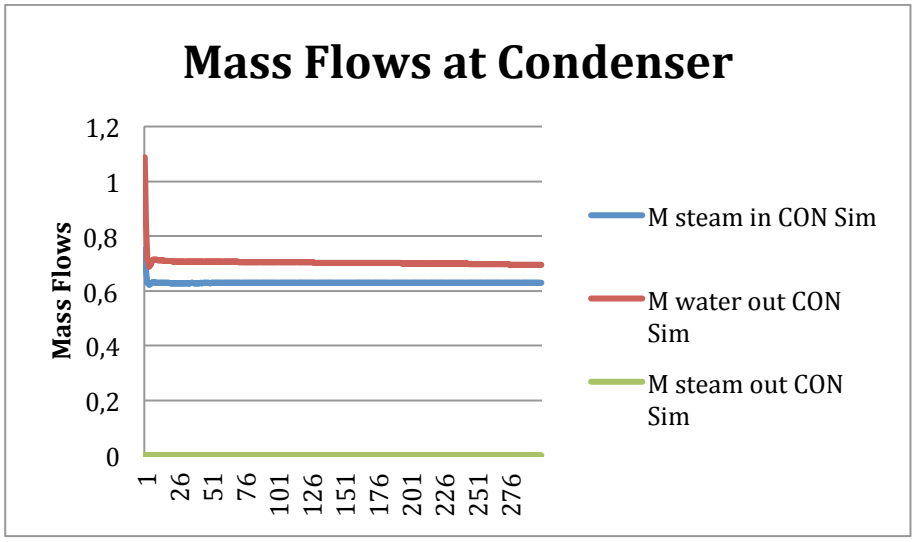

Figure 21.19: Mass flows balance in the condenser

Figure 21.19 shows that the condenser transforms all the steam that exits the low-pressure turbine into water by extracting heat. The vapor mass flow that enters the condenser (blue) is completely condensed into water; hence, the final mass flow of water in the condenser (red) is the sum of all the condensed steam and the little amount of water present in the fluid at the exit of the low-pressure turbine, which explains that the red line is higher than the blue one. Finally, the mass flow of steam at the exit of the condenser is zero (green).

5.3. First Transient Simulation for the New Turbine

The first transient is simulated for 1300 seconds and is realised through a decrease of the mass flow inserted by the fill, and hence the pressure at the inlet of the high-pressure turbine.
Since ATHLET simulations should start under normal operational conditions, the first 100 seconds of simulation are the same as for the steady state, until the second 101 when the transient is introduced.
The mass flow entering the high-pressure turbine is represented in the following graphic.

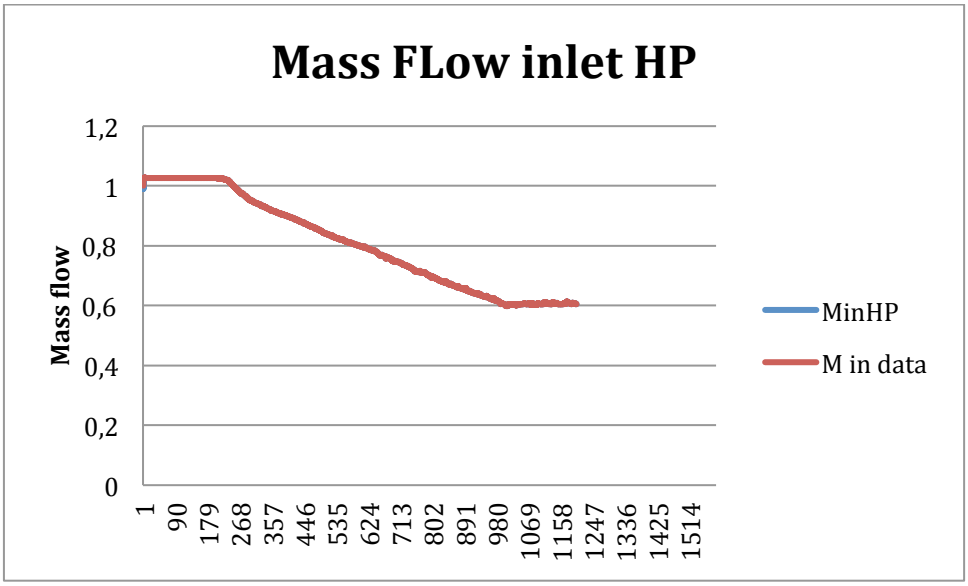

Figure 22.1: Mass flow introduced by the fill (normalized values) during transient

As Figure 22.1 shows, Transient 1 simulates a decrease of around the 40% mass flow in 700 seconds.
The available measured data for the transient simulation is:

- Mass flow at High-Pressure Turbine Inlet
- Pressure at High-Pressure Turbine Inlet
- Pressure at High-Pressure Turbine Extraction
- Pressure at High-Pressure Turbine Outlet
- Pressure at Separator Outlet
- Pressure at Low-Pressure Turbine First Extraction
- Pressure at Low-Pressure Turbine Second Extraction
- Pressure at Condenser Inlet

Therefore, all these sets of data can be compared to those obtained from the simulation. For this reason, the results obtained from the ATHLET simulations

have been interpolated within intervals of time of 1 second in order to be compared to the available measurements.
The mass flow at the inlet of the high-pressure turbine is an input for the fill simulation; thus, it coincides exactly with the measurement data as Figure 22.1 shows.
The pressure at the inlet of the high-pressure data obtained with the simulation is compared to the pressure from the measurements in Figure 22.2.
This comparison shows that the pressures are pretty closed. The bigger difference appears when the transient data is introduced (second 101 of simulation).

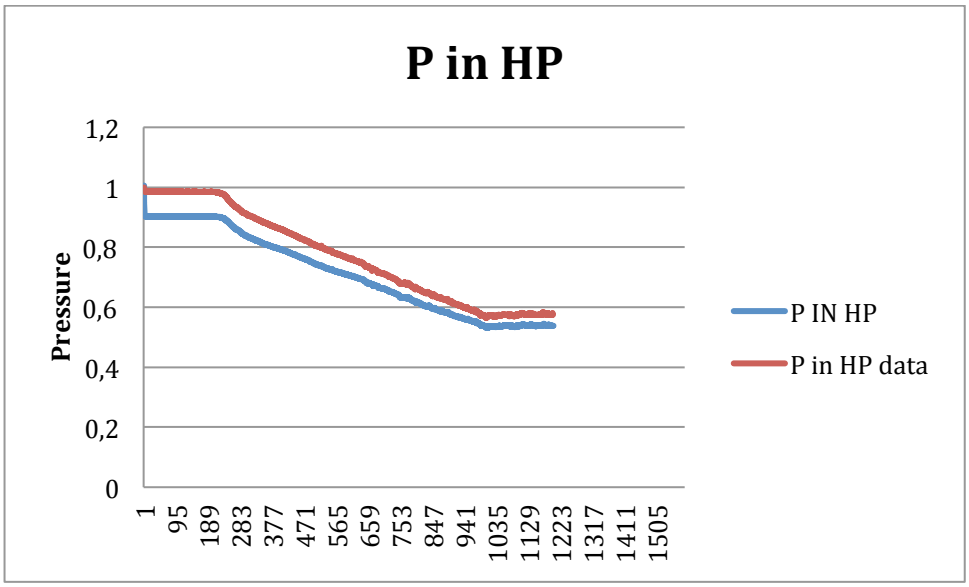

Figure 22.2: Pressure at the inlet of the high-pressure turbine during transient simulation

Since the available measured data is for the transient simulation, the comparison between the properties has been performed only for the transient part, which means, from 101 seconds until the end of the simulation because there is no available measured data under normal operational conditions.
The simulated pressure at the extraction of the high-pressure turbine has been measured in the turbine CV where the extraction is situated, and it has been compared to the measured one. In addition, although there is no measure to compare with, the mass flow of the extracted steam is represented in Figure 22.4. This mass flow decreases as the total mass flow of the high-pressure turbine inlet decreases.

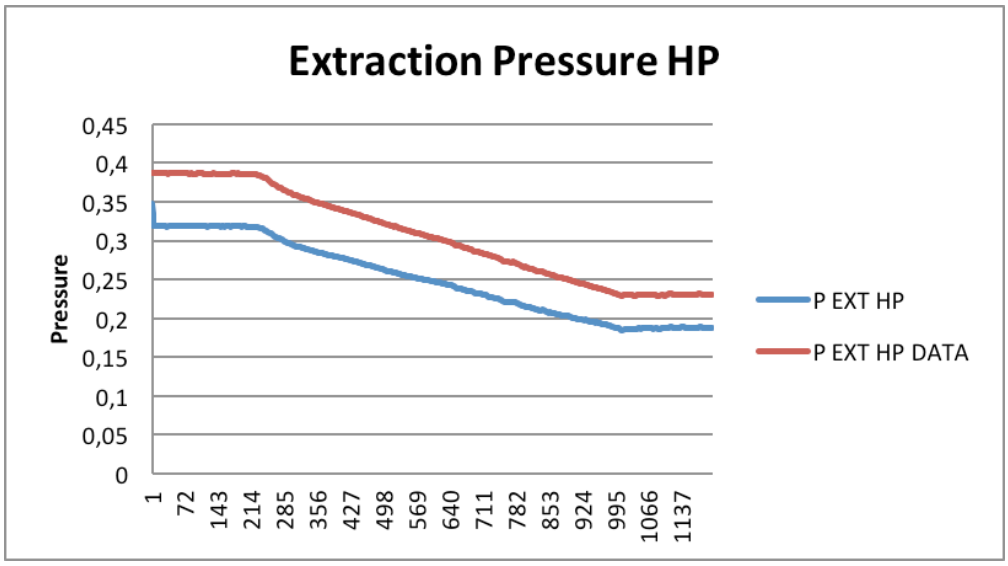

Figure 22.3: Pressure at the high-pressure turbine extraction during transient simulation

The mass flows of steam extracted by the HP turbine extraction decreases over time as the total mass flow at its inlet decreases during the transient.

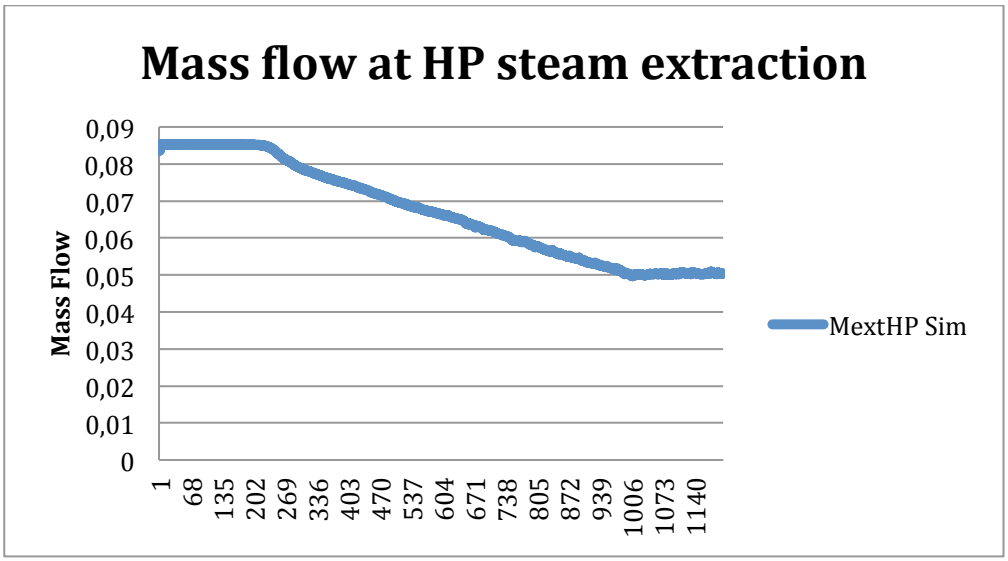

Figure 22.4: Steam mass flow extracted in the high-pressure turbine

The pressure at the outlet of the high-pressure turbine has also been compared to the measured one.

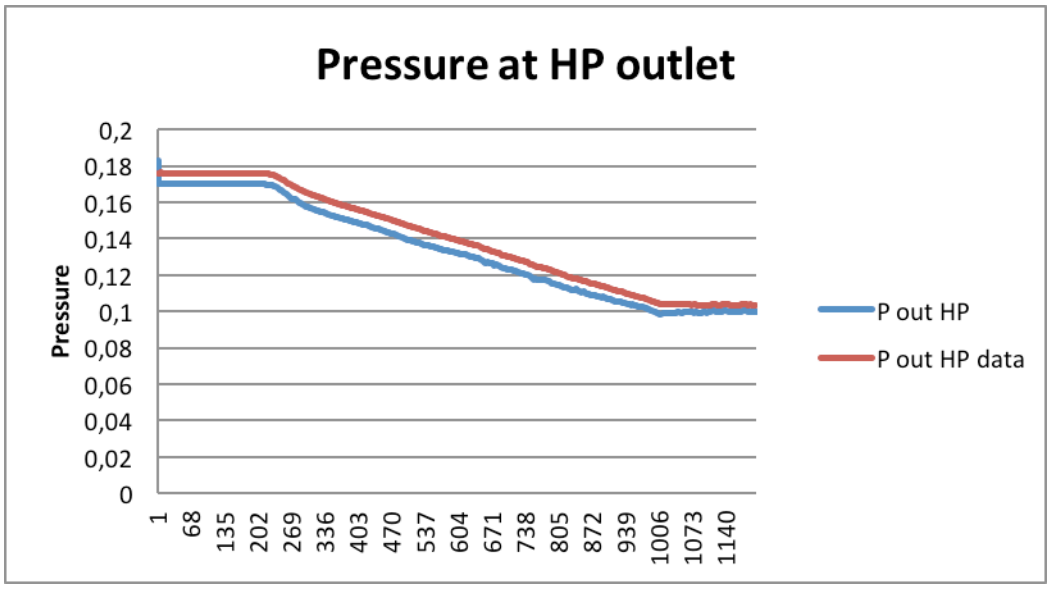

Figure 22.5: Pressure at the outlet of the high-pressure turbine during transient simulation

The pressure drop in the high-pressure turbine can also be calculated during the transient as the difference between the inlet and outlet pressure.

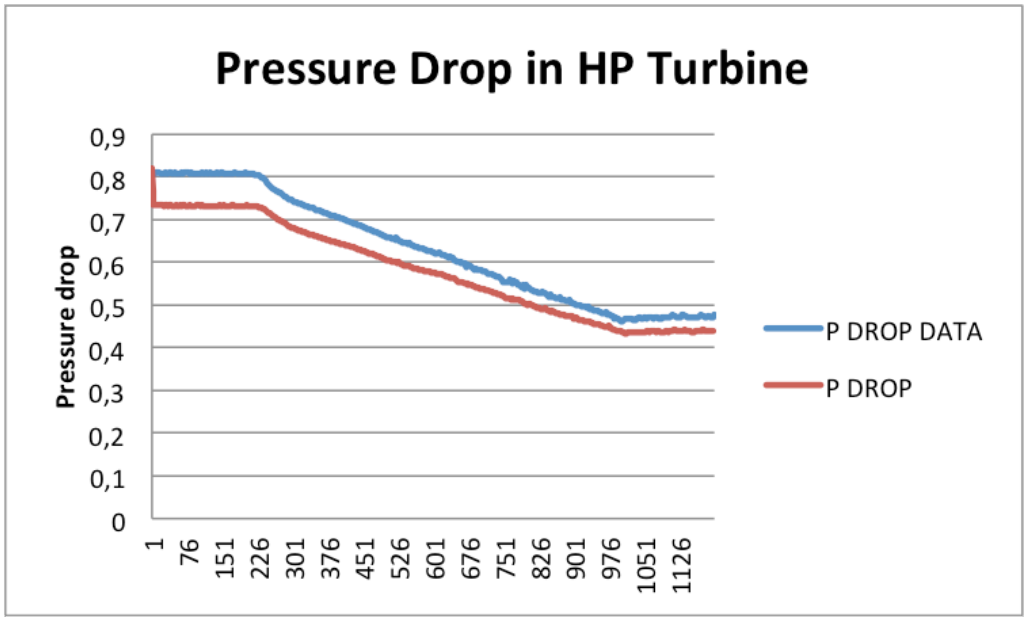

Figure 22.6: Pressure drop in high-pressure turbine comparison for simulation and measurements

The mean percentage error of the simulated pressure drop in the high-pressure turbine during the first transient is 7,779%, with a maximum of 9,507% and a minimum of 5,08%.

The pressure at the steam outlet of the steam-water separator has been compared to the real measurement data as well.

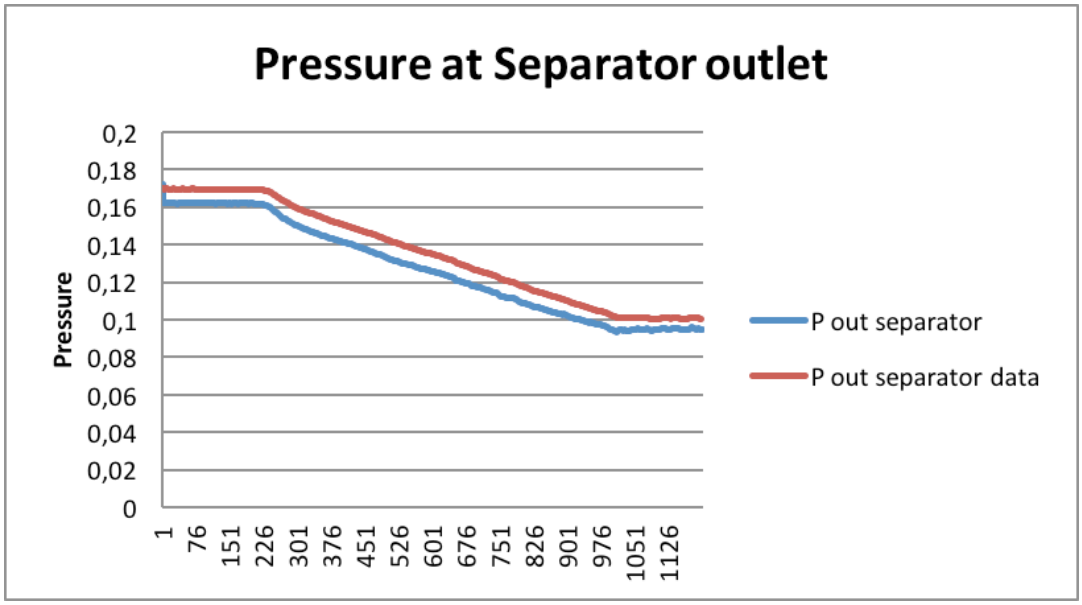

Figure 22.7: Pressure at the exit of the steam-water separator during transient simulation

Although there is no real measurement data related to the over-heater, it is interesting to see the evolution of the heat addition as the mass flow is reduced. The heat addition has been defined as a constant source that provides the nominal heat per unit length; thus, at the same rate as the mass flow through the over-heater decreases, the temperature difference between the over-heater inlet and outlet is expected to increase, as well as the steam enthalpy increment, as Figure 22.8 shows.

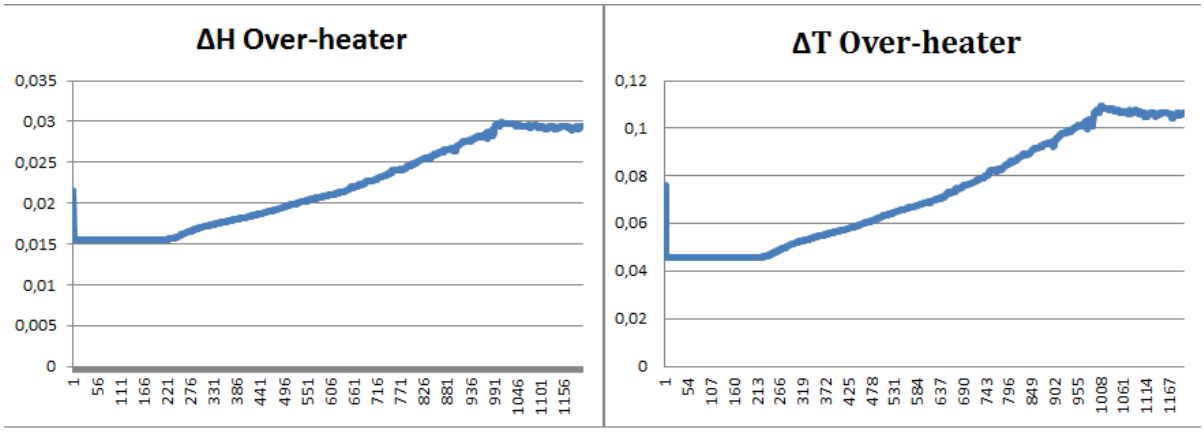

Figure 22.8: ΔT and ΔH in the over-heater during the first transient simulation

$$Q = \dot{m} \cdot (h_{out} - h_{in}) = \dot{m} \cdot \Delta H \qquad \textit{(Equation 31)}$$

The previous equation justifies the increment of ΔH as the mass flow decreases for a constant Q.

Moreover, the pressures at the first and second extractions of the low-pressure turbine have also been measured at the corresponding turbine CVs where they are located and compared to the available measures during the transient.

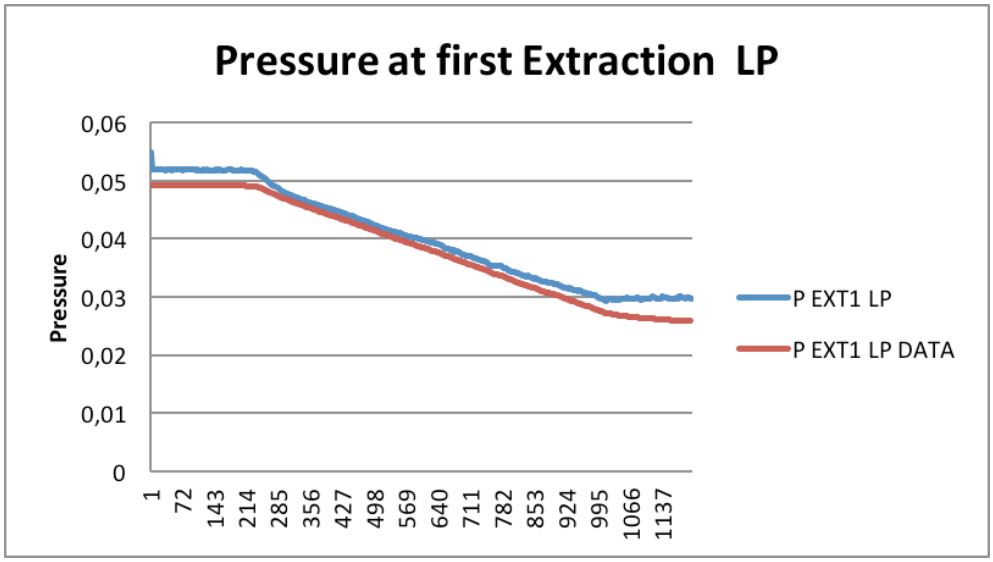

Figure 22.9: Pressure in the first extraction of the low-pressure turbine

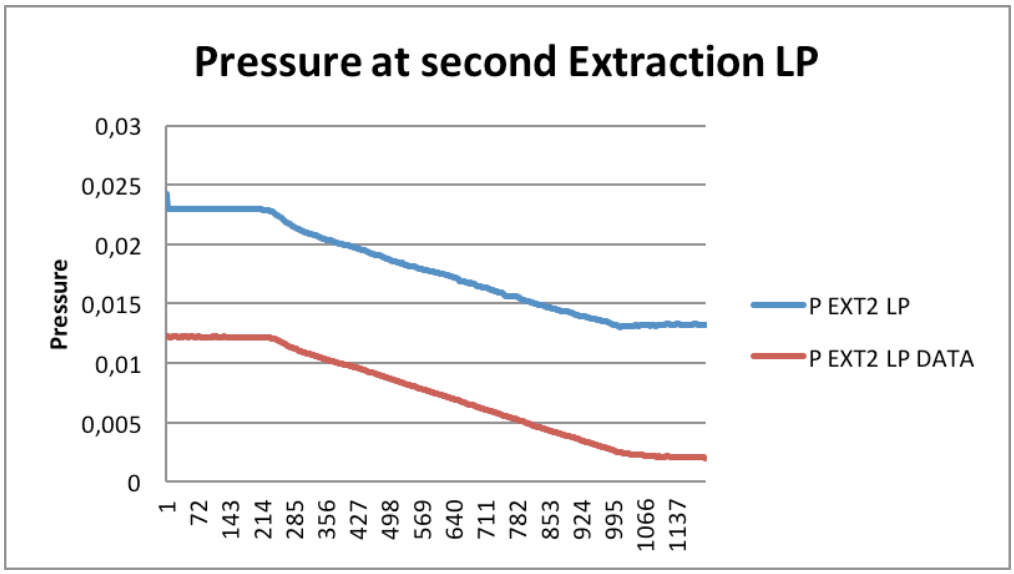

Figure 22.10: Pressure in the second extraction of the low-pressure turbine

Although the difference between the simulated and measured pressure for the second extraction seems large, actually the difference becomes smaller when considering the real values without normalizing.

The mass flows of steam extracted in the first and second extractions of the low-pressure turbine are also shown in Figures 22.11 and 22.12 to prove that they both decrease at the same rate as the mass flow at the inlet of the turbine does.

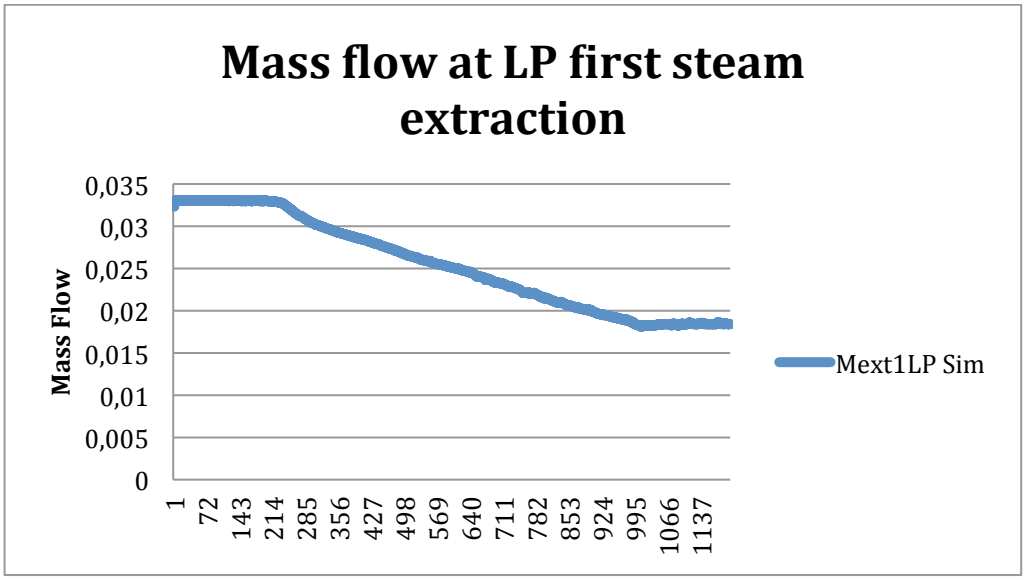

Figure 22.11: Steam mass flow extracted in the first steam extraction of the low-pressure turbine

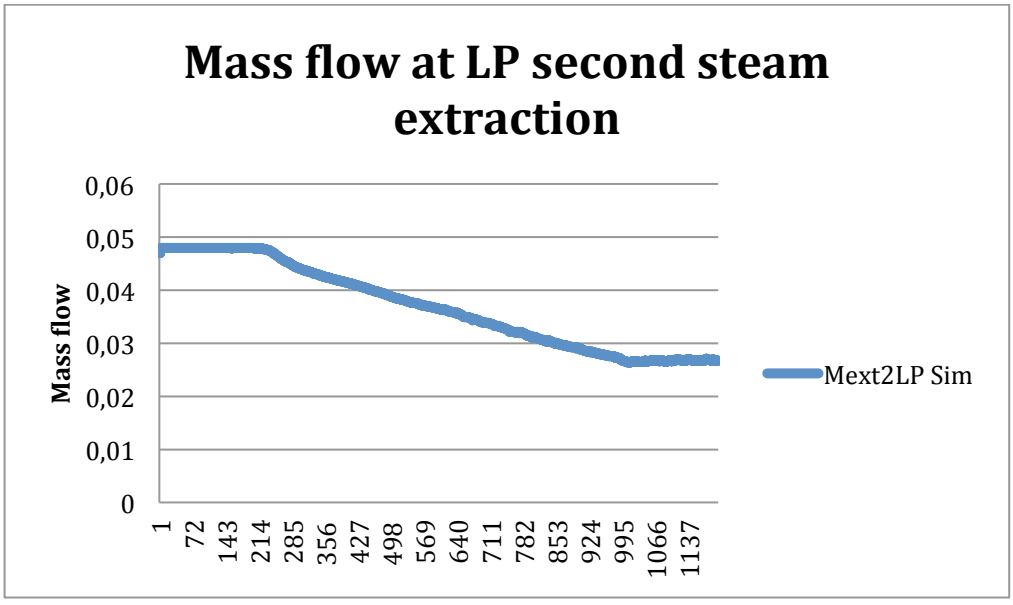

Figure 22.12: Steam mass flow extracted in the second steam extraction of the low-pressure turbine

The last measured pressure is the one at the inlet of the condenser, which has been compared with the given by the ATHLET simulation.

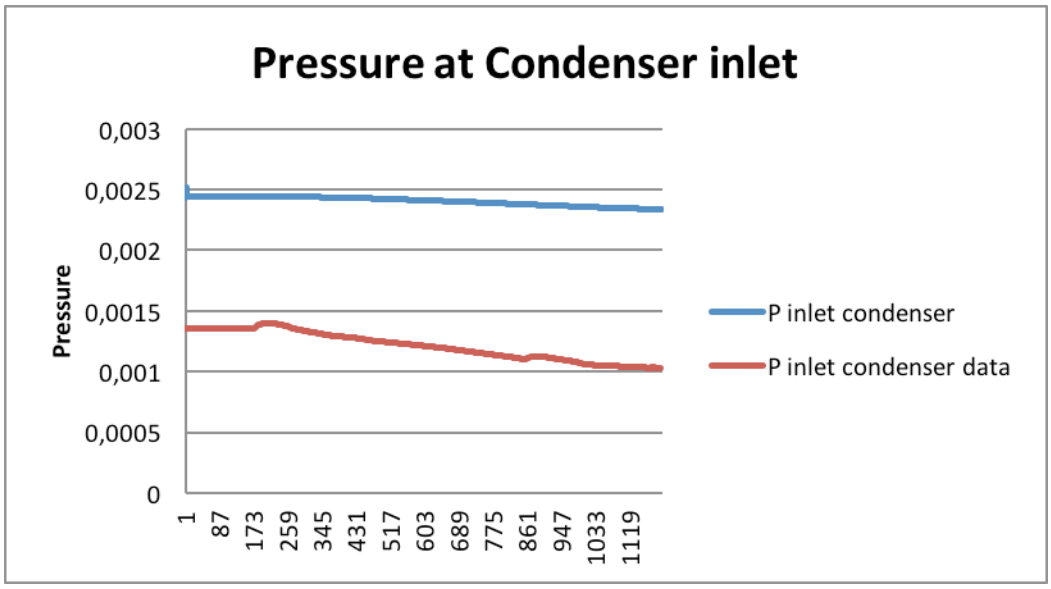

Figure 22.13: Pressure at the inlet of the condenser during transient simulation

As already explained for the steady simulations, the pressure at the inlet of the condenser is higher than the nominal value because of the lack of the last stage in the low-pressure turbine.

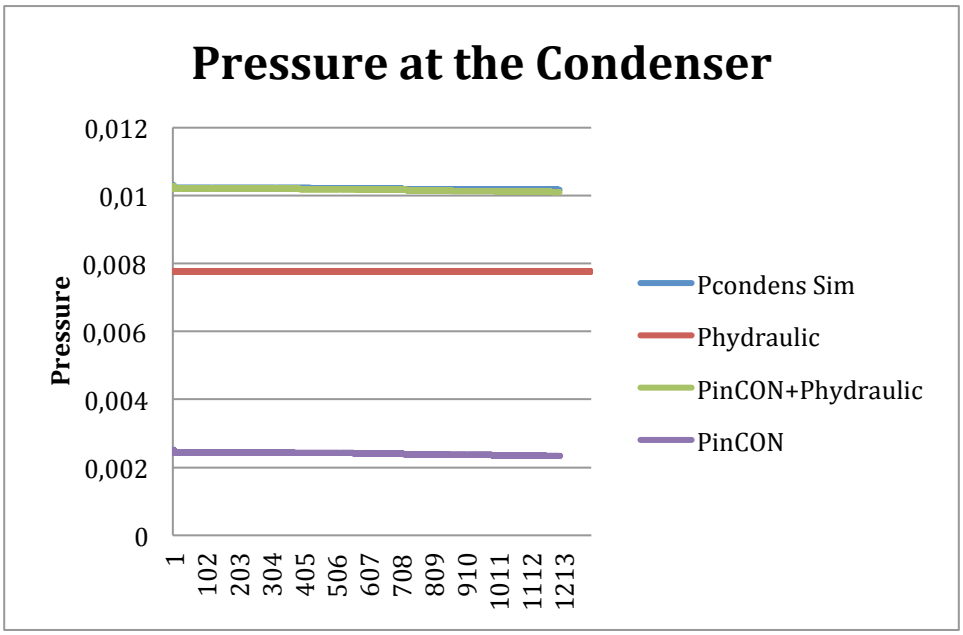

Figure 22.14: Pressure in the condenser

The hydrostatic pressure already mentioned for the steady state simulations affects the condenser CV pressure. Figure 22.14 demonstrates that, indeed the pressure given by ATHLET in the condenser pipe includes the pertinent hydraulic at that point.

5.4. Second Transient Simulation for the New Turbine

The second transient is simulated for 1687 seconds and simulates an increase of the mass flow inserted by the fill, and hence the pressure at the inlet of the high-pressure turbine.
Similar as for the first transient, the first 100 seconds of simulation are steady state, until the second 101 when the transient is introduced. Since the results have been compared to the available measurements for transients, the first 100 seconds of simulation are not included in the graphics.
The mass flow entering the high-pressure turbine is represented in the following graphic.

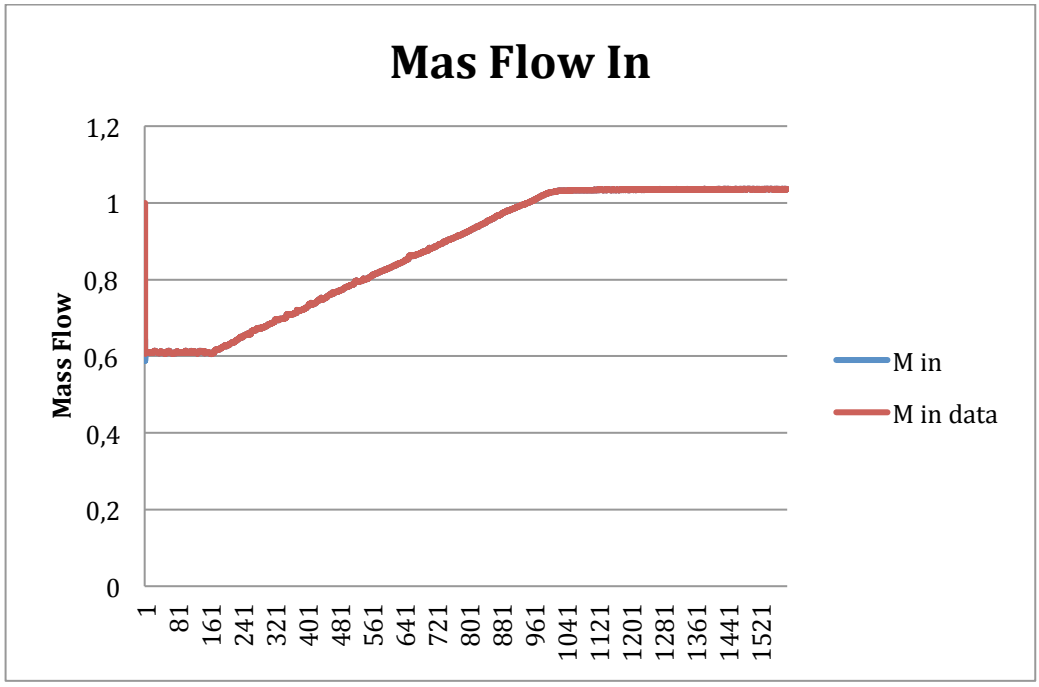

Figure 23.1: Mass flow introduced by the fill (normalized values) during transient

As Figure 23.1 shows, Transient 2 starts with a mass flow value of 60% the nominal one. The following 800 seconds simulate an increase in the mass flow value of around the 40%, ending a little above the nominal mass flow value.
The available measured data for the transient simulation is the same mentioned for Transient 1. Therefore, all these sets of data are compared in the same way as already described for the first transient, after interpolating the obtained values as well.
The pressure at the inlet of the high-pressure data obtained with the simulation is compared to the pressure from the measurements in Figure 23.2.

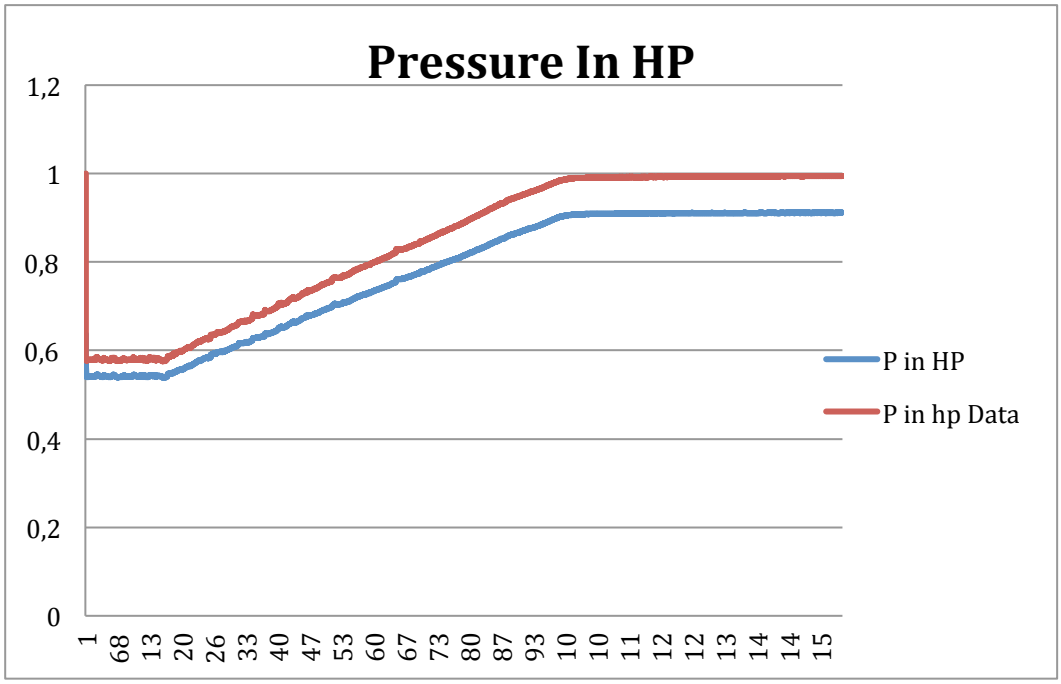

Figure 23.2: Pressure data at the inlet of the High-Pressure Turbine during transient simulation

The simulated pressure at the extraction of the high-pressure turbine has been measured in the turbine CV where the extraction is situated, and it has been compared to the measured one, as well as the pressure at the outlet of the turbine.

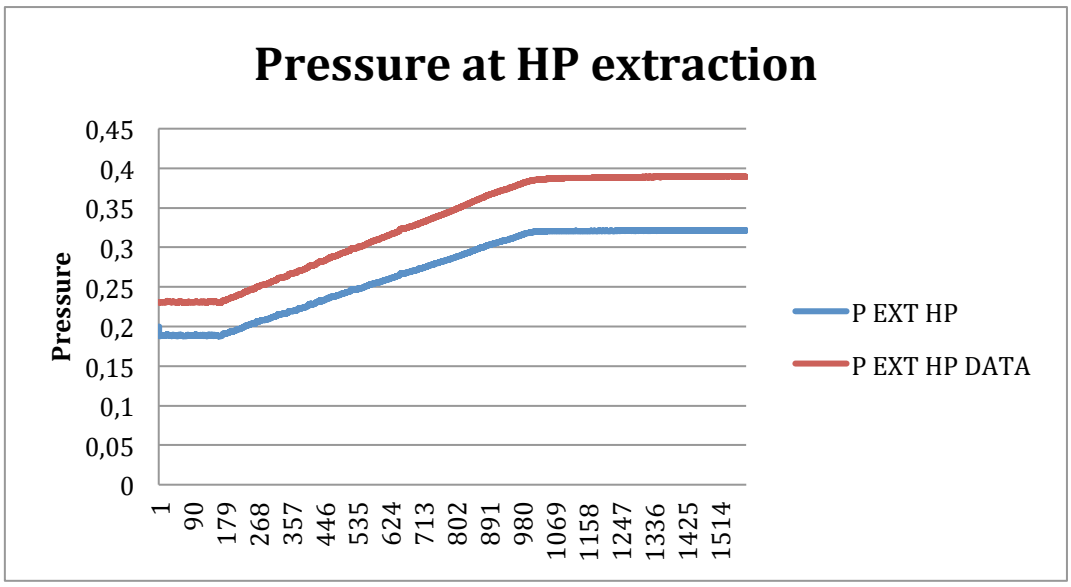

Figure 23.3: Pressure at the extraction of the high-pressure turbine during transient simulation

The steam mass flow extracted in the HP turbine is represented in the annexes as Figure A.9.

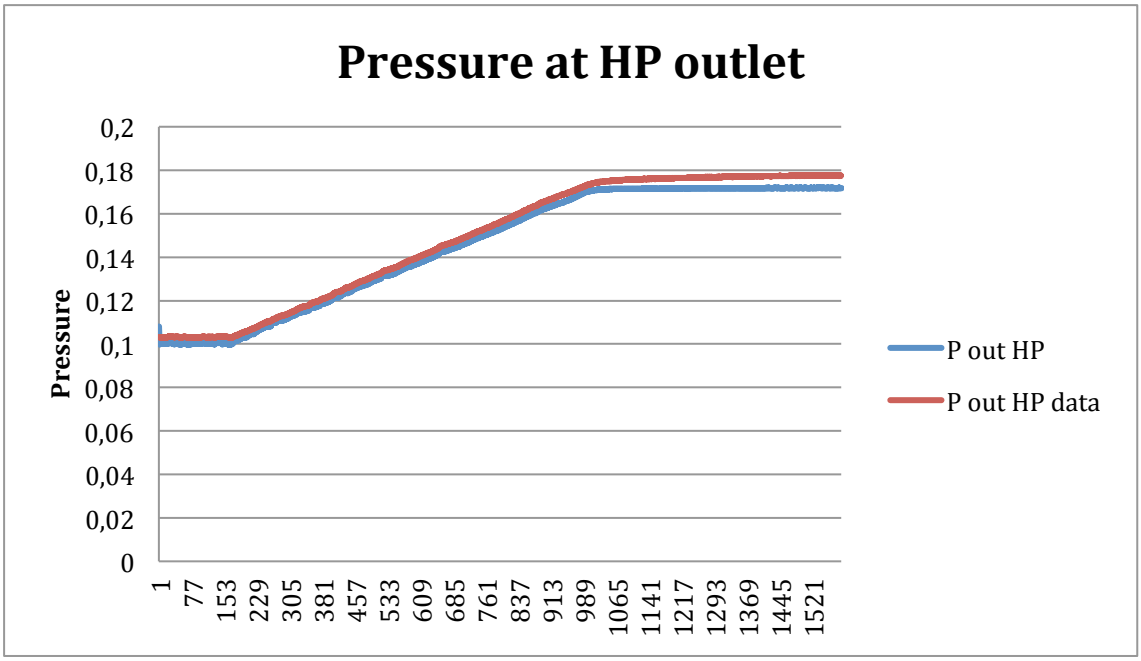

Figure 23.4: Pressure at the outlet of the high-pressure turbine during transient simulation

The pressure drop in the high-pressure turbine can also be calculated during the transient as the difference between the inlet and outlet pressure.

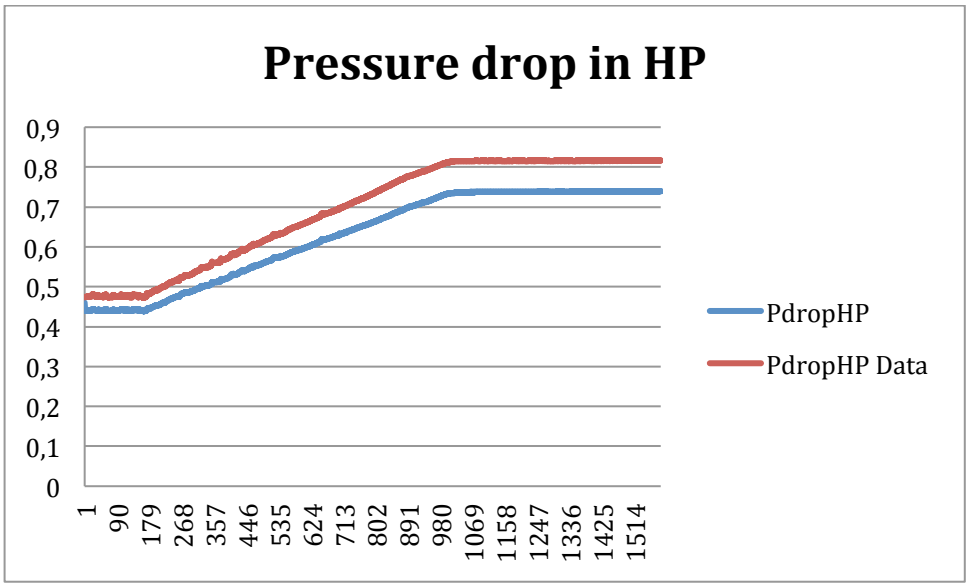

Figure 23.5: Pressure drop within the high-pressure turbine for the measured and the simulated data

The pressure drop through the high-pressure turbine in the simulation is lower than the calculated pressure drop from the measured data. The maximum percentage error is 10,13%.

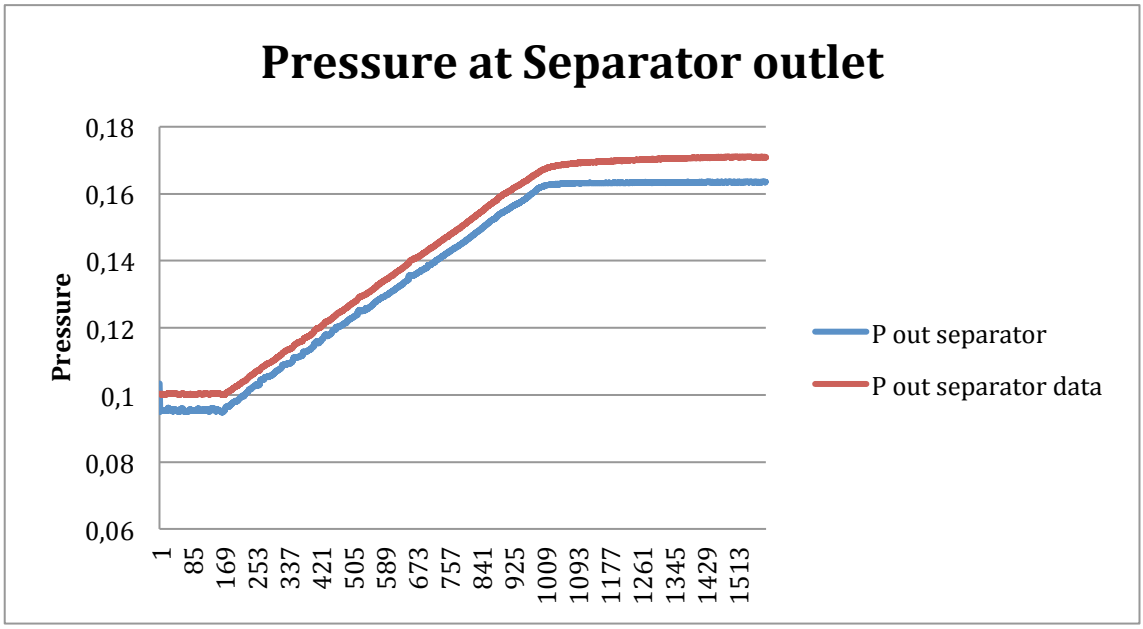

Figure 23.6: Pressure at the exit of the steam-water separator during transient simulation

Regarding the over-heater, in contrast to the increment in ΔT and ΔH during the first transient, the second transient causes a decrement in ΔT and ΔH because the mass flow increases over time (Equation 31).

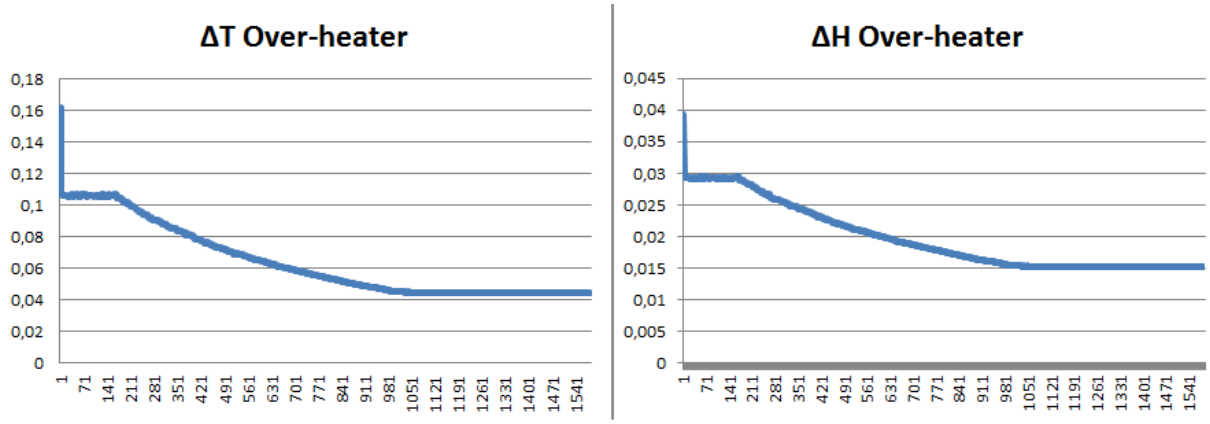

Figure 23.7: ΔT and ΔH in the over-heater during the second transient simulation

Moreover, the pressures at the first and second extractions of the low-pressure turbine have also been measured at the corresponding turbine CVs where they are located and compared to the available measures during the transient.

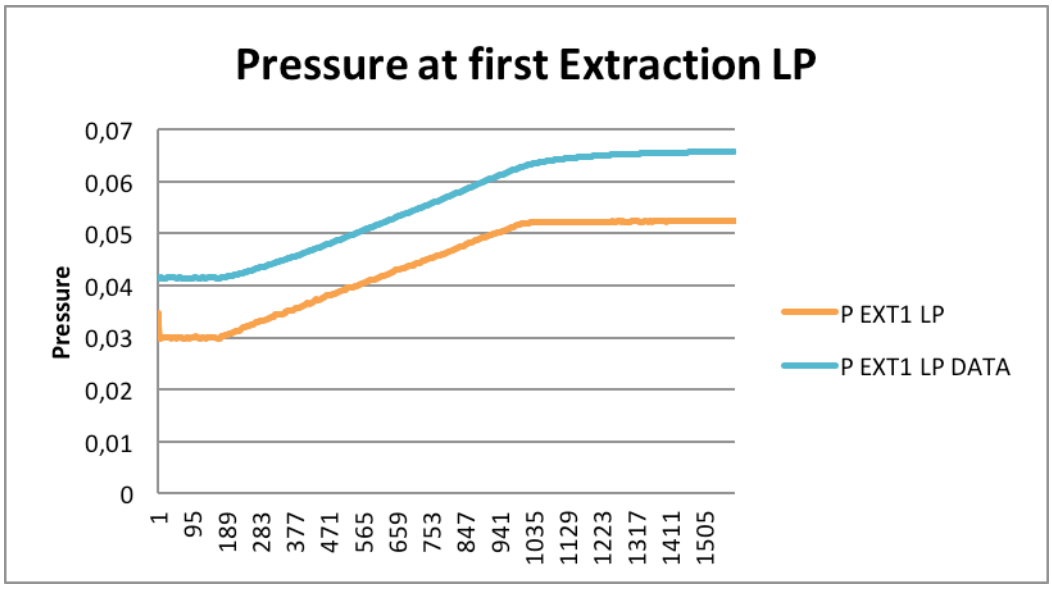

Figure 23.8: Pressure in the first extraction of the low-pressure turbine

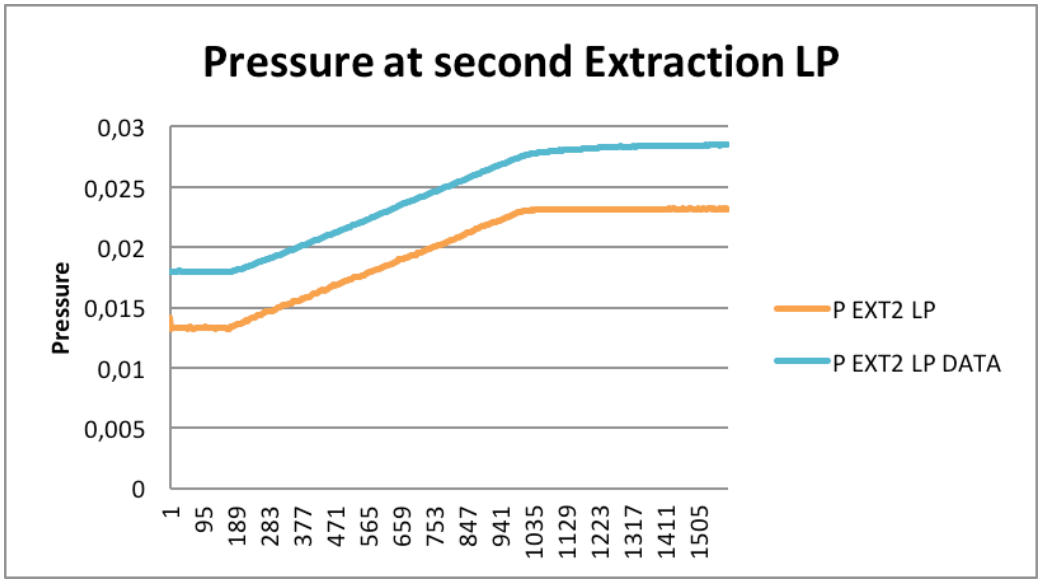

Figure 23.9: Pressure in the second extraction of the low-pressure turbine

Although the difference between the simulated and measured pressure for the second extraction seems large, actually the difference becomes smaller when considering the real values without normalizing.

The mass flows of these extractions cannot be compared to measured data but they increase at the same rate as the mass flow at the inlet does, and their graphics have been included in annexes (Figures A.10 and A.11).

The simulated pressure at the inlet of the condenser, which corresponds to the exit of the low-pressure turbine, is higher than the nominal value, because the last stage of the turbine is not modeled.

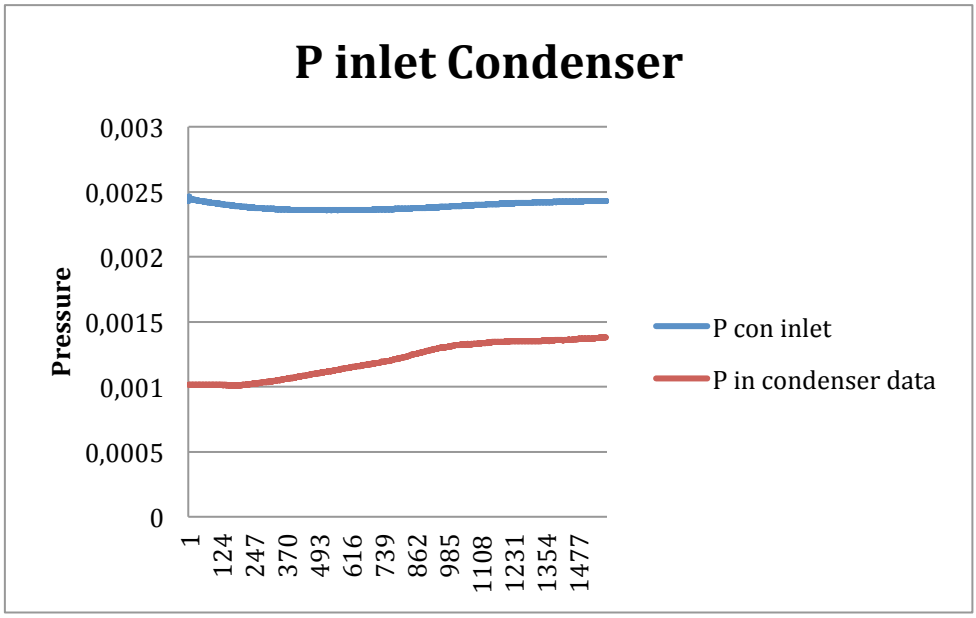

Figure 23.10: Pressure at the inlet of the condenser during transient simulation

As already explained for the previous simulations, the pressure in the condenser is higher than the fluid pressure because of the term of the hydraulic pressure water. Figure 23.11 shows the relation between the pressure of the steam at the inlet of the condenser, the hydraulic pressure and the total pressure in the center of the condenser CV, which is the one given by ATHLET.

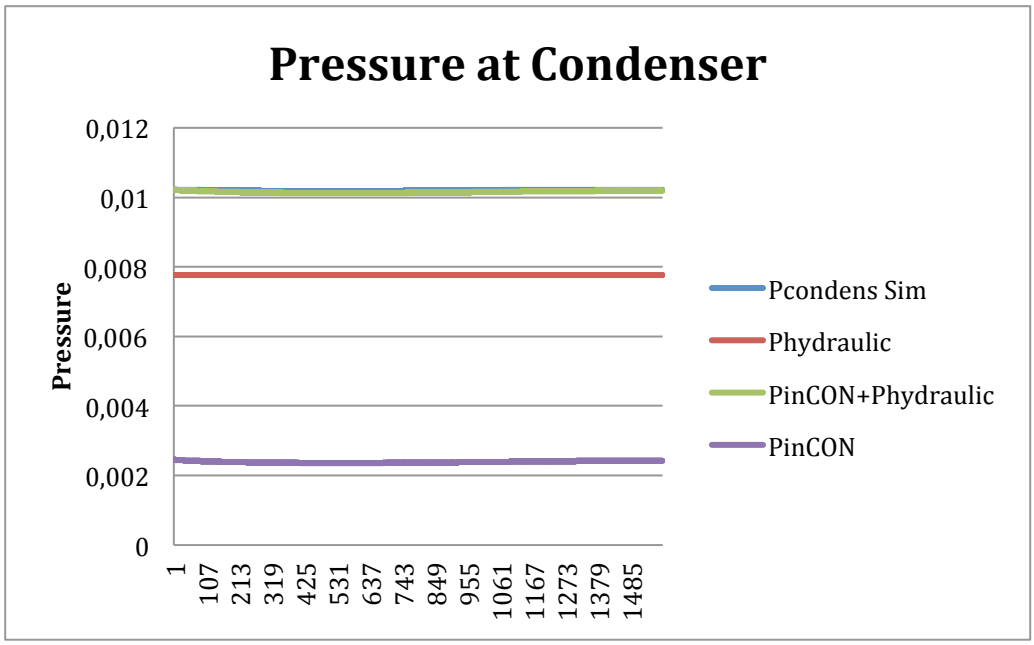

Figure 23.11: Pressure in the condenser

5.5. Third Transient Simulation for the New Turbine

The third transient is simulated for 2000 seconds and is given by a decrease of the mass flow inserted by the fill, and hence the pressure at the inlet of the high-pressure turbine.
As well as for the first and second transients, the first 100 seconds of simulation are the same as for the steady state, until the second 101 when the transient is introduced.
The mass flow entering the high-pressure turbine is represented in the following graphic.

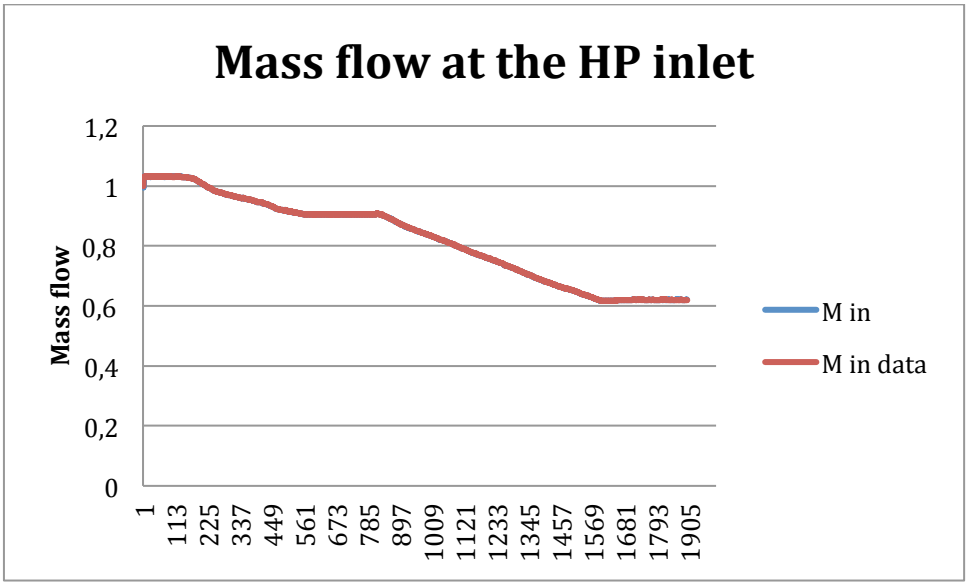

Figure 24.1: Mass flow introduced by the fill (normalized values) during transient

As Figure 24.1 shows, Transient 3 starts with a mass flow around the nominal one, and it decreases during around 1300 seconds until it is reduced to the 60% of the nominal value.
The available measured data for the transient simulation is the same mentioned for the first transient. Therefore, all these sets of data are compared in the same way as already described for the first and second transients, after interpolating the obtained values as well.
The pressure at the inlet of the high-pressure data obtained with the simulation is compared to the pressure from the measurements in Figure 24.2.

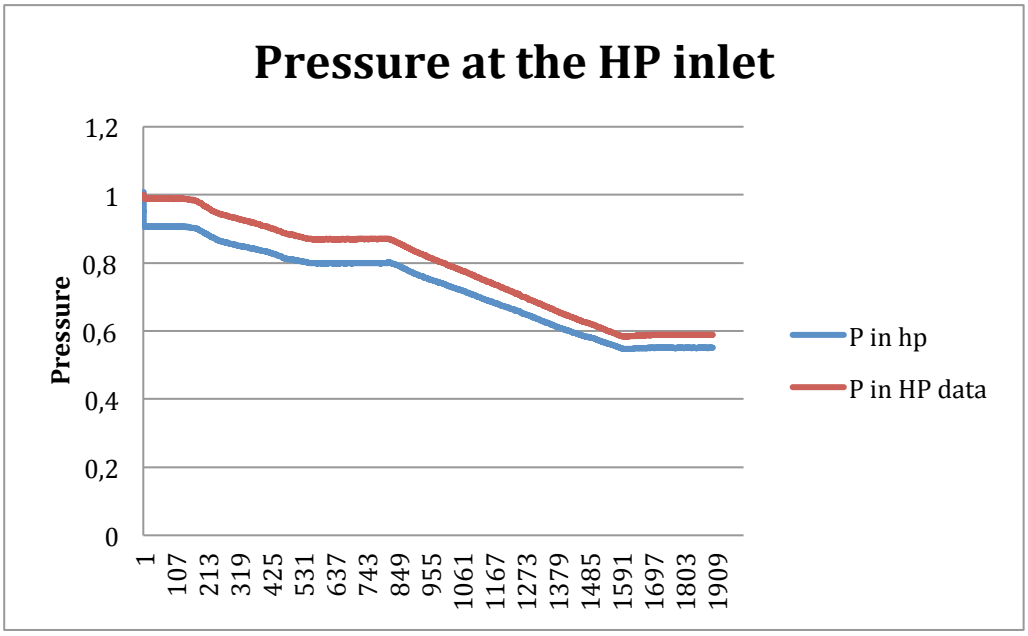

Figure 24.2: Pressure at the inlet of the high-pressure turbine during transient simulation

The simulated pressure at the extraction of the high-pressure turbine has been measured in the turbine CV where the extraction is situated, and it has been compared to the measured one.

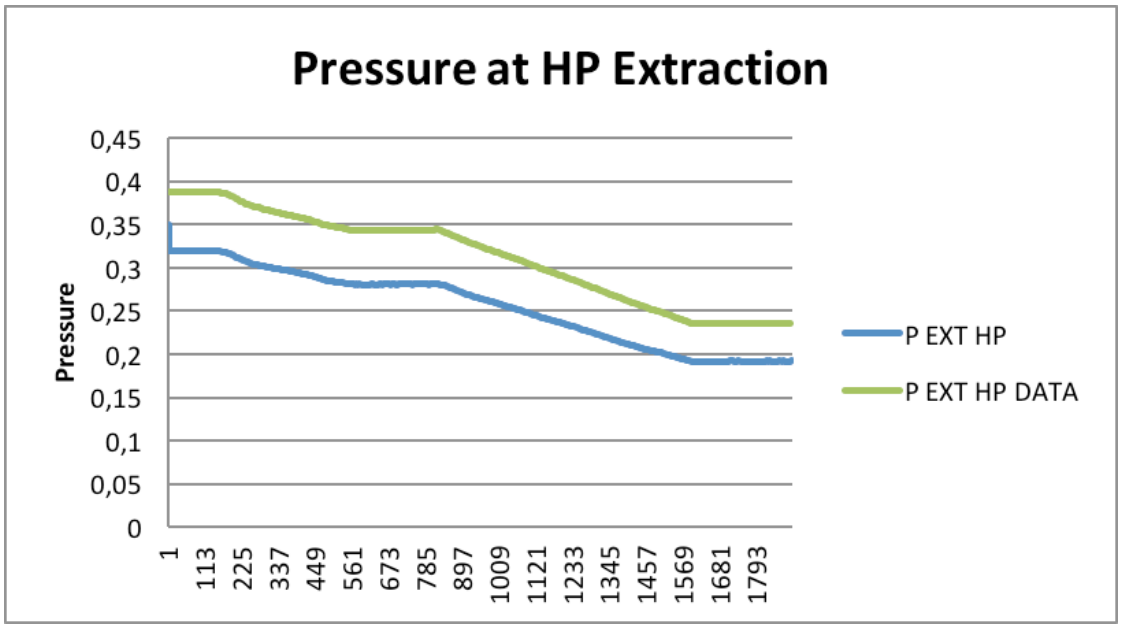

Figure 24.3: *Pressure at the extraction of the high-pressure turbine during transient simulation*

The steam mass flow extracted in the HP turbine is represented in Figure A.13 within the annexes section.

The pressure at the outlet of the high-pressure turbine has also been compared to the measured one.

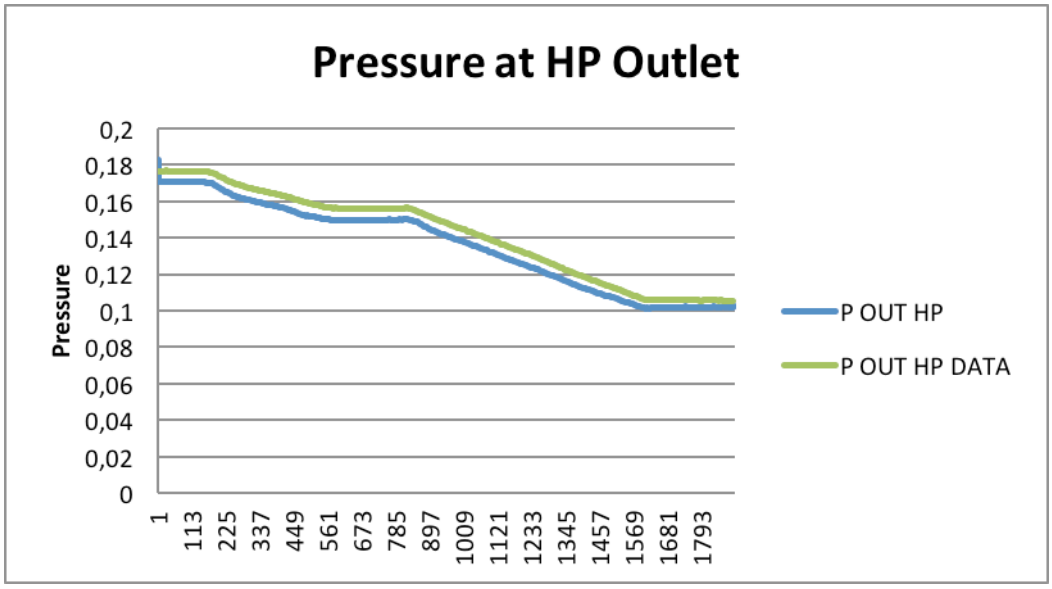

Figure 24.4: Pressure at the outlet of the high-pressure turbine during transient simulation

The pressure drop in the high-pressure turbine can also be calculated during the transient as the difference between the inlet and outlet pressure.

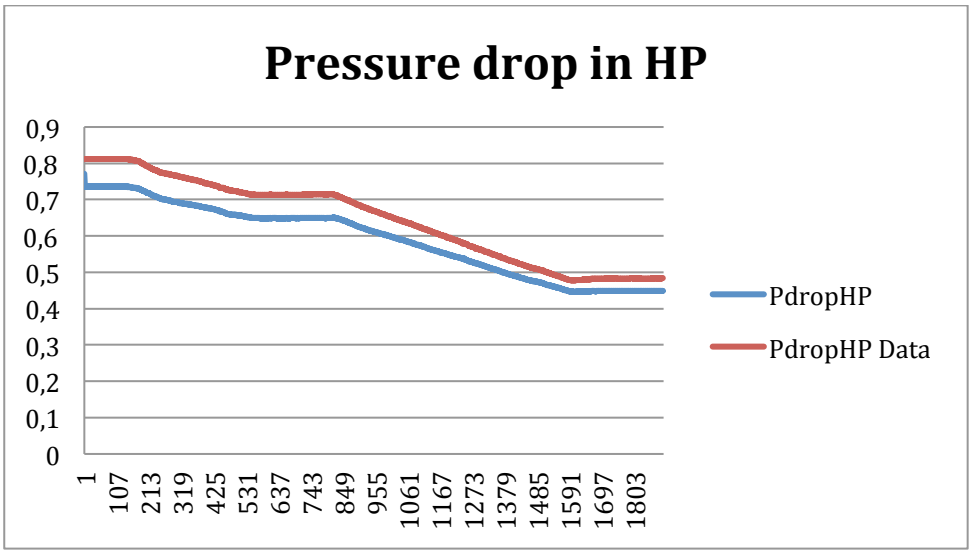

Figure 24.5: Pressure drop within the high-pressure turbine for the measured and the simulated data

The mean percentage error of the simulated pressure drop is 8,23%, with a maximum of 9,45%.
The pressure at the steam outlet of the steam-water separator has been compared as well.

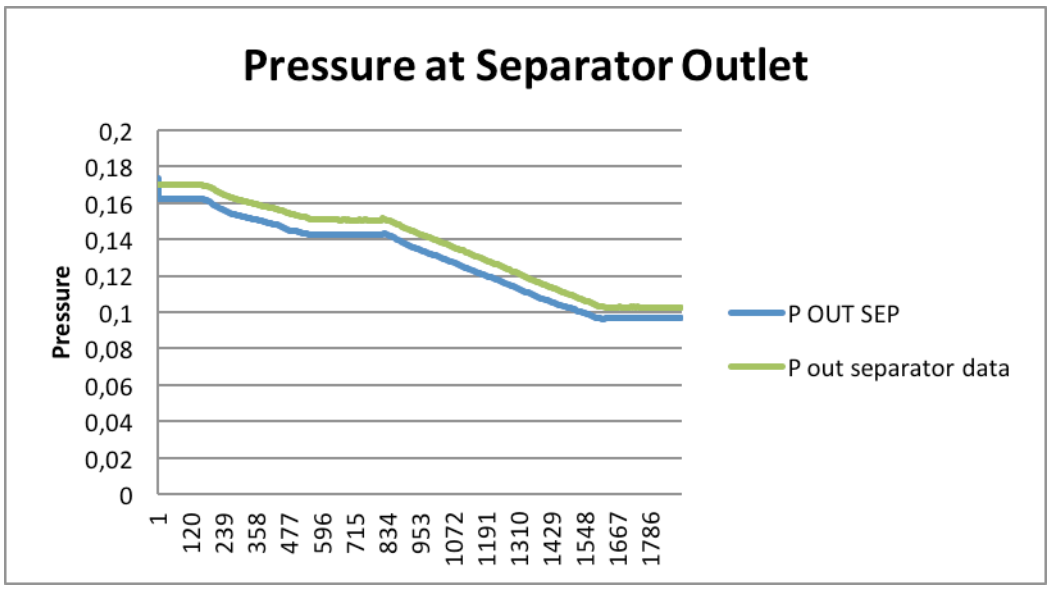

Figure 24.6: pressure at the exit of the steam-water separator during transient simulation

As well as for the previous transients, the pressures at the first and second extractions of the low-pressure turbine have also been measured at the corresponding turbine CVs where they are located and compared to the available measures during the transient.

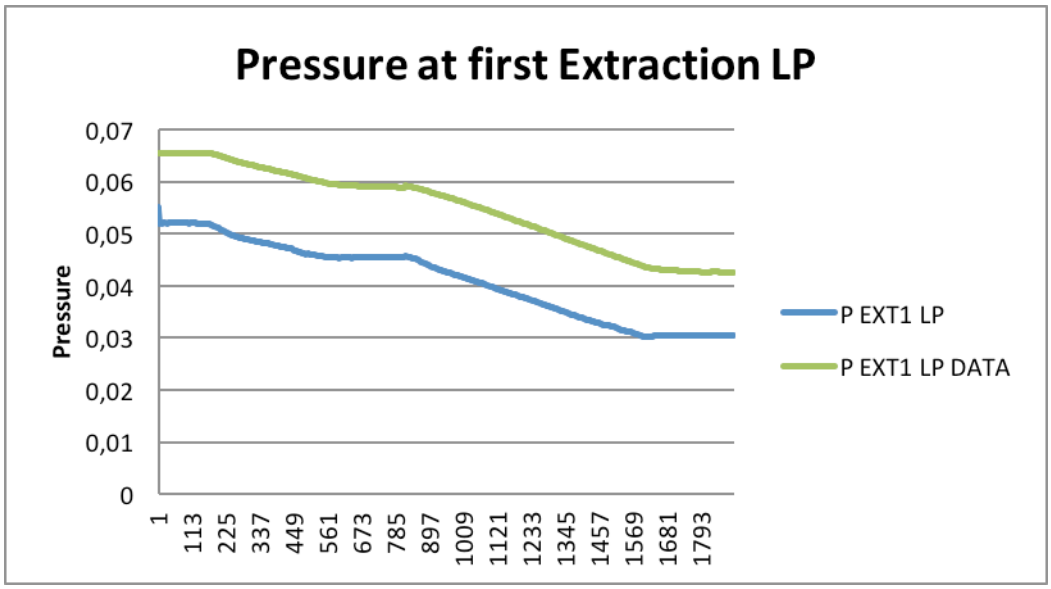

Figure 24.7: Pressure in the first extraction of the low-pressure turbine

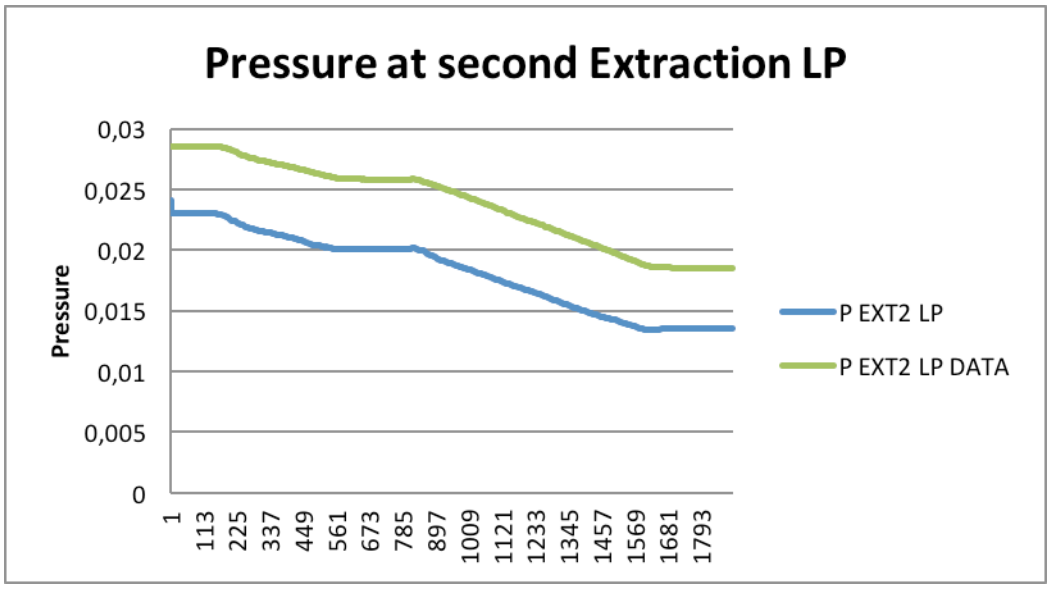

Figure 24.8: pressure in the second extraction of the low-pressure turbine

The mass flows extracted by these extractions decrease over time at the same rate as the inlet mass flow decreases, and its graphics are included as annexes (Figures A.14 and A.15).

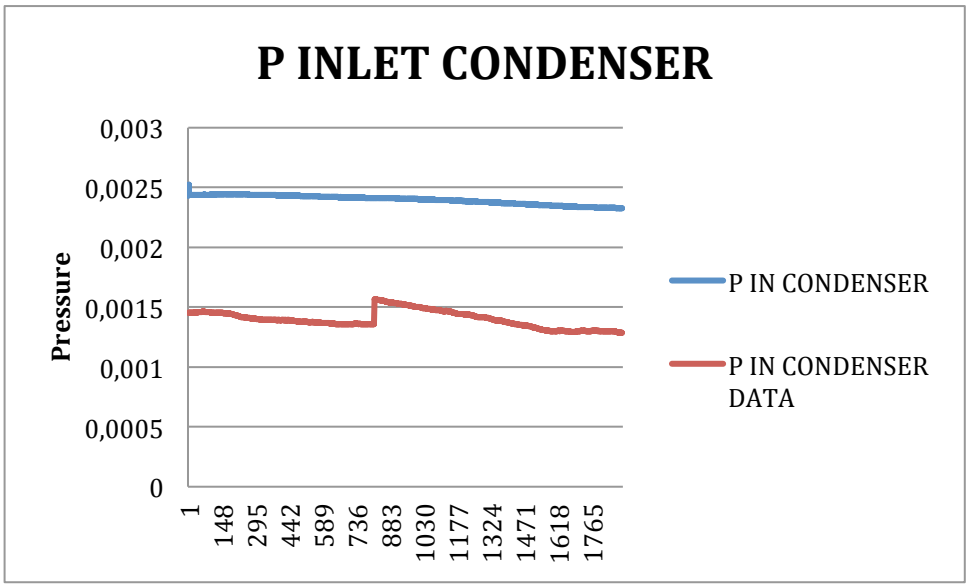

Figure 24.9: Pressure at the inlet of the condenser during transient simulation

The pressure at the inlet of the condenser is higher than the real measurements because the last stage of the turbine is not modeled. Figure 24.10 explains the condenser pressure value given by ATHLET, which takes into account the hydrostatic pressure caused by the condensed water.

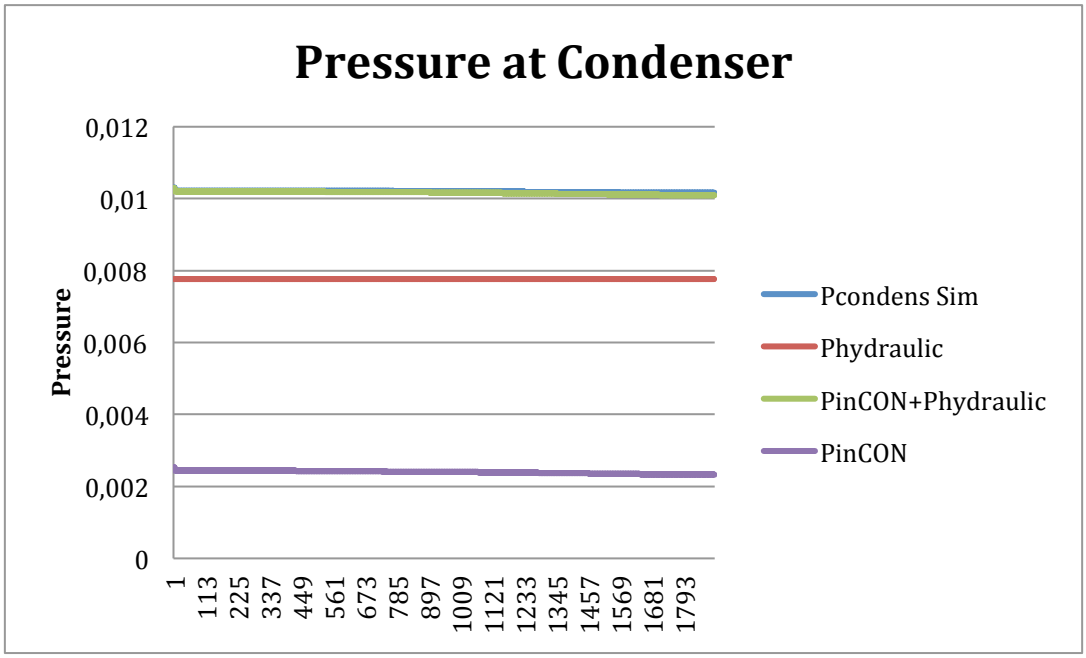

Figure 24.10: Pressure in the condenser

In addition, the ΔT and ΔH increase in the over-heater due to the variation of the mass flow is represented in the same way as for the previous transient simulations, but these graphics are included in the annexes section (Figures A.17 and A.18).

6. CONCLUSIONS

The ATHLET model developed in this work is able to describe relatively well the behavior of the steam turbine of a typical German PWR during normal operation as well as load change transients.
The model has been designed starting from two separated models for the HP and LP turbines. These turbine models were improved and then connected through several pipes and additional components such as water separator and over-heater in order to obtain a more realistic turbine system.
The main objective of the Master´s Thesis was to simulate the steam turbine of a NPP during normal as well as transient operation. This has been achieved and the results obtained are presented and analyzed in the fifth chapter of the thesis. Both steady state and transient simulations results were close to the real plant measurements.
Although the model returns very good results, it can be of course further improved, and the proposed optimization approaches are presented in the next chapter.

7. POSSIBLE FUTURE IMPROVEMENTS OF THE MODEL

This section describes some possible improvements of the model that have not been carried out because of the limited time.

7.1. High-pressure turbine and low-pressure turbine at the same elevation

The model developed for this master thesis can be further optimized by adding additional components in order to obtain the same elevation for the HP turbine and the LP turbine. Here this has not been done, as the focus was on coupling of the HP and LP parts with as little additional losses as possible and the mechanical side of the turbine has not been considered in detail. In the current model, the separator component requires vertical pipes that increase the elevation of the system; that is why the high and low-pressure turbines are not placed at the same elevation. In reality their shafts spin together because they are both connected to the same generator; thus, their shafts are at the same elevation. This could be done next by inserting a vertical pipe in the model at the end of the over-heater which would drive the steam down until the turbine shaft was reached.

7.2. Model over-heater as a heat exchanger

The real over-heater is a heat exchanger that uses part of the steam provided by the steam generator, which means with the same thermal-hydraulical properties as at the inlet of the high-pressure turbine, to heat up the steam after the separator component. In order to simplify the model, a pipe connected to a heat conduction object has been simulated, but the over-heater can be designed by assigning a heat conduction object between two pipes; one containing the steam to be heated up, and the other one containing the saturated steam that transfers its heat and condensates. With this model, the transferred heat would not be a constant source but it would depend on the properties of the saturated steam given by the steam generators.

7.3. Heat source controlled by a signal instead of a constant source for the over-heater

The heat conduction object connected to the over-heater pipe can be designed in a way that the heat addition is controlled by a GCSM signal instead of a constant heat source. This would be interesting to be modeled for the transients' simulation,

since the provided heat power could change as the mass flow varies, while the increment of temperature and enthalpy between the inlet and outlet of the pipe would remain constant. However, additional measured data about temperatures or enthalpies in the over-heater during the transient simulation would be required, or some approximations would be necessary in order to control this heat addition with a GCSM signal.

8. BIBLIOGRAPHY

[1] *Macián (2014), TU Munich, Course: Fundamentals of Nuclear Engineering, Page 11.*

[2] *Macián (2014), TU Munich, Course: Fundamentals of Nuclear Engineering, Page 78.*

[3] *Macián (2014), TU Munich, Course: Fundamentals of Nuclear Engineering, Page 11.*

[4] *Pressurized Water Reactor (PWR) Systems, USNRC Technical Training Center, Reactor Concepts Manual.*

[5] *Richard Schreiber, Nuclear Engineering Handbook, Section 1, Chapter 2 PWR.*

[6] *R. K. Kapooria, S. Kumar, K. S. Kasana, Journal of Energy in Southern Africa, Vol 19 No 1, February 2008.*

[7] *Woodford, Chris (2010) Steam Turbines.*

[8] *ATHLET User's Manual*

[9] *ATHLET Models and Methods*

ANNEXES

This section includes graphics representing some obtained results that have not been included within the results section.

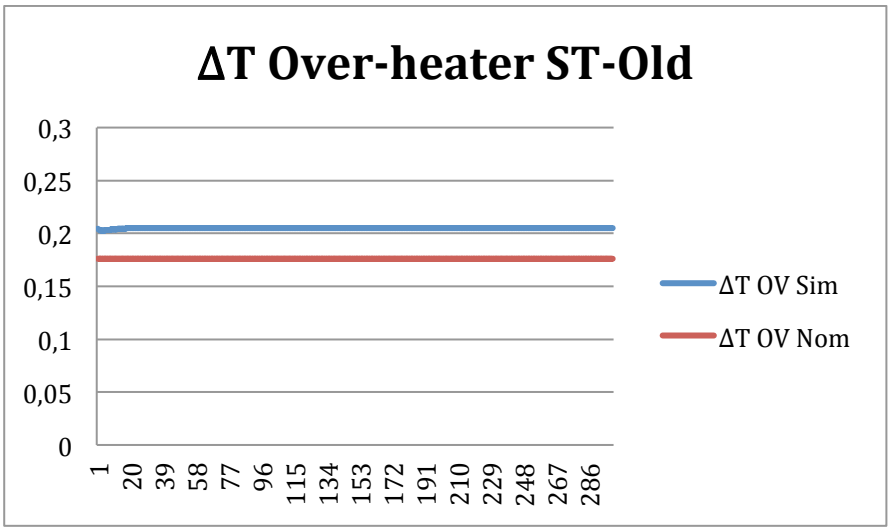

Figure A.2: ΔT in the Over-heater during the old turbine´s steady state model

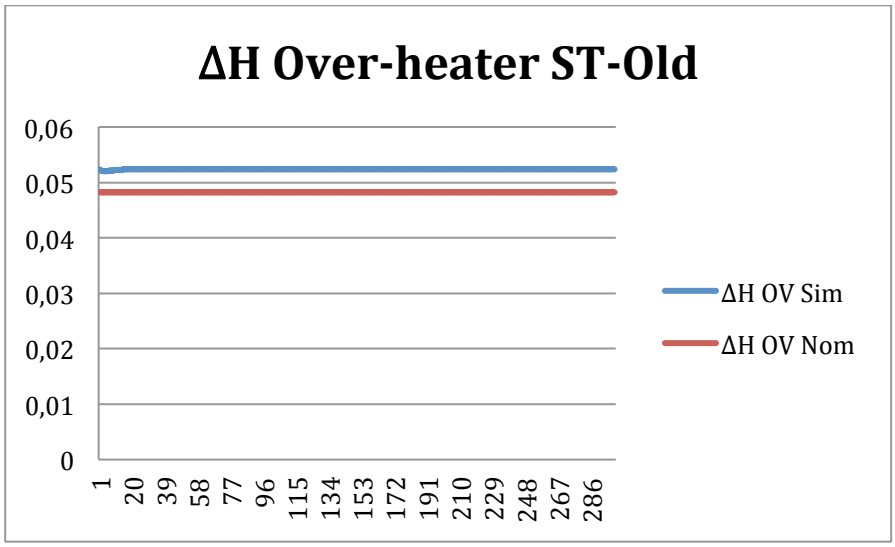

Figure A.3: ΔH in the Over-heater during the old turbine´s steady state

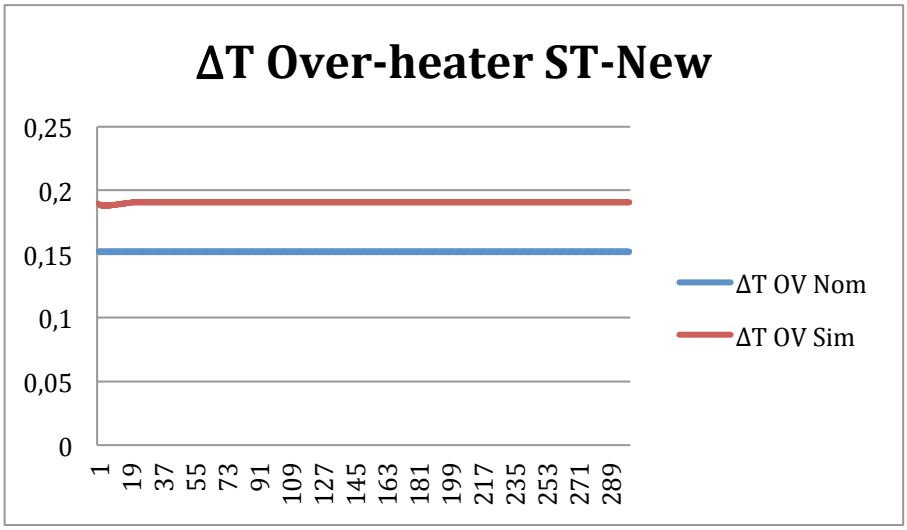

Figure A.4: ΔT in the Over-heater during the new turbine´s steady state model

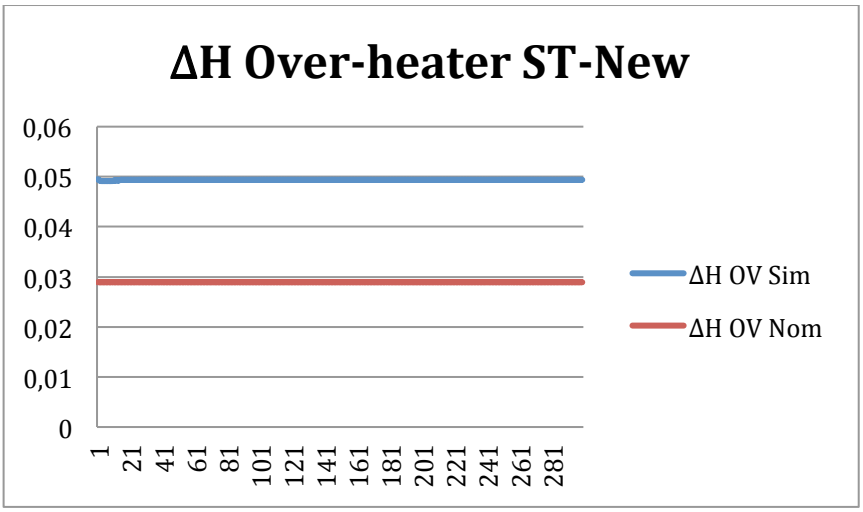

Figure A.5: ΔH in the Over-heater during the new turbine´s steady state model

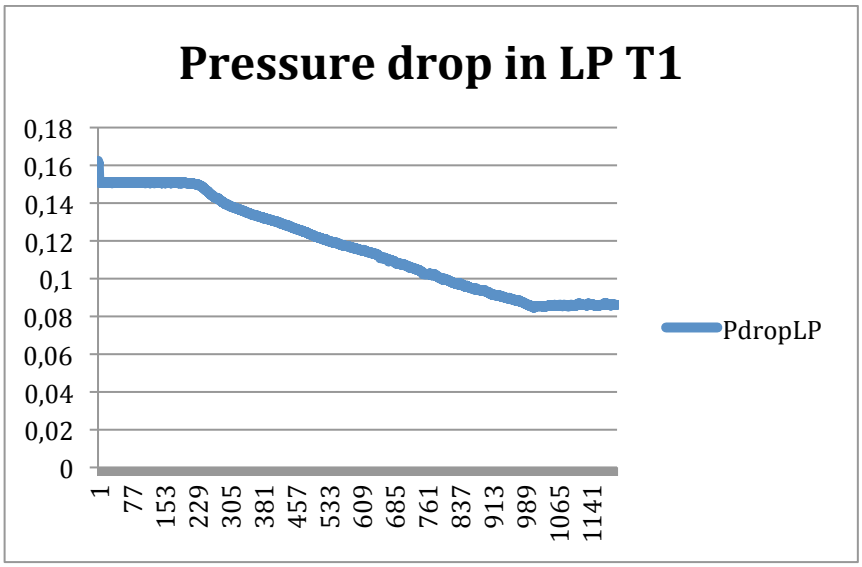

Figure A.6: Pressure drop in LP turbine during the first transient simulation

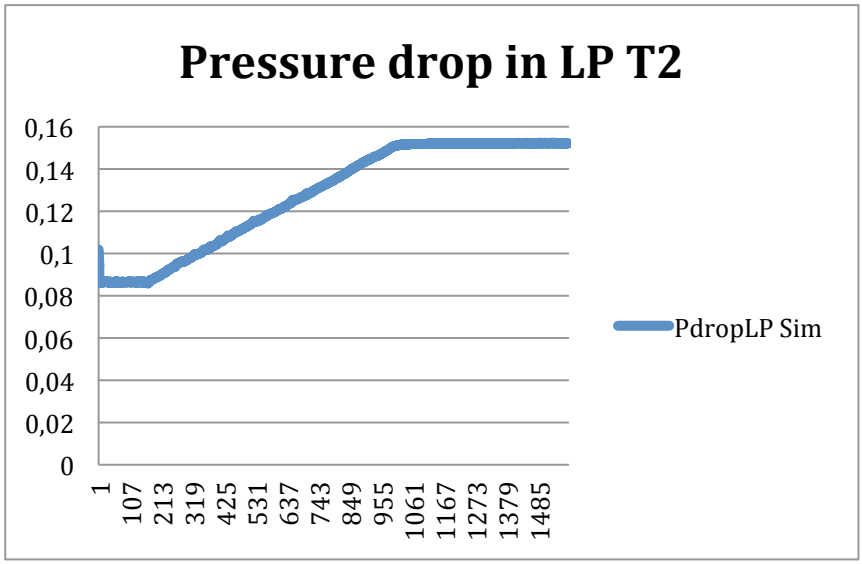

Figure A.7: Pressure drop in LP turbine during the second transient simulation

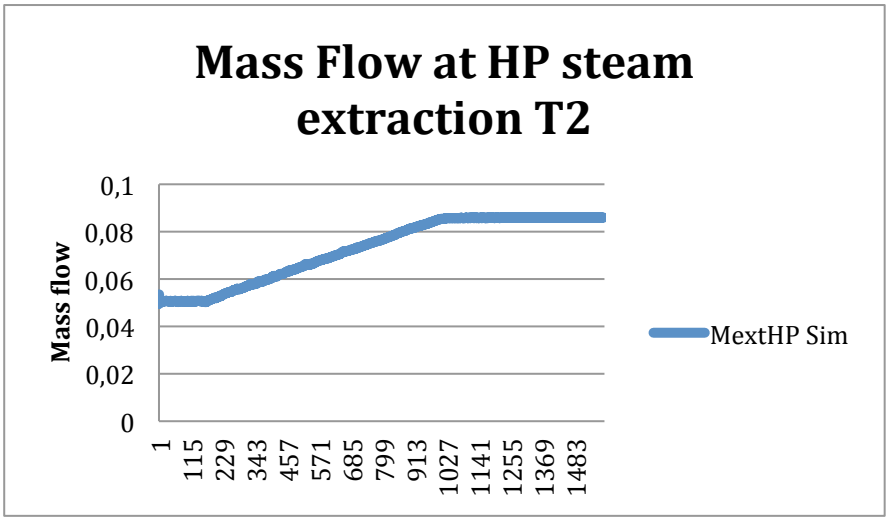

Figure A.8: Mass flow at HP steam extraction during the second transient simulation

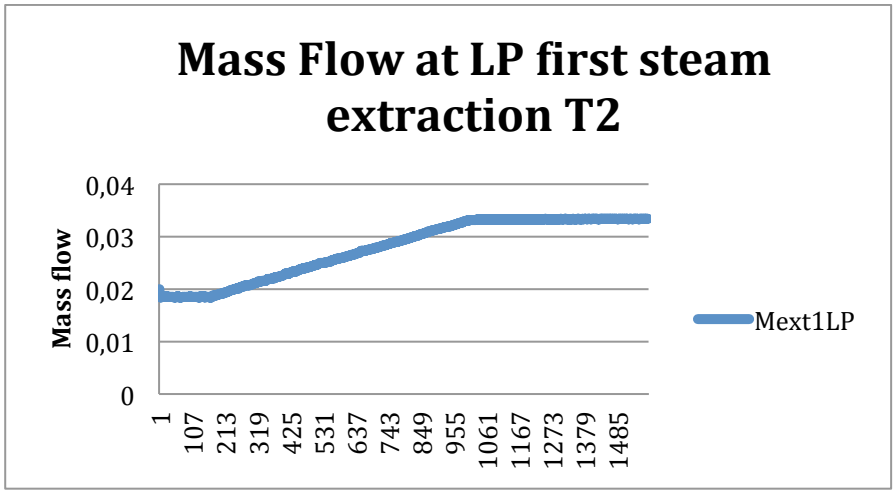

Figure A.9: Mass flow at LP first steam extraction during the second transient simulation

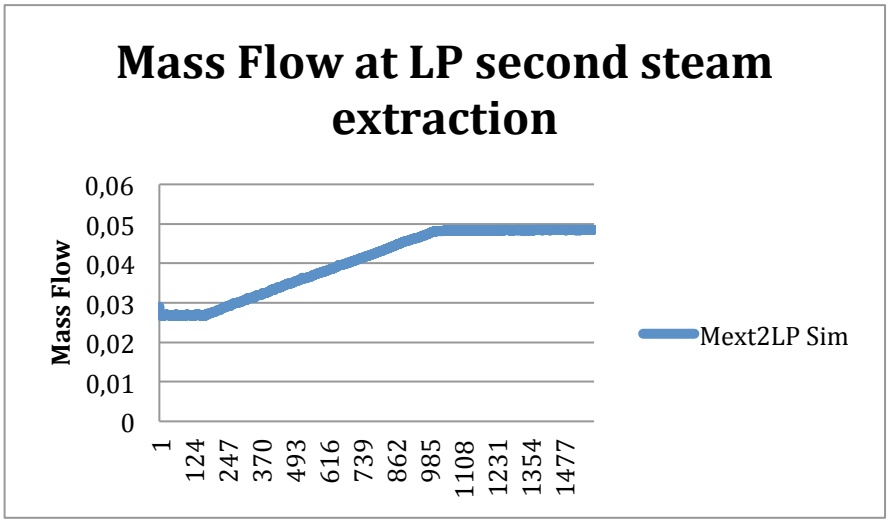

Figure A.10: Mass flow at LP second extraction during the second transient simulation

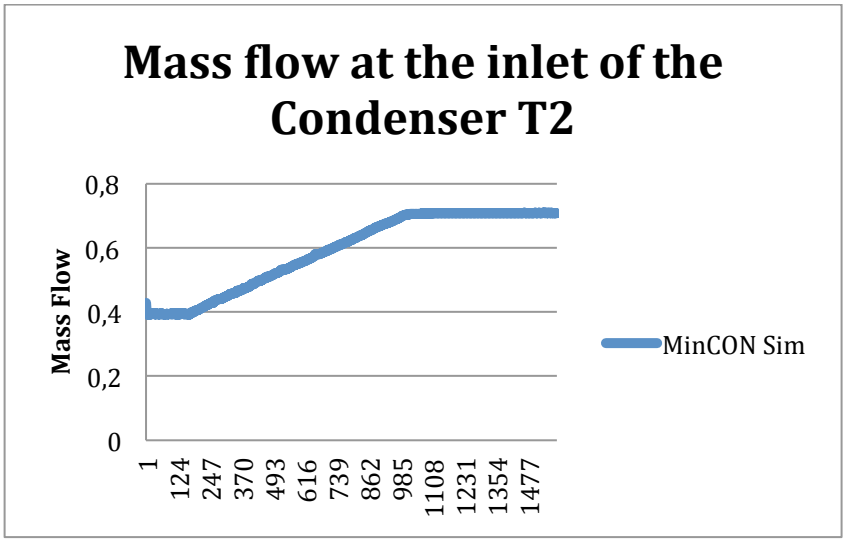

Figure A.11: Mass flow at the inlet of the condenser during the second transient simulation

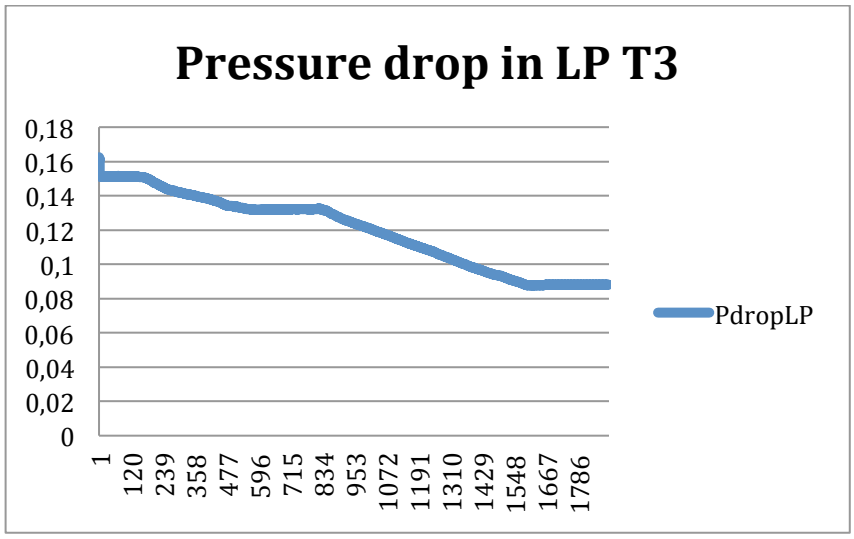

Figure A.12: Pressure drop in LP turbine during the third transient simulation

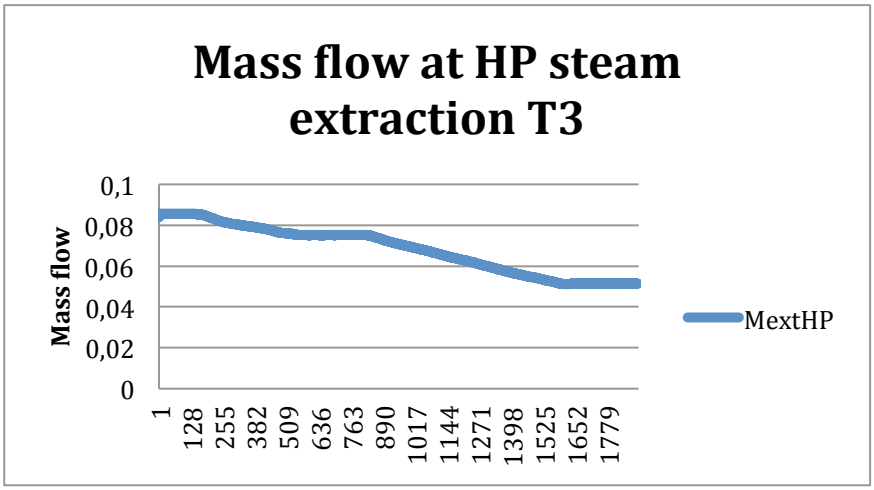

Figure A.13: Mass flow at HP steam extraction during the third transient simulation

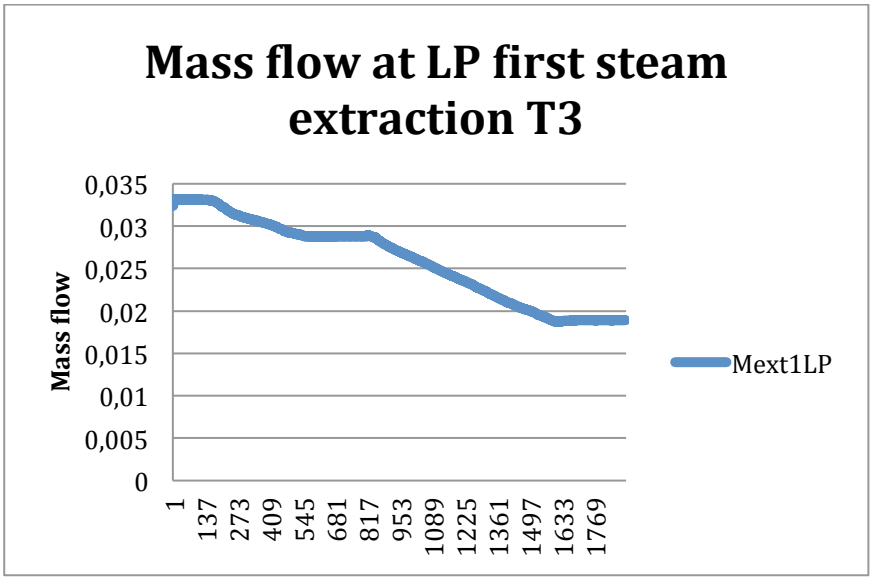

Figure A.14: Mass flow at LP first steam extraction during the third transient simulation

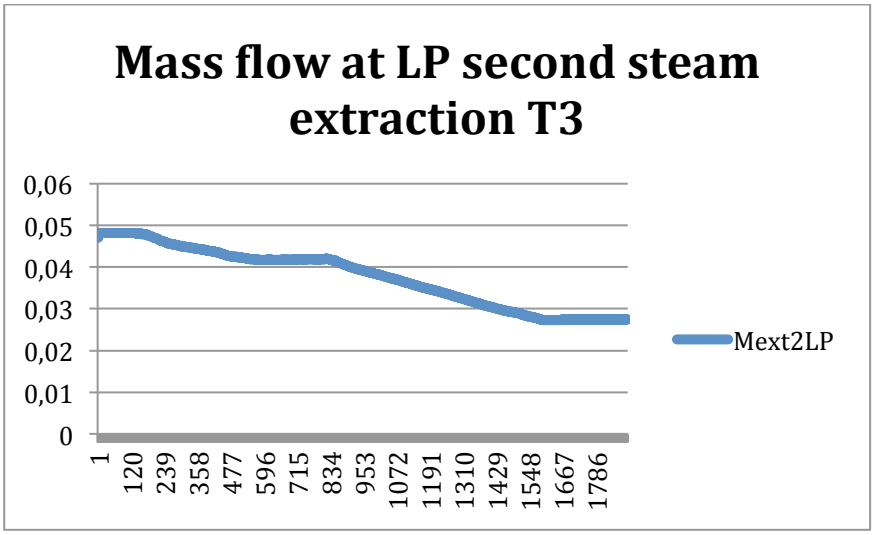

Figure A.15: Mass flow at LP second steam extraction during the third transient simulation

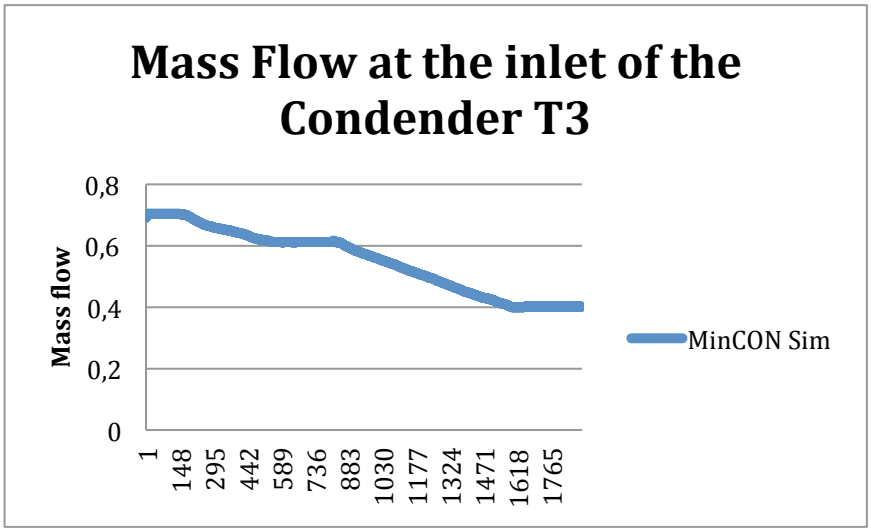

Figure A.16: Mass flow at the inlet of the condenser during the third transient simulation

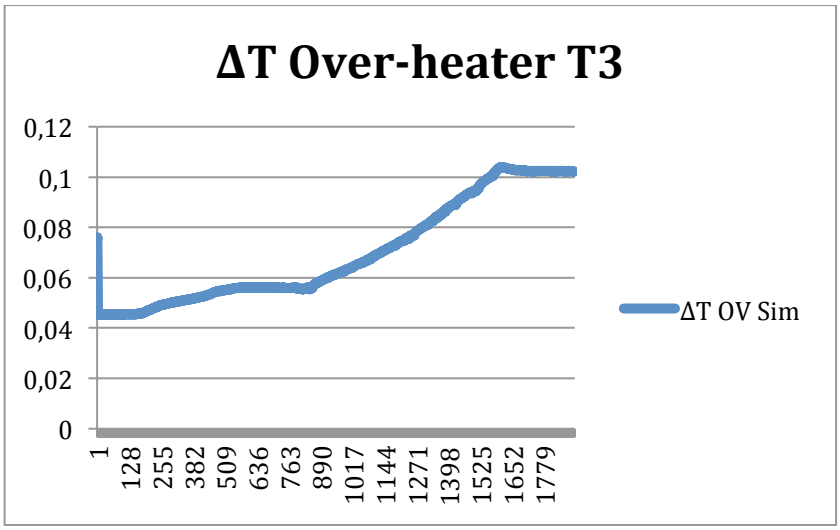

Figure A.17: ΔT in the over-heater during the third transient simulation

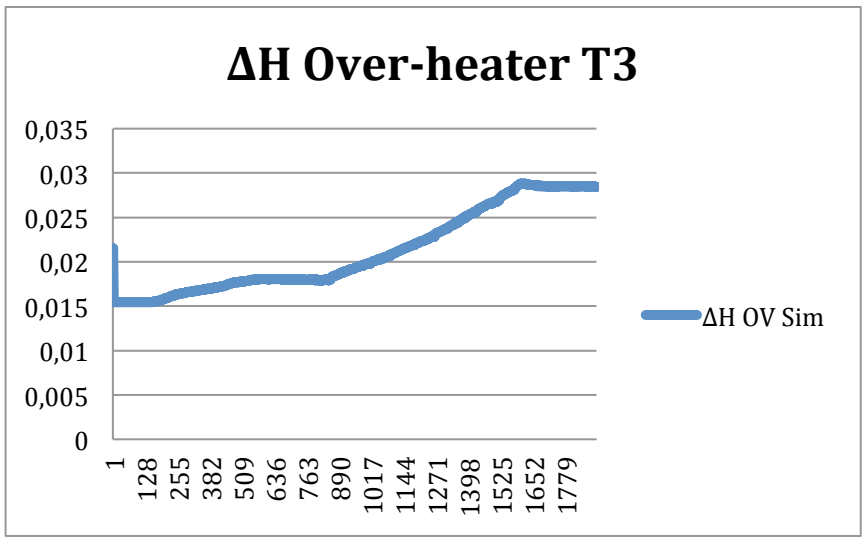

Figure A.18: ΔH in the over-heater during the third transient simulation



SIMULACIÓN DE UNA TURBINA DE VAPOR DE UNA CENTRAL NUCLEAR CON ATHLET

Vega Gómez de la Rosa